FRACTURE TOUGHNESS IN DUCTILE TO BRITTLE TRANSITION REGION AND MASTER CURVE

Thesis submitted by

KUSHAL BHATTACHARYYA

DOCTOR OF PHILOSOPHY (ENGINEERING)

DEPARTMENT OF MECHANICAL ENGINEERING
FACULTY COUNCIL OF ENGINEERING & TECHNOLOGY
JADAVPUR UNIVERSITY
KOLKATA, INDIA

2019

JADAVPUR UNIVERSITY
KOLKATA-700 032

Index No. 289/14/E**.**

1. Title of the Ph.D. (Engg.) Thesis:

FRACTURE TOUGHNESS IN DUCTILE TO BRITTLE TRANSITION REGION AND MASTER CURVE.

2. Name, institute & designations of the supervisors:

Prof (Dr.) Sanjib Kumar Acharyya
Professor, Department of Mechanical Engineering,
Jadavpur University,
Kolkata – 700032, INDIA.

3. List of Publications (Referred Journals):

I. Bhattacharyya K, Acharyya S, Dhar S, Chattopadhyay J. Variation of Beremin Model Parameters With Temperature by Monte Carlo Simulation. Journal of Pressure Vessel Technology. 2019 Apr 1;141 (2):021401.

II. Bhattacharyya K, Acharyya S, Dhar S, Chattopadhyay J. Calibration of Beremin Parameters for 20MnMoNi55 Steel and Prediction of Reference Temperature (T 0) for Different Thicknesses and a/W Ratios. Journal of Failure Analysis and Prevention. 2018 Dec 1;18(6):1534-47.

III. Bhattacharyya K, Acharyya S, Dhar S, Chattopadhyay J. To Study the Effect of Loss of Constraint on Reference Temperature (T0) With the Help of Q-Stress, Triaxiality Ratio and T-Stress. Materials Today: Proceedings. 2018 Jan 1;5(13):27260-8.

IV. Bhattacharyya K, Acharyya SK, Chattopadhyay J, Dhar S. Study of constraint effect on reference temperature (T0) of reactor pressure vessel material (20MnMoNi55 Steel) in the ductile to brittle transition region. Procedia Engineering. 2014 Jan 1;86:264-71.

4. List of Patents: Nil

5. List of Presentations in International Conferences:

1. K.Bhattacharyya, S.Acharyya, S.Dhar, J.Chattopadhyay. "Variation of Weibull Modulus (m) & Weibull Scalar Parameter (σu) with temperature, for RPV material 20MnMoNi55 steel in the Ductile to brittle transition region with the help of Master Curve methodology", 2017,4th International Conference on Advance In Materials And Materials Processing. Department Of Metallurgical and Materials Engineering, IIT Kharagpur
2. K.Bhattacharyya, S.Acharyya, S.Dhar, J.Chattopadhyay. "Variation of Weibull Modulus (m) & Weibull Scalar Parameter (σu) with temperature, for the Brittle Dominated portion of Ductile to Brittle Transition region with the help of Monte Carlo Simulation for 20MnMoNi55 steel"" Proceedings of 62nd Congress of ISTAM, 2017, University College of Engineering, Osmania University, India.

CERTIFICATE FROM THE SUPERVISOR/S

*This is to certify that the thesis entitled "**FRACTURE TOUGHNESS IN DUCTILE TO BRITTLE TRANSITION REGION AND MASTER CURVE**" submitted by **Shri Kushal Bhattacharyya**, who got his name registered on **27.03.2014** for the award of **Ph.D. (Engineering) degree** of **Jadavpur University**, is absolutely based upon his own work under the supervision of **Prof. Sanjib Kumar Acharyya**, that neither his thesis nor any part of the thesis has been submitted for any degree/diploma or any other academic award anywhere before.*

.....

Prof. (Dr.) Sanjib Kumar Acharyya

Signature of the Supervisor
and Date with Office Seal

About the Author

The author, Sri ***KUSHAL BHATTACHARYYA*** was born at Dum Dum West Bengal. He did his diploma in Automobile Engineering from Air Technical Training Institute, Kolkata in 2003. He graduated in Mechanical Engineering from Jadavpur University in 2011, he completed Master of Mechanical Engineering in Machine Design specialization from Jadavpur University in 2013. He got registration for pursuing PhD work in the Department of Mechanical Engineering from Jadavpur University on 27/03/2014.Presently he is working as an Assistant Professer in Netaji Subhas Engineering Collage (Techno India Group)

Acknowledgement

This thesis would not have been possible without the help of so many people in so many assorted ways. So I would like to take this opportunity to express my heartfelt gratitude to them for supporting me of this thesis.

Last five years in this thesis outcome of my research work carried out at Jadavpur University. Thank you Jadavpur University for given me this kind of rear opportunity.

I am as grateful of Prof. Sanjib Kumar Acharyya as my honourable supervisor. He had support me through my thesis with his patience and knowledge. It is his endless guidance and constant encouragement. It will cherish me every moment of his wise company.

I would like to thank Bhaba Atomic Research Centre (BARC) for providing the experimental setup and materials required for execution of the thesis

In the last few years of my thesis I work on Fatigue and Fracture laboratory. Thanks to all of past and present members of Fatigue and Fracture Laboratory, research scholars and postgraduate students. Their valuable suggestions and input have certainly helped to improve the overall content of the thesis.

Special thanks goes to my friends Amit Banerjee research scholar Design of Machine element Laboratory Jadavpur University who helped me in various way in completion of the thesis and also to Subhabrata Mondal a senior faculty and colleague of Netaji Subhash Engineering Collage.

I would like to convey my thanks to the Head of the Department and all the academic and technical staffs of Mechanical Engineering Department, Jadavpur University, Kolkata.

In this respect, I would also like to grab this opportunity to express my heart-felt gratitude to my wife Nandini Nag who helped me a lot in the last phase of my work, her suggestions and helping attitude helped my way out to the completion of the thesis.

Thank you Babon (Father) without your moral support I would not be able to complete this thesis. He always support me, his contribution always encourage me lots.

Kushal Bhattacharyya

To,

Babon, Mamuni

and

my sweet little Princesses

Ushasree Bhattacharyy

CONTENTS

LIST OF FIGURES

LIST OF TABLES

ABSTRACT

The thesis deals with the determination of reference temperature (T_0) using master curve methodology proposed by Kim Wallin (ASTM E1921-02) from TPB specimen for the material 20MnMoNi55 steel using single temperature and multi temperature method. The effect of test temperature on reference temperature (T_0) has been studied for both TPB and CT specimens. A study is performed on the censor parameter M for both TPB and CT specimen and a correction value is suggested for TPB specimen for the material 20MnMoNi55 steel. To study the effect of constraint (a/W and thickness) on reference temperature (T_0), the value of (T_0) is calculated for different a/W ratio and thickness of TPB specimen. The results are compared with the results obtained from CT specimen for the same material to study the effect of geometry on reference temperature (T_0).

In the next part of the thesis a series of experiments are performed in the ductile to brittle region on TPB specimens with different thickness and a/W ratio and a variation of T_0 is obtained, which indicates constraint dependence of T_0. Then an attempt is made to correlate T_0 with Q-stress, Tstress and Triaxiality ratio to count for the constraint loss. Both the average value and also the maximum value of the finite element parameters are considered to predict T_0 at different constraint label and compared with the experimental results.

Then Weibull stress at the crack tip is calculated from FE analysis of each fracture test using FE software ABAQUS. Calibration of Beremin parameters, like Weibull modulus (m), scaling parameter (σ_u), and $C_{m,n}$ is done using linear regression analysis of a large number of fracture test data at single test temperature.T_0 for different thicknesses and a/W ratios are also evaluated from corresponding Weibull stress based on Beremin model using calibrated m, σ_u and $C_{m,n}$ which are compared with experimental results showing case-specific good matching. The same calibrated values of Beremin parameters and $C_{m,n}$ are also used to evaluate T_0 for CT specimen of the same material using Beremin model, and an excellent matching with the experimental result is found.

After that, variation of the Beremin parameters with temperature for reactor pressure vessel material 20MnMoNi55 steel is studied. Beremin model is used, including the effect of plastic strain as originally formulated in the Beremin model. A set of six tests are performed at a temperature of -110°C in order to determine reference temperature (T_0)and master curve for the entire ductile-to-brittle transition (DBT) region as per the ASTM Standard E1921. Monte Carlo simulation is employed to produce a large number of 1T three-point bending specimen (TPB) fracture toughness data randomly drawn from the scatter band obtained from the master curve, at different temperatures of interest in the brittle dominated portion of DBT region to determine Beremin model parameters at different temperatures.

In the last part of the thesis the results obtained from Monte Carlo simulation are compared with that of experimentally obtained values from the direct calibration strategy for three different temperatures as discussed previously. Utilization of Monte Carlo simulation transcends the burden of performing a huge number of experiments for proper calibration of Beremin parameters for a fixed temperature. Once the Beremin parameters are calibrated for different temperatures in the brittle portion of DBT region then with the help of $C_{m,n}$,another Beremin model parameter, K_{JC} is predicted for 5%,50%and 95% probability of failure for the corresponding temperatures and compared with the existing Master Curve.

Abbreviations

W =Specimen width

a/W= Crack length-to-width ratio of the specimen

RPV= Reactor pressure vessel

DBT= Ductile-to-brittle transition

TPB= Three-point bending

CT =Compact tension

SYMBOLS

m =Weibull modulus

σ_u= Scaling parameter

$C_{m,n}$ =Beremin coefficient

σ_w= Weibull stress

a =Physical crack size (mm)

B =Gross thickness of specimens (mm)

B_{1T}= Thickness of 1T (one inch) specimen

B_0 =Thickness of tested specimen (mm)

P_f =Probability of fracture

K_{JC} =Converted value of J_C equal to critical K

K_{min} =Minimum possible fracture toughness

$K_{JC(median)}$ =Median fracture toughness

K_0 =Scale parameter dependent on test temperature and specimen thickness

M =Censor parameter

Chapter 1

Introduction

1.0 Introduction

Fracture toughness of ferritic steel is the most important material property for failure assessment related to design and maintenance of Reactor Pressure vessel components. Like other ferritic steel Reactor Pressure Vessel Materials show a peculiar behaviour of fracture with variation in temperature. In the upper shelf of temperature the material fails purely by ductile fracture mode, and in the lower self, i.e. in the cryogenic condition, the failure behaviour is completely cleavage fracture. In both the cases there is fairly constant fracture toughness value at a fixed temperature. But the material shows a mixed mode of failure that is ductile initiation followed by uncontrolled brittle fracture in the transition region, reflecting a probabilistic fracture toughness value which shows a scatter at a fixed temperature. Fracture toughness and its scatter in this region depend on temperature. Modelling of this complex failure behaviour of ferritic steel in the transition temperature zone attracts the attention of several researchers for the last few decades. Kim Wallin's [1, 2, 3] proposition of non-dimensional Master curve along with ASTM standard E1921 [4] becomes a pervading axiom to describe the failure behaviour of ferritic steel in the transition region. The propositions given in Master Curve and E1921are adopted worldwide for predicting fracture toughness of various types of ferritic steel as irradiated and virgin material in the Ductile To Brittle Transition (DBT) region. Capturing the constraint effect in the fracture behaviour is the major area where the Master Curve methodology fails to earn its success. This inherently affects the transferability of Fracture Toughness value from the specimen level to component level, which is investigated explicitly in this work.

1.1 Reactor Pressure Vessel

In terms of plant safety, the reactor pressure vessel (RPV) represents the most critical pressure boundary component. It performs a vital safety function as a barrier to fission product release. In addition, the RPV serves several operating functions: it supports and guides control rods, supports vessel internals, provides reactor coolant around the reactor core, and directs the reactor coolant flow that facilitates transfer of heat generated in the core to the steam generator. The RPV is cylindrical with a hemispherical bottom head and a flanged and gasketted upper head. The bottom head is welded to the cylindrical shell while the top head is bolted to the cylindrical shell via the flanges. The cylindrical shell course may or may not utilize longitudinal weld seams in addition to the girth (circumferential) weld seams. The body of the vessel is of low-alloy carbon steel. To minimize corrosion, the inside surfaces in contact with the coolant are clad with a minimum of some 3 to 10 mm of austenitic stainless steel. Numerous inlet and outlet nozzles, as well as control rod drive tubes and instrumentation and safety injection nozzles penetrate the cylindrical shell. The number of inlet and outlet nozzles is a function of the number of loops or steam generators.

1.2 Reactor Pressure Vessel Materials

In RPVs different materials are used for the different components (shells, nozzles, flanges, studs, etc.). Moreover, the choices in the materials of construction changed as the PWR products evolved. For example, the Westinghouse designers specified American Society for Testing and Materials (ASTM) SA 302 Grade the shell plates of earlier vessels and ASTM SA 53 Grade B Class 1 for later vessels. Other vessel materials in common use include American Society of Mechanical Engineers (ASME) SA 508 Class2 plate in the USA, 22NiMoCr37 and 20MnMoNi55 in Germany, and 16MnD5 in France. SA-302, Grade B is a manganese-molybdenum plate steel used for a number of vessels made through the mid-1960s. Its German designation is 20MnMoNi55. As commercial nuclear power evolved, the sizes of the vessels increased. For the greater wall thicknesses required, a material with greater hardening properties was necessary.

The addition of nickel to SA-302, Grade B in amounts between 0.4 and 0.7 weight per cent provided the necessary increased hardening properties to achieve the desired yield strength and high fracture toughness across the entire wall thickness. This steel was initially known as SA-302, Grade B Ni Modified. Forging steels have also evolved since the mid-1950s. The SA-182 F1 Modified material is a manganese-molybdenum-nickel steel used mostly for flanges and nozzles in the 1950s and 1960s. Another forging material used then was carbon-manganese molybdenum steel, SA-336 Fl. Large forgings of these materials had to undergo a cumbersome, expensive heat treatment to reduce hydrogen blistering. Eventually these steels were replaced with steel, first described as ASTM A366 Code Case 1236 and are now known as SA-508 Class 2 that did not require this heat treatment. This steel has been widely used in ring forgings, flanges and nozzles. It was introduced into Germany with the designation 22NiMoCr36 or 22NiMoCr37. With slight modifications, this steel became the most important material for German reactors for a long time. In addition, SA3 508 Class 3 (20MnMoNi55 in Germany and 16 MnD5 and 18MnD5 in France) is used in the fabrication of RPVs.

1.3 Neutron Embrittlement

A unique feature of the environment of nuclear power reactors is the presence of high energy neutron radiation, which can lead to degradation processes in the materials of critical components. This is a central issue, since many components are designed for full service life.

Components in or near the cores of thermal and fast reactors are exposed to fluxes of neutrons with energies ranging from several MeV down to ~0-025 eV and ~10 keV, respectively. The neutrons are produced from fissioning (splitting apart) of the nuclei of atoms of suitable isotopes of uranium (U) or plutonium (Pu) fuel. In most thermal reactors the fuel is principally uranium enriched up to ~5% in the fissile isotope uranium-235 and in modern systems is usually in the form of the oxide The reactor core must also contain a moderator (i.e. a material containing low atomic mass elements such as H or C, e.g. water or graphite) to slow the fission neutrons down to thermal energies by efficient

neutron- nucleus elastic collisions. This is required to sustain a chain reaction, since U-235 is most effectively fissioned by thermal neutrons.

This type of embrittlement concerned with structural steel, can increase the ductile-to-brittle transition temperature as much as 200 °C. In addition, neutron irradiation reduces the upper shelf energy value. The degree of embrittlement increases with neutron fluency (neutron flux x time) and decreases with temperature of exposure.

This type of embrittlement is also observed in case of RPV material at low temperature. The fracture toughness changes drastically over a small temperature range. At low temperatures, steel is brittle and fails by cleavage. At high temperatures, the material is ductile and fails by micro void coalescence. Ductile fracture initiates at a particular toughness value. The crack grows as load is increased. Eventually, the specimen fails by plastic collapse or tearing instability. In the transition region between ductile and brittle behaviour, both micro mechanisms of fracture can occur in the same specimen. In the lower transition region, the fracture mechanism is pure cleavage, but the toughness increases rapidly with temperature as cleavage becomes more difficult. In the upper transition region, a crack initiates by micro void coalescence but ultimate failure occurs by cleavage. On initial loading in the upper transition region, cleavage does not occur because there are no critical particles near the crack tip. As the crack grows by ductile tearing, however, more material is sampled. Eventually, the growing crack samples a critical particle and cleavage occurs. Because fracture toughness in the transition region is governed by these statistical sampling effects, the data tend to be highly scattered. In transition zone the analyses use probability distribution functions to describe the fracture toughness data which vary from fully cleavage at lower temperatures to fully ductile at higher temperatures. Assessment of degree of embrittlement (reduction in value of fracture toughness) plays the most crucial role in advanced structural integrity assessment. This embrittlement may be caused due to low temperature as well as by irradiation, change in microstructure or corrosion. The components in nuclear power plants which are subjected to irradiation or any other components facing low temperature are required to be continuously monitored for assessment of loss of ductility during the operational life. Therefore a comprehensive methodology to describe the fracture

toughness of structural steels encompassing the ductile, ductile to brittle transition (DBT) and completely brittle fracture influenced by temperature, irradiation and other causes has been attempted to be developed during the last few decades.

1.4 Transition-Temperature Curve and Nil Ductility Temperature (NDT)

The notched-bar Charpy impact tests are conducted over a range of temperatures to generate Transition-Temperature Curve [5] so that the temperature at which the ductile-to-brittle transition takes place can be determined. A well-defined criterion is to base on the transition temperature on the temperature at which the fracture becomes 100 percent cleavage. This point is known as Nil Ductility Transition Temperature (NDTT) ASTM E208 - 06(2012)**[6]**. The NDTT is the temperature at which fracture initiates with essentially no prior plastic deformation. Below the NDTT, the probability of ductile fracture is negligible. Later another reference temperature for nil ductility for transition (RT_{NDT})**[7]** was defined as the temperature at which the Charpy impact energy for failure is observed to be equal to 41J. If a material is embrittled then this reference temperature will be increased and the shift in this temperature can be a measure of degree of embrilltlement. ASME Code K_{IC} curve characterizing for static crack initiation and the K_{ID}/ K_{IA}/ K_{IR} curve for dynamic crack arrest are based upon an approach that utilizes a material normalizing and indexing parameter,**[**8] RT_{NDT}. By establishing appropriate RT_{NDT}, the K_{IC} curve can be positioned appropriately for use in RPV integrity assessment. The appropriate position of K_{IC} curve for irradiated material can be adjusted by finding RT_{NDT} of irradiated material. The shift in RT_{NDT} is the measure of loss of ductility due to irradiation. The adjusted K_{IC} curve is to be considered for structural integrity analysis at this stage. However, the ASME Code fracture toughness curves, K_{IC} and K_{IR}, are lower bound curves that are not based on probability assessment and hence very much conservative. Although it is helpful to provide a method for evaluating the fracture toughness parameters, the main drawback is that

1. Charpy test cannot provide fracture toughness by itself.
2. It gives only the Lower bound of fracture toughness curve.

3. It could not arrest the Statistical scatter of the fracture toughness values in the ductile to brittle transition region

Fig.1.1 shows the variation of Charpy energy with Temperature showing clearly the Brittle behaviour in the lower self and ductile behaviour in the upper shelf temperature and Fig1.2 also shows the scatter of fracture toughness data in the transition region.

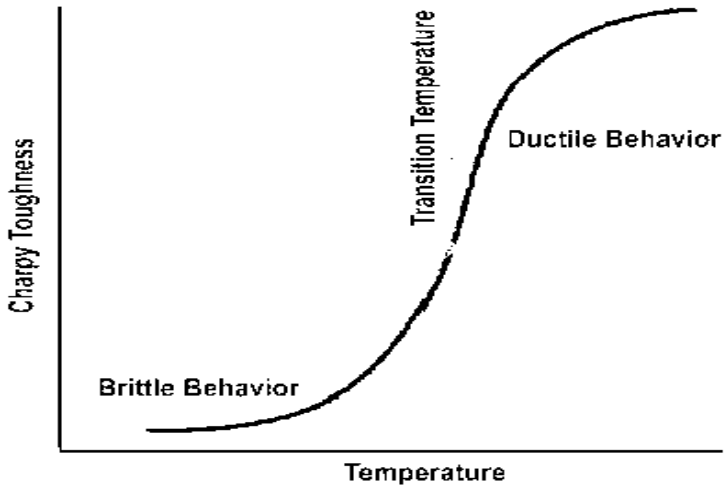

Fig. 1.1: CVN energy variation

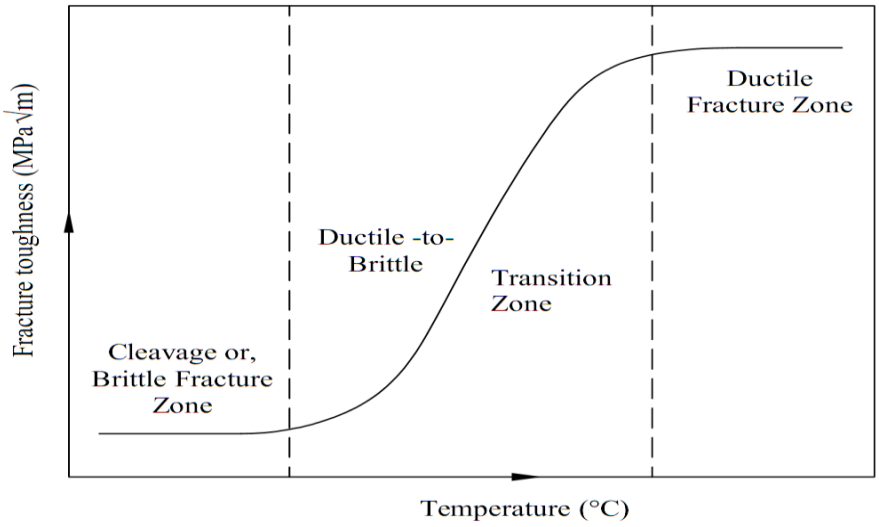

Fig.1.2: Scatter of fracture toughness data in the transition range

1.5 Master Curve Approach

In order to overcome the drawbacks of Nil Ductility Temperature (NDT) approach, later Wallin developed the concept of a common fracture toughness-temperature Curve for all the ferritic steel known as Master Curve (adopted in ASTM E 1921-02) [9] specifically to provide a measurement of fracture toughness transition temperature (T_0) that properly accounts for specimen size, strain rate (over a range of nearly static loading rates), and specimen notch acuity (fatigue pre-cracked). This Master Curve procedure to determine T_0 provides a more reliable prediction of actual material behaviour. The master curve defines both the variation of the median value of fracture toughness with temperature and the scatter of fracture toughness about this median value. The Master Curve [10] together with reference temperature (T_0) value defines the complete transition fracture toughness curve in a manner appropriate for use in both probabilistic and deterministic analysis. In the master curve method, a fracture toughness curve is determined by a single parameter that establishes the position of the master curve on temperature scale. This parameter is termed as T_0 and is defined as the temperature at which the median fracture toughness for 1T–CT fracture toughness specimen equals 100 MPa [11]. The master curve method is also used to construct a bounding curve on the fracture toughness. Typically a bounding curve with a 95% degree of confidence is used as lower bound on the fracture toughness values. This implies that 95% of all fracture measurements should fall above the confidence/ tolerance bound. Wallin [12, 13] described the cleavage fracture toughness behaviour in the lower ductile-to-brittle transition (DBT) range of ferritic steels. Using the J integral based cleavage fracture toughness, K_{JC}, it was demonstrated on many materials that the temperature dependence of the median fracture toughness has a unique shape, the so-called ‘‘Master Curve’’ (MC), which can be adjusted with a reference temperature T_0. The MC approach postulates four assumptions:

1. the statistical analysis using a three-parameter Weibull distribution,
2. the statistically derived specimen size adjustment,
3. a unified temperature dependence and
4. material homogeneity at the macroscopic level.

In this analysis, the scatter of fracture toughness value in DBTT is explained assuming that cleavage fracture in the transition range is initiated at the randomly distributed nucleation sites in the material matrix and followed by crack propagation. The factors (temperature, thickness, loading rate, irradiation) influencing this phenomenon make the fracture to be probabilistic. The fracture toughness is not a definite value rather for each value of fracture toughness there is a value of probability of failure.

It is derived theoretically and verified experimentally that the scatter is best fitted by Weibull characteristics. The basis of the master curve approach is a three parameter Weibull model which the relationship between K_{JC} and the cumulative probability failure P_f where,

$$P_f = 1 - \exp\left[-\left(\frac{K_{JC} - K_{\min}}{K_0 - K_{\min}} \right)^4 \right] \tag{1.1}$$

and

$$K_{JC} = \sqrt{\frac{J_C E}{1-\nu^2}} \tag{1.2}$$

Where, K_{JC} is the fracture toughness corresponding to P_f, K_0 is the scale factor of Weibull distribution and is the value of fracture toughness corresponding to 63.2% cumulative failure probability and K_{min} is the lower bound fracture toughness. From experimental and theoretical observations it appears that for all ferritic steels, the value of Weibull modulus is best fit at 4 and the value of K_{min} can be taken as 30 MPa$\sqrt{m}$. Therefore, for particular steel the value of K_{JC} is to be estimated experimentally from J-R curve test. The distribution of fracture toughness value at a particular temperature is completely available by the values of K_{JC}. Using maximum likely-hood principle and Weibull distribution the value of K_0 is determined from the following equation:

$$K_0 = \left[\sum_{i=1}^{N} \frac{\left(K_{JC(i)} - K_{\min} \right)^4}{N} \right]^{1/4} + K_{\min} \tag{1.3}$$

Where K_{JC}(i)s are determined from experiments with different specimens and N must be at least six .

Then $K_{JC(med)}$ is computed by the equation,

$$K_{JC(med)} = K_{\min} + (K_0 - K_{\min})(\ln 2)^{1/4} \quad (1.4)$$

In this way $K_{JC(med)}$ can be determined at different test temperatures. The variation of $K_{JC(med)}$) with temperature is observed to be best fitted exponentially as

$$K_{JC(med)} = 30 + 70\exp\left[0.019(T - T_0)\right] \quad (1.5)$$

Where T_0 is a reference temperature at which the median fracture toughness of 1T–CT fracture toughness specimen is 100 MPa. For specimens with other thicknesses the following equation is used to compute 1T–CT equivalent fracture toughness.

$$K_{JC(1T)} = K_{\min} + \left[K_{JC(x)} - K_{\min}\right]\left(\frac{B_x}{B_{1T}}\right)^{1/4} \quad (1.6)$$

The different observations and recommendations regarding Master curve of fracture toughness in DBTT range have been explored in last two decades through organized experimental and theoretical research activities under the guidance of IAEA [**14**]. The test methodology, specimen standard, guidelines for censoring and size limit, computation of K_{JC} test environment have been described in ASTM E1921.

The reference temperature, T_0 is a measure of degree of embrittlement and useful for comparison of materials. But the T_0 obtained from E1921 is questionable when applied for assessments of structural defects. Structures most often have shallow, surface-breaking or embedded defects and are loaded predominantly in tension not bending, and the local J values vary strongly along the crack fronts. The ‘‘applicability’’ of T_0 values obtained from high-constraint, straight through-cracks to real applications requires additional models that accommodate effect of constraint differences and variations in local J values.

1.6. Effect of constraints on Master Curve and Reference temperature T_0

Capturing the constraint effect in the specimen level is the major area where the Master Curve methodology fails to earn its success. This inherently affects the transferability of Fracture Toughness value from the specimen level to component level, which is studied explicitly in this work.

Other researchers used Q-stress and T-stress [15,16] as the parameters of constraint correction in J Integral and hence in fracture toughness which is extended in this work to capture the effect of constraints on Master Curve.

Recently with the development of local approach model many researchers tried to capture constraint correction on the basic of it. Among them the seminal work of Beremin [17] appears to be most challenging to the researchers as it develops a correlation between micro mechanism of fracture with macroscopic crack driving force such as J-Integral by introducing Weibull Stress(σ_w) ,which is basically a probabilistic fracture parameter. Beremin proposed that σ_w follows a two parameter Weibull distribution, where the shape parameter is identified as Weibull modulus (m) and scale parameter as Weibull Scalar Parameter (σ_u) .By implementation of, any finite element code Weibull Stress (σ_w) can be calculated with the increment in remote or global loading such as J-integral and the failure mechanism can be locally studied on the micro parameter basis. There is a recent trend followed by different researchers to address their transferability model in the light of Weibull Stress [18,19], relying on the fact that unstable cleavage fracture is triggered by a critical value of Weibull Stress (σ_w) due to the effect of increase in remote loading (J-Integral). Different values of Weibull Stress (σ_w) obtained for different crack front conditions reflect a variation in the stress field near the crack tip. The shape parameter of Weibull distribution (ie. Weibull modulus "m") takes a major role in the process to correlate the constraint loss effect for different crack front conditions such as shallow and deep crack and loading conditions such as bending in TPB specimen and Tension in CT specimen.

Therefore proper calibration of Weibull modulus "m" and Weibull Scalar Parameter (σ_u) is a major criterion for the implementation of Beremin model for a given material.

Several methods [18,20,21,22.23,24,25] have been followed for the calibration of the parameters for different materials. Once the parameters are calibrated, the next area of debate put forward by different researchers for the last 20 years is the sensitivity or dependence of the parameters with temperatures.

The direct calibration procedure by calculating the Weibull stress for each experimental data from any FEA package and then using Linear regression analysis is the best solution for the calibration scheme. But testing with a small number of replica specimens creates a lot of uncertainty in the calibrated value of "m" & "σ_u". In the numerical work done by Khalili and Kromp [23],they have shown that testing of at least 30 replica specimens are required to provide a reliable result of the parameters, for a single temperatures. Testing of such huge number of specimens is too much expensive. To transcend the huge burden of testing such a large number of specimens an alternative approach has been put forward by researchers [24, 25,and 26] by employing Monte Carlo technique.

Another important aspect in the study of Beremin modelis calibration of $C_{m,n}$,which is a parameter used for conversion of Weibull stress obtained for Finite Element Analysis to Fracture toughness K_{JC}. This value of Fracture toughness K_{JC} is accounted as the predicted value from the Beremin model and is compared with the values predicted from experiment.

1.7 Literature Review

Assessment and transferability of fracture toughness, from specimen level to component level in the transition region is an important perspective in the design of reactor pressure vessels with reactor pressure vessel (RPV) steels. Many researchers since the last 30 years tried to characterize the fracture toughness for RPV material using different methods and different material model have been put forward to qualitatively asses the transferability of fracture toughness from specimen level to component level considering the constraint affect. To appraise the state of the art in this regard, different methods and models are reviewed here.

1.7.1. Master Curve and effect of constraint on Reference Temperature (T_0):

K. Wallin, A. Laukkanen, P.Nevasmaa and T. Planman [27] stated that "The Master Curve Methodology is a statistical, theoretical, micro mechanism based analysis method for fracture toughness in the ductile to brittle transition region. This method, originally developed at VTT Manufacturing Technology" which simultaneously account for the scatter, size effects and temperature dependence of fracture toughness. The method has been successfully applied to a very large number of different ferritic steels and it forms the basis of the ASTM testing standard for fracture toughness testing in the transition region. In their work, some recent advances of the technology are presented. Such as constraint adjustment, description of warm pre-stress effects, analysis of in homogenous materials and assessment of real three-dimensional flaws

W. J. McAfee, P. T. Williams, B. R. Bass, and D. E. McCabe [28] investigated the variations in the reference indexing parameter T_0 determined from shallow-flaw and deep-flaw fracture-toughness data. The test data were generated from a highly-characterized A533B plate material that had been heat treated to achieve tensile properties similar to a highly irradiated RPV material. A matrix of tests using shallow-flaw (a/W= 0.10) and deep-flaw (a/W= 0.50) 1T SE(B) specimens was conducted at temperatures in the lower transition-temperature region. Constraint loss in the shallow-flaw specimens resulted in a -26.8 °C shift in transition temperature relative to the deep-flaw constraint condition when T_0 was calculated using ASTM E1921-97 procedures.

Iradj Sattari-Far & Kim Wallin [29] illustrated the capabilities of the Master Curve methodology for fracture assessments of nuclear components. Within the scope of their work, the theoretical background of the methodology and its validation on small and large specimens has been studied and presented to sufficiently large extent .The correlations between the Charpy-V data and the Master Curve T_0 reference temperature in the evaluation of fracture toughness is also presented. The work gives a comprehensive report of the background theory and the different applications of the Master Curve methodology.

Kim Wallin [**30**] developed Master Curve method to analyse the scatter of fracture toughness of a large nuclear grade pressure vessel forging 22NiMoCr37 in the ductile to brittle transition regime. The tests were performed on standard CT specimens having thickness 12.5,25,50 and 100mm. The a/w ratio was close to 0.6 for all specimens. Each data set was analysed by standard master curve expression using a fixed K_{min} and the more complicated expression fitting of K_{min}.

Philip Minnebo, César Chenel Ramos, José Mendes, Luigi Debarberis [31] presented the outcome of four fracture test series, addressing the ductile-to-brittle toughness behaviour of a nuclear reactor pressure vessel steel. Each test series corresponds to specific test specimen geometry, tensile or three-point-bend, with a given degree of crack-tip constraint. A brief overview is given of available constraint-based fracture mechanics methodologies in the ductile-to-brittle transition range, including both engineering and local approach procedures.

Z.X.Wang,H.M.li,Y.J.Chao,P.S.Lam [32] has done Finite element method to analyze the three-point bend experimental data of A533B-1 pressure vessel steel obtained by Sherry, Lidbury, and Beardsmore from -160°C to -45°C within the ductile-brittle transition regime. As many researchers have shown, the failure stress (σ_f) of the material could be approximated as a constant. The characteristic length, or the critical distance (r_c) from the crack tip, at which is reached, is shown to be temperature dependent based on the crack tip stress field calculated by the finite element method.

J.A. Joyce1 and R.L. Tregoning [33] used the application of the Master Curve method and associated reference temperature of ASTM E1921 to define the ductile to brittle transition in ferritic structural steels used in commercial nuclear reactor vessels In their experimental program different C(T), SE(B), and pre-cracked Charpy specimen geometries have been investigated including both deep and shallow cracked SE(B) geometries. The differences found between shallow and deep crack specimens is not surprising, but the magnitude of the differences found between the C(T) and deep crack SE(B) specimens was highly unexpected and does not appear to have been previously reported.

H. J. Rathbun, G. R. Odette,T. Yamamoto,M. Y. He,G. E. Lucas [34] investigated the effects of specimen size on the cleavage fracture toughness of a typical pressure vessel steel is reported. Size dependence arises both from: (i)statistical effects, related to the volume of highly stressed material near the crack tip, that scales with the crack front length Band (ii) constraint loss, primarily associated with the scale of plastic deformation compared to the un-cracked ligament dimension b. Previously, it has been difficult to quantify the individual contributions of statistical versus constraint loss size effects. This paper focuses on the possible significance of these results to the Master Curve standard as formulated in ASTM E 1921.

Kim Wallin [12].stated that as the size of the specimen have the effect on fracture toughness data, so the fracture toughness obtained from small laboratory specimens do not directly describe the fracture behaviour of real flawed structures. For validation, a large nuclear grade pressure vessel forging 22NiMoCr37 (A508 Cl.2) has been extensively characterised with fracture toughness testing. The tests have been performed on standard geometry CT-specimens having thickness 12.5 mm, 25 mm, 50 mm and 100 mm. The a/W-ratio is close to 0.6 for all specimens. One set of specimens had 20% side-grooves. The obtained data consists of a total of 757 results fulfilling the ESIS-P2 test method validity requirements with respect to pre-fatigue crack shape and the ASTM E-1921 pre-fatigue load. The master curve statistical analysis method is meticulously applied on the data, in order to verify the validity of the method. Based on their analysis it can be concluded that the validity of all the assumptions in the master curve method is confirmed for this material.

J. Chattopadhyay, B.K. Dutta, K.K.Vaze and S.Acharyya [35] have done a lot of empirical and theoretical correlations to capture the geometry, size and loading rate dependence of fracture toughness .

S.Bhowmik, A.Chattopadhyay, T.Bose, S.K. Acharya, P.Sahoo, J.Chattopadhyay, S.Dhar, [**36**] used the Master curve method proposed by Kim Wallin to estimate the fracture toughness of 20MnMoNi55 in the ductile to brittle transition regime. Reference temperature (T_0) is evaluated both by single temperature method and multiple

temperature method for 1 inch thick compact specimen (1T-CT) specimens. Reference temperature (T_0) is also evaluated from Charpy V-notch test data and compared. It is observed that Charpy test data results yields lower value of Unirradiated T_0 compared to 1T-CT specimen tests. It is also observed that the fracture toughness values falls between 5% and 95% boundary of fracture toughness curves for all evaluations.

S.Bhowmik, S.K. Acharya, J.Chattopadhyay, S.Dhar [37] used the master curve methodology proposed by Kim Wallin (ASTM E1921-02) to evaluate master curve reference temperature (T_0) from full compact tension (CT) and 1/2T-CT specimens for the material 20MnMoNi55 steel using single temperature and multi-temperature method. The effect of temperature range, number of test temperatures and initial crack length on the value of T_0 are also studied. The correction proposed for thickness adjustment has been verified. Master curves are drawn using full and 1/2T-CT specimen separately and compared with best fit characteristic curve and found to be within 95% bound.

1.7.2. Constraint effect in light of Triaxiality ratio, Q-Stress and T-stress

Attempts have been taken by different researchers to capture the constraint effect on fracture toughness with the help of the above parameters. A detail review has been done to coagulate the effect of all of them.

B. S. Henry and A. R. Luxmoore [38] have done three-dimensional finite element models of low constraint geometries to study the variation of the triaxiality factor, plastic strain and Q-value with the deformation level. Comparisons between the triaxiality factor, the plastic strain and the Q-value are made at different distances ahead of the crack front. Their numerical results show that, for a given material, there exists a unique linear relationship between the triaxiality factor and the Q-value that is independent of specimen geometry, dimensions, crack depth and deformation level.

G. Mirone [39] performed Finite element simulations of the experimental tests to calculate the stress triaxiality evolution on various notched and unnotched specimens. A ductile failure criterion, due to Bao and Wierzbicki, is then applied to evaluate the material damage and predict failure. This procedure is applied to a set of 20 specimens

series made of six metals with 10 different notch shapes. The damage calculations also indicate the material points where failure initiates. These predictions are confirmed by micrographic observation of voids on polished fragments of the broken specimens.

Chen et al, O. Kolednik,J. Heerens,F.D. Fischer [**40**] have investigated the interrelations between the cohesive zone parameters (the cohesive strength, Tmax, and the separation energy, Γ) and the crack tip triaxiality for 10 mm thick smooth-sided compact tension specimens' made of pressure vessel steel 20MnMoNi55.

S. Cravero and C. Ruggieri.[41]used the J-Q approach to characterize constraint effects on cleavage fracture behaviour of cracked structural components. They emphasize features of two-parameter fracture methodologies which extend the limits of applicability of single parameter fracture approaches when LSY effects prevail. Inclusion of the second parameter (Q) in failure assessment procedures leads to the construction of experimentally derived fracture toughness loci, rather than conventional, single-valued definitions of toughness. The plan of the article is as follows. First, the notion of crack tip constraint and its connection with SSY reference fields is introduced. This is followed by a brief description of the J-Q theory to define the hydrostatic parameter Q.

MarcinGraba [15]investigated the values of the Q-stress determined for various elastic-plasticmaterials for centre cracked plate in tension (CC(T)). The influence of the yield strength, the work-hardening exponent and thecrack length on the Q-parameter was tested.

Markku J.Nevalainen [42] have used a wide variety of specimen and flaw dimensions through experiment and finite element analysis in order to infer the constraint effect .T-stress, Q-parameter and Small Scale Yielding conditions are used as the methods for constraint correction.

Philip Minnebo, César Chenel Ramos, José Mendes, Luigi Debarberis [43] presented the outcome of four fracture test series, addressing the ductile-to-brittle toughness behaviour of a nuclear reactor pressure vessel steel. Each test series corresponds to a specific test specimen geometry, tensile or three-point-bend, with a given degree of

crack-tip constraint. A brief overview is given of available constraint-based fracture mechanics methodologies in the ductile-to-brittle transition range, including both engineering and local approach procedures.

M.R. Ayatollahi, M.J. Pavier and D.J. Smith [44] recognised elastic T -stress has been as a measure of constraint around the tip of a crack, in contained yielding problems.They explores direct use of finite element analysis for calculating T .T -stress is determined for a test configuration designed to investigate brittle and ductile fracture in mixed mode loading. It is shown that in shear loading of a cracked specimen T vanishes only when a truly antisymmetricfield of deformation is provided.

Kim Wallin [45] shows that Specimen size, crack depth and loading conditions effect the materials fracture toughness. In case of brittle fracture, essentially three different methods to quantify constraint have been proposed, J small scale yielding correction, Q-parameterand the T-stress. He proposed a relation between the T-stress and the master curve transition temperature T_0which is experimentally developed and verified. As a result, a new engineering tool to assess low constraint geometries with respect to brittle fracture has been developed.

N. P. O 'Dowo and C. F. Shih [46] have shown that within the J-Q annulus, the full range of high- and low-triaxiality fields to be members of a family of solutions parameterized by Q when distances are measured in terms of $J/\sigma 0$, where $\sigma 0$ is the yield stress. The stress distribution and the maximum stress depend on Q alone while J sets the size scale over which large stresses and strains develop.

N. P. O 'Dowo and C. F. Shih [47] show that Q parameter provides a quantitative measure of crack-tip constraint, a term widely used in the literature concerning geometry and size effect on a material's resistance to fracture. They have shown that J Q approach considerably extends the range of applicability of fracture mechanics for shallow-crack geometries loaded in tension and bending and deep-crack geometries loaded in tension.

S.Bhowmik, P.Sahoo, S. Acharyya , S.Dhar , J.Chattopadhyay [48] studied experimentally the effect of test temperature, specimen thickness and crack to width ratio on master curve reference temperature in ductile to brittle transition range of 20MnMoNi55 steel. This effect of loss of constraint on reference temperature is estimated through triaxiality ratio using finite element analysis.

1.7.3. Constraint effect in light of micro-mechanism based local approach model.

The foundation of MC methodology which is developed largely by Wallin, requires Small Scale Yielding (SSY) condition to be met by the specimen. In reality however, this condition of SSY is hardly reached for small and miniature specimens. Moreover the size adjustment to an equivalent 1T SSY condition, described in ASTM E1921 does not completely transform the original experimental value to the equivalent SSY value of K_{JC} at 1T, as the existing thickness correction of ASTM E1921 does not take care of non-SSY condition of stresses in small specimens. Thus, the limitation of Master Curve motivates the development of micromechanical models to address the transferability of cleavage fracture toughness across varying levels of crack front constraints. Local approaches to cleavage fracture (micro mechanics model), which couple macroscopic fracture behaviour with micro scale deformations, captures the constraint effect on cleavage due to crack geometry and loading.

F.M.Beremin [17] performed series of experiments of A508 class 3 steel in order to determine the mechanical conditions for cleavage fracture .These tests were carried out on various geometries including 4-pointbend specimens and axis symmetric notched tensile bars with different notch radii which have been modeled using the finite element method. The temperature range investigated was from77 K to 233 K. He shows that, the probability of fracture obeys the Weibull statistical distribution

Claudio Ruggieri and Robert H. Dodds, Jr. [18] described a computational framework to quantify the influence of constraint loss and ductile tearing on the cleavage fracture process. They adopted the Weibull stress σ_w, as a suitable near-tip parameter to describe the coupling of remote loading with a micromechanics model incorporating the statistics of microcracks (weakest link philosophy). According to their work unstable crack

propagation (cleavage) occurs at a critical value of σ_w which may be attained prior to, or following, some amount of stable, ductile crack extension.

Claudio Ruggieri, Xaosheng Gao, Robert H. DoddsJr [49] focused on the Weibull stress approach to assess the effects of constraint loss on cleavage fracture toughness (Jc). The investigation addresses the significance of the Weibull modulus 'm' on the correlation of macroscopic fracture toughness for varying crack configurations.

Xiaosheng Gao, Robert H. DoddsJr [50]present a simplified approach to parameterize constraint effects on the fracture toughness of ferritic steels in the ductile-to-brittle transition (DBT) region under plane strain, small-scale yielding conditions for non-zero T-stress. The Weibull stress serves to couple near tip and global loading which enables scaling of macroscopic toughness values across varying constraint levels.

Jason P. Petti, Robert H. Dodds Jr. [51] coupled the ASTM E1921 procedure to characterize the ductile-to-brittle toughness of ferritic steels in terms of KJc (or Jc) values with the Weibull stress model, i.e., the ''local approach'' for fracture at the microscale. The E1921 procedures assume that uniform, small-scale yielding (SSY) conditions exist at fracture along the full crack front, which supports the use of a simple thickness scaling relationship to adjust experimental toughness values to an equivalent 1T size.

A H Sherry1, D P G Lidbury, D C Connors and A R Dowling. [52] describe a numerical programme undertaken to investigate the influence of specimen size on the fracture toughness behaviour of submerged-arc weld material in the ductile-to-brittle transition regime. The influences of sampling volume and constraint on ΔT have been assessed for 10 mm thick CT (CT-10) and 20 % side-grooved pre-cracked Charpy specimens (PC-CVN) relative to 25 mm thick standard plane-sided compact-tension (CT-25) specimens.

Claudio Ruggieri [53] describes a probabilistic model based upon a local failure criterion incorporating the potential effects of plastic strain on cleavage fracture coupled with the statistics of micro cracks. A central objective is to explore and further extend application of a multiscale methodology incorporating the influence of plastic strain on

cleavage fracture phrased in terms of a modified Weibull stress (σ_w) to correct fracture toughness for effects of geometry and constraint loss.

Xiaosheng Gao , Guihua Zhang, T.S. Srivatsan [54] present a modified Weibull stress model which accounts for the effects of plastic strain and stress triaxiality at the crack tip region. The proposed model is applied to predict cleavage fracture in a modified A508 pressure vessel steel. It is demonstrated that the Weibull modulus (m) remains a constant in the temperature range considered. The threshold value for the Weibull stress model, σ_{w-min}, decreases with temperature due to decrease of the yield stress with temperature.

Wei-Sheng Lei [55] proposed a critical flaw in the Beremin model and suggested modifications. A new statistical model with the power-law distribution of microcracks is obtained to describe the cumulative probability of cleavage fracture. A set of cleavage fracture toughness data of a nuclear pressure vessel steel is used to highlight the difference between the new model and the Beremin model.

A. Andrieu , A. Pineau, J. Besson, D. Ryckelynck, O. Bouaziz [56] present a short and efficient way to apply the original Beremin model, published in 1983, to predict the scatter in the brittle part of the brittle-to-ductile transition curve of ferritic steels. From an engineering point of view, the application of this model has been hampered by the lack of an analytical solution for one of its parameters, $C_{m;n}$. Thus in this work, particular attention is paid to calculating it numerically, and to providing a table of accurate values. The proposed approach is validated by comparing the results given by the application of the unimodal Beremin theory to an existing Euro fracture toughness database.

Claudio Ruggieri and Robert H. Dodds, Jr [57] describe a micromechanics methodology based upon a local criterion incorporating the effects of plastic strain on cleavage fracture coupled with statistics of microcracks. A parameter analysis is conducted under well-contained plasticity, where near-tip fields with varying constraint levels are generated through a modified boundary layer formulation.

Claudio Ruggieri, Rafael G. Savioli and Robert H. Dodds, Jr [58] extended a micromechanic model for cleavage fracture incorporating effects of plastic strain to

determine the reference temperature, T_0, for an A515 Gr 65 pressure vessel steel based on a modified Weibull stress (σ_w). Non-linear finite element analyses for 3-D models of plane-sided SE(B) and PCVN specimens define the relationship between σ_w and J from which the variation of fracture toughness across different crack configurations is predicted. The modified Weibull stress methodology yields estimation of T_0 from small fracture specimens which are in good agreement with the corresponding estimates derived from testing of larger crack configurations.

Hessamoddin Moshayedi ,IradjSattari-Far [59]proposed a linear relationship to improve the cleavage failure probability prediction of preloaded specimens using the modified Beremin model. Maximum stress triaxility factor shows fracture load independency for enough high loads and a good sensitivity to crack tip stress changes due to residual stresses and preloads.

AbhishekTiwari, R. N. Sing, Per Ståhle [60] investigated cleavage fracture in upper region of DBT and a modified master curve approach is presented which can satisfactorily describe the fracture toughness as a function of temperature as well as amount of ductile tearing preceded by cleavage.

B.Z.Margolin, V.N. Fomenko, A.G. Gulenko, V.I. Kostylev, V.A. Shvetsova[61] modified the probabilistic model of brittle fracture known as the Prometey model. The modified model (referred to as the Prometey-M model) has been used for analysis of the transferability of the experimental results on brittle fracture for smooth and notched cylindrical tensile specimens and cracked specimens from Reactor Pressure Vessel (RPV) steel in the initial and embrittled conditions.

M.K. Samal, J.K. Chakravartty, M. Seidenfuss, E. Roos [62] proposed a combined model for ductile and cleavage fracture is used to predict the fracture toughness scatter and its variation with temperature in the DBTT range. It is demonstrated that the above data for fracture toughness can be predicted once we know the material stress–strain data at different temperatures and a single set of Weibull statistics parameters for cleavage fracture. Extensive experimental investigations have been carried out on two types of

pressure vessel steels in the DBTT region using different kinds of specimens to validate the predictions of the model.

Kim Wallin[63] explained the Master Curve methodology for describing cleavage fracture toughness, scatter, size-effects and temperature dependence has been standardized in ASTM E1921. The scatter and size-effects predicted by the method are based on theory, whereas the temperature dependence is the result of empirical observations. This presentation gives some more insight into the factors that lead to the experimentally observed temperature dependence. Finally, a new more material specific temperature dependence usable instead of the standard expression is given.

Carl von Feilitzen, Iradj Sattari-Far[64] describe the implementation of the Master Curve concept into the code ProSACC. The code gives fracture toughness values at the given temperature based on input data on T_0 from fracture toughness testing, or Charpy impact test results (T28J or T41J) or K_{IC} value from fracture toughness testing on the actual material. There is also a possibility in the code to make crack-size correction on the evaluated fracture toughness.

Andrey P Jivkov,, Peter James[65] coupled ductile damage models with Beremin-like failure probability which could be useful in the transition region, uncoupled models with "a posteriori" probability calculations are advantageous to the engineering community. Cleavage toughness predictions in the transition regime, which can be extended to low constraint conditions, are here made with improved criterion for particle failure and experimentally based size distribution of initiators for specific RPV steel. The model is shown to predict experimentally measured locations of cleavage initiators.

Y. Lei, N.P. O'Dowd, E.P. Busso and G.A. Webster[66] used Weibull stress as a measure of the probability of cleavage failure. In this work analytical and semi-analytical expressions for the Weibull stress are developed in terms of the remote loading parameters, *J* or *K*, and material properties. Results are presented for sharp cracks and notches in elastic and elastic-plastic materials under plane stress and plane strain conditions.

N.P. O'Dowd *, Y. Lei, E.P. Busso[67] examined Weibull stress as a measure of the failure probability of a cracked body. Closed form expressions for the Weibull stress are presented for linear elastic and power law materials. These expressions allow Weibull stress values and failure probabilities to be estimated without the need for finite element analyses and provide insight into the use of the Weibull stress as a parameter for the prediction of cleavage failure of cracked bodies.

Avinash Gopalan , M.K. Samal , J.K. Chakravartty.[68] characterised the fracture behaviour of 20MnMoNi55 reactor pressure vessel (RPV) steel in the ductile to brittle transition regime (DBTT) is. Compact tension (CT) and single edged notched bend (SENB) specimens of two different sizes were tested in the DBTT regime. Reference temperature 'T_0' was evaluated according to the ASTM E1921 standard. The effect of size and geometry on the T_0 was studied and T_0 was found to be lower for SENB geometry.

Jason P. Petti, Robert H. Dodds Jr.[**69**] stated that according to new testing standards (e.g., ASTM E1921) remain under continuing development to measure the fracture toughness of ferritic steels over the ductile-to-brittle transition. The procedures assume that relatively small, deep-notch test specimens maintain near small-scale yielding conditions at fracture, which simplifies greatly the interpretation of measured values. However, 3-D finite element analyses suggest that the geometry and small size of common fracture specimens leads frequently to constraint loss, e.g., the decay of small-scale yielding conditions, at only moderate levels of deformation.

1.7.4. Calibration of Beremin Model Parameters.

For the effective use of the above discussed micro-mechanical model proper calibration of its parameters Weibull modulus (m) and Scalar parameter (σ_u) for a specific material is utmost important**.** A number of calibration scheme proposed by different researches for different ferritic steel based RPV materials which are review in the following paragraph.

F. Minami , A. Bruckner-Foit , D. Munz And B. Trolldenier.[21] present a procedure for the determination of the Weibull parameters m and σ_u. This procedure consists of the

determination of the plastic zone ahead of the crack tip, from which cleavage fracture originates, and of the maximum likelihood estimation of the parameters m and σ_u based on the stress distribution in the plastic zone. Calculations using this procedure confirm that the distribution of the Weibull stress σ_w is a material property independent of specimen thickness, and in particular that the shape parameter m depends on the material.

X. Gao, C. Ruggieri and R.H. Dodds, Jr.[20].demonstrated numerically, that a non-uniqueness arises in the calibrated values of Beremin parameters (m &σ_u) i.e., many pairs of m &σ_u provide equally good correlation of critical Weibull stress values with the distribution of measured (SSY) fracture toughness values. They proposed a new calibration scheme to find m &σ_u which uses toughness values measured under both low and high constraint conditions at the crack front. The new procedure reveals a strong sensitivity to m and σ_u provides the necessary micromechanical values to conduct defect assessments of flawed structural components operating at or near the calibration temperature in the transition region.

X. Gao, R.H. Dodds, Jr,R.LTregoning, J.A.Joyce and R.E.Link[70]. applied a recent advancement in probabilistic modelling of cleavage fracture to predict more accurately fracture behaviour of surface crack plates fabricated with A 515-70 pressure vessel steel. They have introduced a new Parameter in Beremin Model referred as $\sigma_{w\text{-}min}$ to predict the fracture toughness more accurately in comparison with experimental data and no separate experimental data is required for calibration of this parameter. A new calibration scheme for Beremin parameters (m & σ_u) is presented in this work based on toughness transferability model which eliminates the non-uniqueness that arises in calibration strategy ,using only small-scale yielding toughness data.

M.C. Burstow[71]. employed commonly used technique to tune the Weibull parameters within the Beremin cleavage model in an iterative scheme using a maximum likelihood method applied to available fracture data. For reliable results, this can require results from a large number of specimens, which is rarely practicable. A new tuning method has been proposed which seeks to scale the history of Weibull stress of one geometry onto that of another. This possesses a number of advantages over maximum likelihood

schemes since reliable predictions can be obtained from fewer experimental results. The technique has been applied to fracture data from two specimen geometries over a range of temperatures, and compared with results obtained from the maximum likelihood method. The technique has been extended to allow tuning of a single, temperature-independent, value of the Weibull modulus, m.

A.H.Sherry, D.P.G.Lidbury, B.R.Bass and P.T.Williams[72] predicted amount of pre-cleavage ductile tearing and the timing of the subsequent cleavage event are compared with the observed fracture behaviour of the defect. Then they highlight several areas in which Local Approach methodology has been developed since the initial work on PTS. These include: Calibration of the cleavage model across a range of temperatures and constraint states.

1.7.5. Variation of Beremin Model Parameters with temperatures.

Once the parameters are calibrated, the next area of debate put forward by different researchers for the last 20 years is the sensitivity or dependence of the parameters with temperatures.

Hojo et al.[73] calibrated distribution of Weibull stress in the brittle fracture region using notched round bar specimens and CT specimen for A533B steel and showed that m & σ_u are insensitive to temperature at least in the lower self-portion of DBT region.

Gao et al. [74] also showed in their work that m does not vary with temperature for A508 steel in the transition region. They used a 3-parameter Weibull Distribution model where the first parameter m remains constant with temperature while the Second parameter σ_u increases with temperature and third parameter the threshold value Weibull stress $\sigma_{w\text{-}min}$(below which cleavage fracture does not occur) decreases with temperature.

Bogdan Wasiluk et al.[75] studied the variation of Beremin parameters on 22Ni–MoCr37 steel similar to ASTM A508 Cl.3. They also used a 3-parameter Weibull Distribution model where the first parameter is “m” the Second parameter “σ_u” and third parameter the threshold value Weibull stress $\sigma_{w\text{-}min}$(below which cleavage fracture does not occur).They have calibrated the parameters at two extreme temperatures of DBT

region that is at -40°C & at -110°C.From the results they have concluded that "m" remains practically insensitive to temperatures,(m=20 at -40°C &m=18 at -110°C) while "σ_u" & $\sigma_{w\text{-}min}$ shows a marked increases with temperature.

Petti and Dodds [76] proposed from their study on A533B and A508 steels that, "σ_u", increases with temperature, while they assumed "m" remains invariant with temperature. They have also proposed a calibration scheme of "σ_u" with variation in temperature, by employing the Master Curve methodology.

But the work done by **C.S. Wiesner and M.R. Goldthorpe [77]** revealed a different trend. They studied on three types of specimen ,notched tensile specimen , notched (Charpy-type) four point bend and fracture mechanics specimens of BS 4360 Grade 50D structural steel at different temperatures. The results reveals that the parameters remains invariant with temperature for notched tensile specimen but for other two specimens notched bend and fracture mechanics specimens, the parameters shows clear dependence on temperature.

In the numerical work done by **Khalili and Kromp [23]** have shown that testing of at least 30 replica specimens are required to provide a reliable result of the parameters, for a single temperatures. Testing of such huge number of specimens is too much expensive. To transcend the huge burden of testing such a large number of specimens an alternative approach has been put forward by researchers [24,25]by employing Monte Carlo technique.

Yupeng Cao et al[24] studied dependence of Beremin Parameters on temperature for C–Mn steel (the 16MnR steel in China) by using a huge number of sample size randomly selected from the band specified by Master Curve E-1921 technique and finally employing Monte Carlo simulation .In their technique the simulation is stopped once the calibrated value of "m" coincides with the predicted value.

Similar work has been done by **Guian Qian.et al[25]** for the unirradiated and irradiated RPV material .Only difference is that the simulation is not stopped once the calibrated value of "m" coincides with the predicted value. Rather it is treated as the result of one

loop of convergence. Similar loop is repeated for “n” number of times and the predicted values of “m” coinciding with the calibrated results from each iteration are taken separately. The average of all the values of “m” values is recognized as the calibrated value for that temperature.

1.8 Motivation of the thesis work :

Inspired with all the researches that has taken place over the years in characterization of fracture toughness in DBT region; the work in this thesis is focused, to capture the constraint effect on T_0 using ductile stress parameters like T-stress, Q-stress and Triaxiality ratio in the upper shelf of the DBT region .Beremin brittle failure model is used to capture the constraint effect on T0 in lower self of the DBT region. Calibration of Beremin parameters for 20MnMoNi55 steel and to investigate the dependence of Beremin parameters with temperatures in the lower self are also attempted explicitly. The direct calibration procedure by calculating the Weibull stress for each experimental data from any FEA software and then using linear regression analysis is the best solution for the calibration scheme. But testing with a small number of replica specimens, 10 to 15 creates a lot of uncertainty in the calibrated value of “m” & “σ_u”. Monte Carlo simulation is also explored to determine the Beremin Parameters from Master Curve requiring six tests only and verified against experimental results.

1.9 Planning of the thesis Work :

1. To study the Effect of a/W ratio and thickness on reference temperature (T_0), a series of experiment on TPB specimen is performed at a constant temperature of -110°C in accordance with ASTM standard E1921.The variation of a/W ratio includes 0.4,0.45,0.5,0.55,0.6,0.65 and variation in thickness of specimen includes 10mm,12mm,15mm,20mm,25mm,30mm.
2. To study the Effect test temperature on reference temperature (T_0), a series of experiment on standard 1T TPB specimen is performed at temperature of -100°C , -110°C , -120°C , -130°C , -140°C in accordance with ASTM standard E1921.

3. To study the Effect of geometry and loading pattern on reference temperature (T_0) the TPB specimen results are compared with the results of CT specimen of same material.

4. To study the effect of Censor Parameter (M) on reference Temperature T_0, both for TPB and CT specimen.

5. Finite Element Analysis is to be done in order to quantify the constraint effects in light of stress based parameters which are Tri-axiality ratio, Q-parameter and T-Stress.

6. For getting better prediction in lower transition , a Local Approach based micro-mechanical model (Beremin model) is to be used tocapture effect of constraints, which correlates the global parameters J-Integral or K_{JC} with micro mechanism based probability of failure by a stress based term coined as Weibull Stress (σ_W).

7. Calibration of the essential parameters Of Beremin Material model are required for the flawless application of the micro-mechanical model is determined for the material.

8. An effective way of determination of $C_{m,n}$, a parameter which is used to convert the value of Weibull Stress (σ_W) for a certain condition of constraint, loading geometry and temperature to the Predicted value of K_{JC} at the specified condition is to be explored.

9. Effect of test temperature on the calibrated parameters, in the brittle failure dominated regime of Ductile to Brittle Transition is to be studied by introducing a strain correction in the model.

10. In order to transcend the burden of performing a huge number of experiments for effective calibration of the parameters, Monte Carlo simulation is to be investigated as the calibration scheme for the variation of the parameters with temperature .

11. The results of the Monte Carlo simulation are to be compared with the calibrated value obtained from the direct calibration of physical experimental results for two test temperatures, which paved a basis for relaying the predicted calibrated values of the parameters for other temperatures from Monte Carlo simulation in the brittle dominated portion of DBT region.

1.10 Chapter-wise Outline of the thesis.

In **Chapter 1**, review of previous studies was undertaken and the research gaps were identified, which sets a framework for the present investigations

The **second chapter** deals with

- Experimental determination of fracture toughness at low temperatures
- Determination of Master curve and Reference temperature T_0 for different thickness and a/W ratio.
- The constraint effect (like thickness and a/w ratio) on the reference temperature T_0 of TPB specimen.
- The effect of test temperature on the reference temperature T_0. For TPB specimen.
- The effect of geometry and loading conditions on the reference temperature T_0 , CT and TPB results are compared.
- The effect of Censor Parameter (M) on reference Temperature T_0, both for TPB and CT specimen.
- Tri axiality ratio is calculated using finite element analysis for all the tested TPB samples and its variation is studied with reference temperature T_0 for different thickness and a/w ratios, with a frame of mind that whether Tri axiality ratio can be an co related with reference temperature T_0, so that by simply doing a finite element analysis on a given model we could find out the T_0.

Third chapter deals with Variation of reference temperature (T_0) with a/W ratio and thickness of the specimen which are observed from experimental results and discussed in second chapter. In order to analyze this variation of T_0 some finite element parameters are put forward to account for this variation. The parameters which are nurtured in this work are T stress, Q-Stress and Triaxiality ratio. An attempt has been put forward to predict T_0 with the help of these parameters with respect to a reference specimen with a/W ratio 0.5 and thickness of 25 mm for TPB specimen. Predicted results are compared with experimental observations.

In **the fourth chapter**, a large number of fracture tests (38 in number) are performed at (-110^0 C) on a variety of TPB specimens to determine the effect of thickness and a/W ratio on Reference temperature T_0. FE simulation of all the fracture tests are done and Weibull stresses are computed at failure load with an assumed Weibull modulus (m). Then Weibull modulus (m) and Scaling parameter (σ_u) and C_{mn} are finalized iteratively using linear regression analysis between failure probability measured from experimental results and Weibull stress obtained from FE analysis. Fracture test results of 38 TPB specimens of different thickness and a/w ratio at a fixed temperature of -110^0C have been used in regression analysis to capture the probabilistic nature of the failure process and to extract the material parameters valid over a wide range of thickness and a/w ratio. The value of Beremin coefficient $C_{m,n}$ is also determined from fracture test results using Beremin formulation. $C_{m,n}$ is actually a function of Weibull modulus (m) and Power Law Hardening (n) for a given material. Variation of the Beremin parameters (m & σ_u) with temperature are studied . A series of 30 fracture toughness data of standard 1T TPB specimen are generated from experiment for each temperature -100°C and -130°C, then calibrating the parameters with linear regression analysis.

In the **Fifth chapter** variation of the Beremin parameters with temperature is studied using Modified Beremin model where strain correction is imposed in the Beremin model formulation. The variation of the parameters with temperature is studied from a set of six number of tests performed at a temperature of -110°C in order to determine Reference Temperature (T_0) and Master Curve for the entire DBT region as per the ASTM Standard E1921. Monte Carlo simulation was employed to produce a large number of 1T TPB (Three Point Bending specimen) fracture toughness data randomly drawn from the scatter band obtained from the Master curve, at the different temperatures of interest in order to determine Beremin model parameters at different temperatures. The results of 'm' & 'σ_u' obtained for temperatures -100°C,-110°C,-120°C,-130°C and -140°C. The results are compared with direct calibration procedure obtained by generating a series of 30 fracture toughness data set from experiment for each temperature -100°C and -130°C methods and a matching trend is

observed, which provides a basis for relaying on the prediction of ‘m’ & ‘ σ_u’ from the Monte Carlo simulation , for other temperatures.

In the **Sixth and last** chapter, assessment of the targeted objective and its appraisal from overall observations and conclusions are compiled including the work which could not be attained in this work.

Chapter 2

Effect of constraints on Reference Temperature (T_0) for 20MnMoNi55 steel from Experimental Results

Outline of the chapter

*This chapter focuses on the determination of Reference Temperature (T_0) for the special nuclear grade steel 20MnMoNi55 from Three Point Bending specimen and then study the effect of constraint, on it. To characterize the fracture properties of the material first tensile tests are performed to determine the tensile properties at different temperature in the range from 22°C to –140°C on ASTM E8 standard round bar tensile specimen using Bluehill software .Then fracture toughness tests are performed as per ASTM E399–90 standard to determine Reference Temperature (T_0) for (Three Point Bending)TPB specimen of different thickness (10mm,12mm,15mm,20mm,25mm,30mm) and different a/W (*Crack length-to-width ratio) of the specimen *ratio (0.4,0.45,0.5,0.55,0.6,0.65) at a fixed temperature -110°C in order to quantify the effect of thickness and a/W ratio on Reference Temperature (T_0). Then fracture toughness tests are performed to determine Reference Temperature (T_0) for a standard TPB specimen at different test temperatures such as -100°C,-110°C, -120°C ,-130°C, -140°C to study the effect of Test Temperature on Reference Temperature (T_0). To introduce sharp crack, fatigue pre–cracking was done on standard TPB and CT specimens at room temperature in the range of a/W = 0.40–0.65 according to ASTM E647 standard on servo–hydraulic universal testing machine using commercial da/dN fatigue crack propagating software. Now to determine J–integral values, the pre–cracked TPB and CT specimens are tested in Universal testing machine at different temperatures range as discussed using J_{IC} software according to ASTM E1820 standard. All the test results are discussed in details from different respect.* **In order to study the effect of geometry and loading pattern on Reference Temperature**

(T_0) results of TPB specimen are compared to that of Compact Tension specimen. The effect of Censor Parameter (M) on reference Temperature T_0, both for TPB and CT specimen are also studied and a basis for selection of suitable M is proposed.

2.1. Introduction:

Wallin [12] described the cleavage fracture toughness behaviour in the ductile -to-brittle transition (DBT) range of ferritic steels. The master curve together with an ASTM E1921 reference temperature (T_0) value defines the complete transition fracture toughness curve in a manner appropriate for use in both probabilistic and deterministic analysis. The master curve methodology [78] is based on a cleavage fracture model that assumes randomly distributed fracture initiators in a macroscopically homogeneous matrix. The transition curve definition for ferritic steels, as specified in ASTM E1921, was originally derived in 1991 from data measured on various quenched and tempered structural steels. After the statistical thickness correction of these data, which had been measured with different size specimens, the curve shape was determined from the maximum likelihood fit to the data. Then it was proposed for a universal functional form of the temperature dependence of fracture toughness in the transition region and afterwards it was included in ASTM E1921.The master curve defines both the variation of the median fracture toughness with temperature and the scatter of fracture toughness about this median value. For all the ferritic steels this curve is common and varies only in the location along temperature axis. In the master curve method, a fracture toughness curve is characterised by a single parameter T_0 (temperature at which the median fracture toughness for one inch thick compact tension (1T–TPB) fracture toughness specimen equals 100 MPa$\sqrt{m}$. that establishes the position of the master curve on temperature scale. Hence for any ferritic steel T_0 is only the parameter to characterize fracture toughness in Transition temperatures.

The basis of the master curve approach is a three parameter Weibull model in which the relationship between fracture toughness of a specimen K_{JC} and the cumulative probability failure P_f [12] as given below,

$$p_f = 1 - \exp\left[-\left(\frac{K_{JC} - K_{\min}}{K_0 - K_{\min}} \right)^4 \right] \qquad (2.1)$$

Where K_{JC} is the fracture toughness corresponding to P_f, K_0 is the fracture toughness corresponding to 63.2% cumulative probability and K_{min} is the lower bound fracture toughness. K_0 is a material property to be determined from experiment and K_{min} is taken to be 20 MPa√m for all the ferritic RPV material as suggested by Wallin and International Atomic Energy Agency [79]

Censoring is performed with respect to excessive ductile tearing prior to cleavage. The K_{JC} limit is calculated according to the ASTM E1921-02 [80] standard as given below

$$K_{JC(\lim it)} = \sqrt{\left[\frac{E b_0 \sigma_{ys}}{M\left(1-\nu^2\right)} \right]} \qquad (2.2)$$

2.2. Size Effects and Transition Temperature

Master Curve considers a three-parameter Weibull model which defines the relationship between K_{JC} and the cumulative probability of failure, P_f as shown in equation. 2.1. The statistical weakest link theory is used to model the effect of specimen size on the probability of failure in the transition range. Fracture toughness determined for a specimen of thickness other than 25 mm, the measured K_{JC} value is to be adjusted for thickness correction as

$$K_{JC(1T)} = K_{\min} + \left[K_{JC} - K_{\min} \right] \left(\frac{B_0}{B_{1T}} \right)^4 \qquad (2.3)$$

where B_0 is the thickness of the tested specimen (side grooves are not considered); B_{1T} is the thickness B = 1T (25.4 mm); $K_{JC\ (1T)}$ is the fracture toughness of a specimen with a thickness of B = 1T; $KJC_{(}X)$ is the fracture toughness of the tested specimen; K_{min} is the lower bound fracture toughness fixed at 20 MPa√m in ASTM E 1921-02.

The lower validity criterion for the Weibull statistics, on which the Master Curve is based, is 50 MPa√m. The K_{JC} values below 50 MPa√m need not be size adjusted.

2.3. Determination of T_0

The value of T_0 is calculated after inclusion of all valid and censored values according to the single or multi temperature methods as discussed below.

2.3.1. Single Temperature Evaluation:[79]

Evaluation of the scale parameter, K_0, is performed according to equation. 2.4 and the fracture toughness for a median (50%) cumulative probability of fracture, K_{JC} (med), according to equation. 2.5 of a data set at the applied test temperature:

$$K_0 = \left[\sum_{i=1}^{N} \frac{\left(K_{JC(i)} - K_{\min} \right)}{N} \right]^{1/4} + K_{\min} \qquad (2.4)$$

Where, K_{JC} (i) is the individual K_{JC} (1T) value and N is the number of K_{JC} values. The term N is replaced by the number of valid K_{JC} values, r, if censored K_{JC} values are included in the calculation:

$$K_{JC(med)} = K_{\min} + \left(K_0 - K_{\min} \right) \left(\ln 2 \right)^{1/4} \qquad (2.5)$$

The K_{JC} (med) value determined for the data set at test temperature is used to calculate T_0 at K_{JC} (med) of 100 MPa√m by equation. **2.5**:

$$T_0 = T - \left(\frac{1}{0.019} \right) \ln \left(\frac{K_{JC(med)} - 30}{70} \right) \qquad (2.6)$$

2.3.2. Multi temperature evaluation:[80]

The multi temperature option of ASTM E 1921-02 represents a tool for the determination of T_0 with K_{JC} values distributed over a restricted temperature range, namely, $T_0 \pm 50^oC$. The value T_0 can be evaluated by an iterative solution of Eq. (**2.7**):

$$\sum_{i=1}^{N}\frac{\delta_i \exp\left[0.019\left(T_i - T_0\right)\right]}{11+77\exp\left[0.019\left(T_i - T_0\right)\right]} - \sum_{i=1}^{N}\frac{\left(K_{JC(i)} - K_{\min}\right)^4 \exp\left[0.019\left(T_i - T_0\right)\right]}{\left\{11+77\exp\left[0.019\left(T_i - T_0\right)\right]\right\}^5} = 0 \quad (2.7)$$

Where Ti is the test temperature corresponding to $K_{Jc(i)}$; δi is the censoring parameter: δi= 1 if the $K_{JC(i)}$ datum is valid (equation. 2.2) or δi = 0 if the $K_{JC(i)}$ datum is not valid and censored.

2.4. Establishment of the Transition Temperature Curve (Master Curve) and Tolerance Bounds

Values of K_{JC} tend to conform to a common toughness versus temperature curve shape expressed by Eq. (2.2). Both upper and lower tolerance bounds can be calculated using Eq. 2.8

$$K_{JC(0.xx)} = 20 + \left[\ln\left(\frac{1}{1-0.xx}\right)\right]^{1/4}\left\{11+77\exp\left[0.019\left(T_i - T_0\right)\right]\right\} \qquad (2.8)$$

Where 0.xx represents the cumulative probability level.

2.5. Material and Experiment Details

2.5.1. Material

The material studied is German steel, used in reactor pressure vessel of Indian PHWR and designated as 20MnMoNi55. The material used in this investigation has received from Bhabha Atomic Research Centre, Mumbai, India. The steel was received in the form of rectangular block. The specimens were made from this block to determine the fracture toughness of the selected steel using J-integral analysis and the Master Curve methodology, to understand the fracture behaviour of the steel. The RPV material properties during operation are defined by their initial values, material type, chemical composition and by operating stressors, mainly operating temperature and neutron influence. Chemical composition of 20MnMoNi55 is shown in Table 2.1**.**

Table 2.1 Chemical Composition of 20MnMoNi55

Name of element	C	Si	Mn	P	S	Al	Ni	Mo	Cr	Nb
%age composition (in wt.)	0.20	0.24	1.38	0.011	0.005	0.068	0.52	0.30	0.06	0.032

2.5.2. Tensile Testing

Tensile tests were done at 22^0C, 0^0C, -20^0C, -40^0C, -60^0C, -80^0C, -100^0C, -120^0C and -140^0C by the previous research fellow in our laboratory for the same material [79,80].The tensile properties for the material at different temperatures are shown in Table 2.2. All data regarding yield strength, ultimate strength and modulus of rigidity have been used as input to determine fracture toughness and reference index temperature.

Table 2.2 Tensile Properties Of 20MnMoNi55 steel different temperatures

temperatures

Temperature (^{0}C)	Modulus of Elasticity (Mpa)	Yield Strength (Mpa)	Ultimate Strength (Mpa)
22	1.99374E+5	488.13	628.25
0	1.92E+5	501.82	647.77
-20	2.3E+5	506.87	664.84
-40	2.02271E+5	518.46	681.51
-60	1.80E+5	538.02	708.92
-80	2.02E+5	562.22	736
-100	1.98E+5	593.43	760.49
-120	1.80E+5	667.06	813.66
-140	1.81E+5	723.47	856.84

2.5.3. Tensile Test Specimens

Round specimens of diameter 6.5mm and gauge length 30mm were fabricated for tensile tests following the ASTM standard E8 from the received blocks. The nominal dimensions of the tensile specimens are shown in Fig.2.1. Specimens were threaded at both ends.

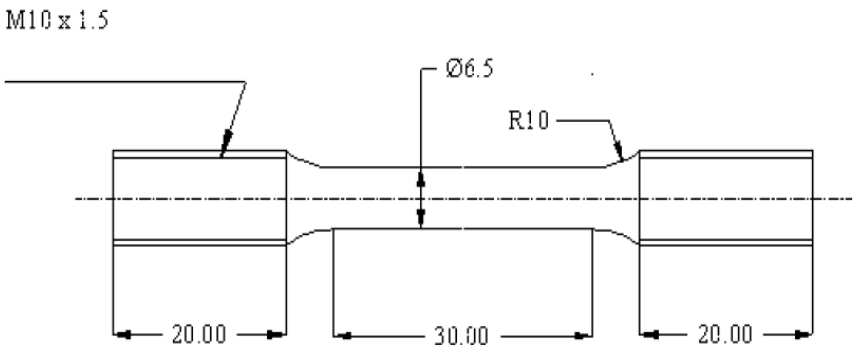

Fig.2.1: Typical round tensile test specimen.

2.5.4. Fatigue Pre-cracking

The fracture toughness tests in this investigation were planned on Three Point Bending (TPB) specimens in L-T orientation as shown in figure 2.2. Standard 1T TPB specimens were machined following the guidelines of ASTM E 399-90. The designed dimensions of the specimens were; thickness (B) = 30mm, 25mm, 20mm, 15mm, 12mm,10mm and width (W) = 25mm which is constant for all the specimen tested and machined notch length (aN) = 7.3mm,10mm and 14mm to provide different a/w ratio of 0.35,0.4,0.45,0.5,0.55,0.6,0.65. Fatigue pre-cracking of the TPB specimens was carried out at room temperature at constant ΔK mode as described in ASTM standard E 647 on servo hydraulic INSTRON UTM (Universal Testing Machine) with 8800 controller having 100 KN grip capacity using a commercial da/dN fatigue crack propagating software supplied by INSTRON Ltd U.K.. The crack lengths were measured by compliance technique using a COD gauge of 10mm gauge length mounted on the load line of the specimen. The gauge was connected to STRAIN 1 connector. The software permitted on-line monitoring of the crack length (a), stress intensity factor range (ΔK) and the crack growth rate per cycle, da/dN. All pre-cracking experiments were carried out at a stress ratio of R = 0.1 using an initial frequency of 10Hz and with a constant ΔK is 30 MPa√m. Later the frequency was increased to 15 Hz.

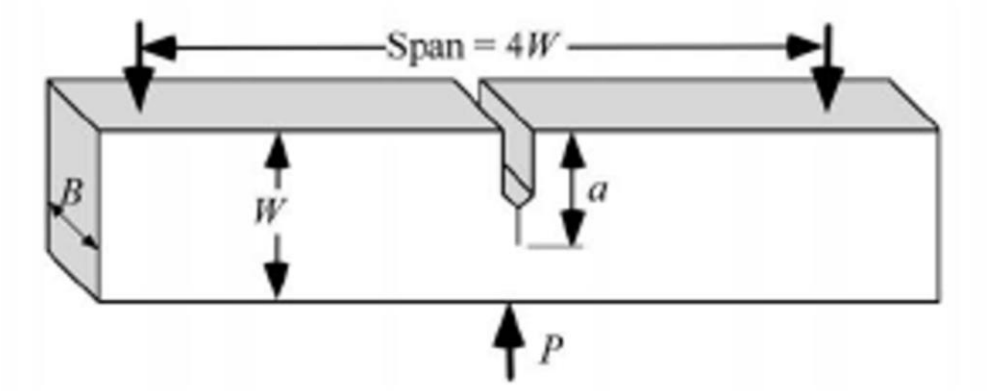

Fig.2.2: 1T TPB specimen

2.5.5. Fracture Test

The estimation of J-integral values of the fabricated specimens were carried out using an INSTRON UTM (Universal Testing Machine) with 8800 controller with 100 KN grip capacity as shown in figure 2.4. Tests were done at different temperatures ranging from 22 ^{0}C to – 140 ^{0}C.

The Instron FAST TRACK J_{IC} Fracture Toughness Program was used to determine the value of J integral. This programme evaluate Fracture Toughness on metallic materials in accordance with the American Society for Testing and Materials (ASTM) Standard test method E813. The method is applied specifically to specimens that have notches or flaws that are sharpened with fatigue cracks. The loading rate was slow, and cracking caused by environmental factors was considered negligible.

The JIC program allows various ways to determine crack growth. Crack growth is usually determined by unloading compliance, but other methods, such as DC Potential Drop (DCPD), can be used. In our case the single specimen unloading compliance technique was used for evaluation of J-integral fracture toughness. In this method the crack lengths are determined from elastic unloading compliance measurements. This is done by carrying out a series of sequential unloading and reloading during the test, the interruptions being made in a manner that these are almost equally spaced along the load versus displacement record. A typical load displacement plot for a specimen tested at room temperature is shown in Fig.2.3

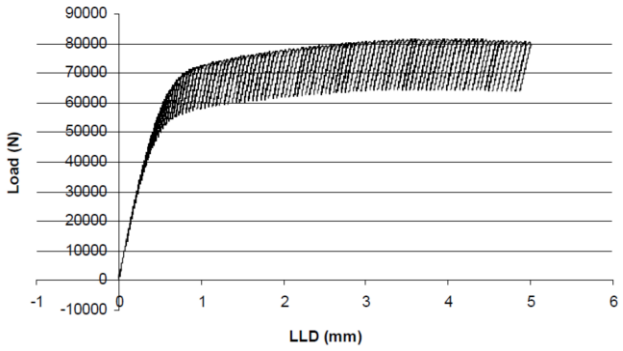

Fig 2.3: Experimental Load – LLD curve of TPB specimen at 22 ^{0}C

The objective of the tests was to determine the value of J_{IC} in case of ductile fracture and J_C in case of cleavage fracture. The method uses pre cracked TPB specimen and determines J as a function of crack growth. Load versus load-line displacement is recorded digitally on a graph screen. The J-integral is determined and plotted against physical crack growth (Δa). These data reflect the material's resistance to crack growth. The J versus crack growth behaviour is approximated with a best-fit power law relationship.

2.5.6. Test procedure

Operation of the J_{IC} test consists of preparing the testing system, entering Parameters into the test programme, running the test programme and retrieving, storing and displaying test results.

Steps that were followed to run the tests were-

(1) Mounting the Cryo-chamber (Model No.-3119-408, Serial No.-0005120) securely in the test position.

(2) Mounting pull rods and adapters.

(3) Connecting COD gauge to the STRAIN 1 connector on the testing system console.

(4) Calibration of all transducer channels.

(5) Setting electronic limits on all three mode control channels.

(6) Turning on the hydraulic system.

(7) Installing a compact tension specimen into the grips.

(8) Mounting the COD gauge on the specimen.

(9) Closing the door of the chamber and cooling it down to the desired temperature.

(10) Entering information and making choices in the appropriate fields on the Main Set up screen.

(11) Allowing the chamber to equilibrate at the set temperature for 30 minutes

(12) Clicking on the START button in the Test Control section.

Steps 1 and 9 were omitted for the tests conducted at room temperature.

2.5.7. Test Set Up Screen

Fig 2.4 Experimental arrangement for ambient temperature J_{IC} tests

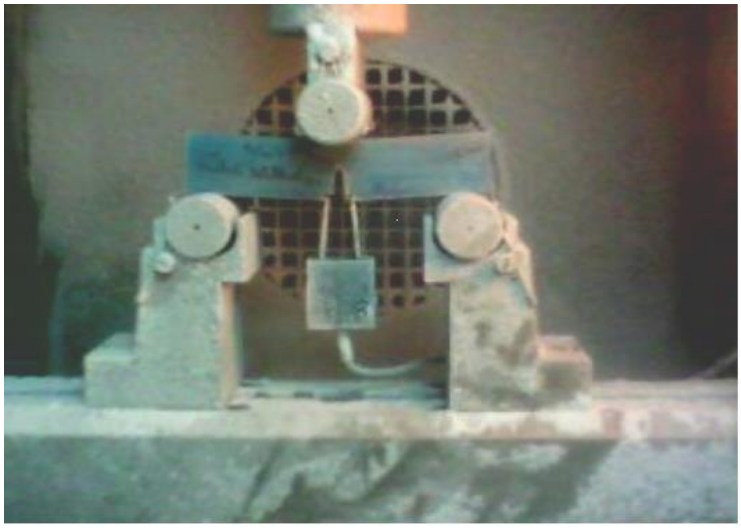

Fig.2.5 Experimental arrangement for cold temperature J_{IC} tests

2.6. Constraint effect on Reference temperature (T_0)

Dependence of Master Curve and reference temperature (T_0) on various constraint levels is explored in this part of the thesis .The schematic diagram representing the effect of various constraints are as shown in the following figure.2.6

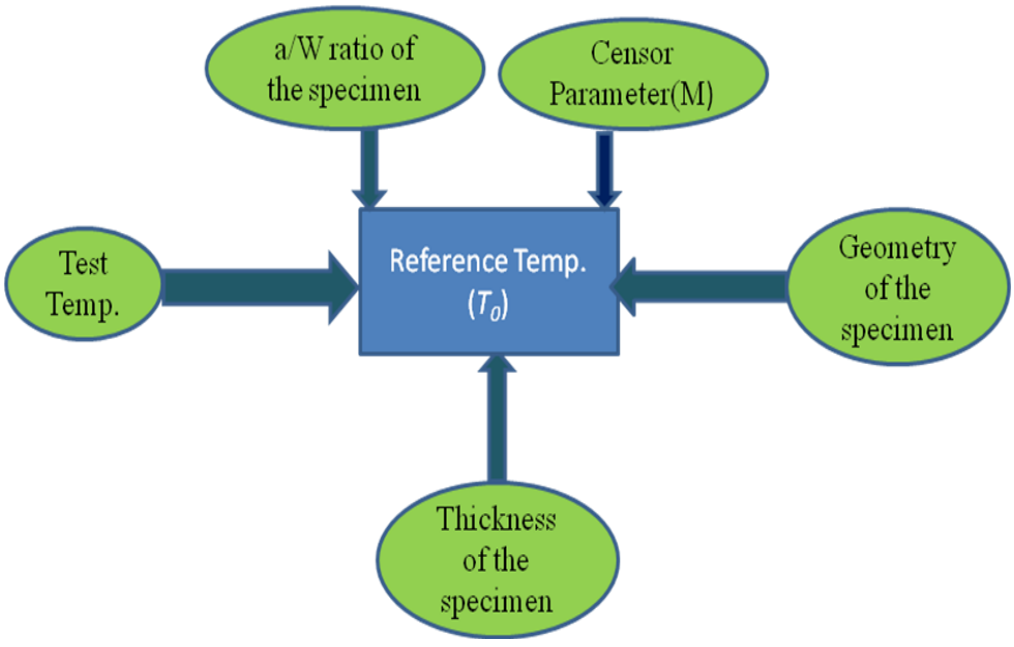

Fig.2.6. Effect of various constraints on Reference Temperature (T_0)

2.7. Results and Discussions

In order to investigate the effect of various constraints on Reference Temperature (T_0) a huge number of experiments are performed at different temperatures in Ductile to Brittle transition region. The detailed values of J_{1C} obtained are shown in the Table below.2.3

Table 2.3. The following Table shows the data of the entire Test matrix

Sl No.	Specimen Id.	Test Temp	Thick-ness (mm)	a/w	J_{1C} kJ/m^2	K1c MPa.m$^{0.5}$	Failure Load, kN	Failure Load Line Disp. LLD (mm)	Failure Crack Tip Opening Disp. COD(mm)
1.	TPB_25_100_8_p45	-110	8	0.45	617.38	368.32	13.95	2.83	1.844069
2.	TPB_25_100_8_p4	-110	8	0.40	151.33	182.37	14.57	0.96	0.485428
3.	TPB_25_100_8_p65	-110	8	0.65	187.69	203.1	14.15	1.53	1.209566
4.	TPB_25_100_10_p4_1	-110	10	0.40	290.5	252.7	19.91	1.55	0.849054
5.	TPB_25_100_10_p4_2	-110	10	0.40	75.84	129.1	17.9	0.69	0.236770
6.	TPB_25_100_10_p5	-110	10	0.50	336.8	272.1	13.93	1.94	1.231514
7.	TPB_25_100_10_p45_1	-110	10	0.45	77.44	130.46	15	0.678	0.292588
8.	TPB_25_100_p45_10_2	-110	10	0.45	146.34	179.35	16.99	0.99	0.497563
9.	TPB_25_100_10_p55	-110	10	0.55	44.28	98.65	9.931	0.537	0.285994
10.	TPB_25_100_12_p4	-110	12	0.40	449.28	314.23	26	2.14	1.199945
11.	TPB_25_100_12_p45	-110	12	0.45	153.25	183.53	19	1.0279	0.507744
12.	TPB_25_100_12_p5	-110	12	0.50	199.89	209.6	16.12	1.36	0.783656
13.	TPB_25_100_12_p6_1	-110	12	0.60	105.08	151.97	10.31	0.95	0.61
14.	TPB_25_100_12_p6_2	-110	12	0.60	65.5	120	9.722	0.69	0.42
15.	TPB_25_100_12_p65	-110	12	0.65	92.7	142.74	8.117	0.92	0.63
16.	TPB_25_100_15_p35	-110	15	0.35	314.10	262.74	36.51	1.645	0.63
17.	TPB_25_100_15_p4	-110	15	0.40	114.39	158.56	28.78	0.887	0.325
18.	TPB_25_100_15_p45	-110	15	0.45	182.47	200.26	25.98	1.167	0.579
19.	TPB_25_100_15_p5	-110	15	0.50	210.70	214.83	20.78	1.37	0.748
20.	TPB_25_100_15_p6	-110	15	0.60	191.55	205.2	9.89	1.676	1.257
21.	TPB_25_100_15_p65	-110	15	0.65	138.92	174.73	10.42	1.64	0.71
22.	TPB_25_100_20_p4	-110	20	0.40	78.398	131.26	30.77	0.75	0.257

23.	TPB_25_100_20_p45	-110	20	0.45	282.12	249	25.6	1.93	1.13
24.	TPB_25_100_20_p5	-110	20	0.50	224.58	222.17	21.64	1.6785	1.0142
25.	TPB_25_100_20_p55	-110	20	0.55	206.76	213.14	23.35	1.446	0.839
26.	TPB_25_100_20_p6	-110	20	0.60	170.27	193.45	12.88	1.5469	1.0915
27.	TPB_25_100_20_p65	-110	20	0.65	153.70	183.79	13.57	1.38	0.96
28.	TPB_25_100_20_p65	-110	20	0.65	121.38	163.33	13.49	1.1873	0.7819
29.	TPB_25_100_20_p65	-110	20	0.65	429.52	307.25	31.63	2.43	1.42
30.	TPB_25_100_25_p4	-110	25	0.40	171.91	196.43	50.79	1.25	0.428
31.	TPB_25_100_25_p45	-110	25	0.45	150.71	183.92	40.88	1.0859	0.401516
32.	TPB_25_100_25_p5	-110	25	0.50	108.33	155.93	34.56	0.9537	0.404
33.	TPB_25_100_25_p55	-110	25	0.55	171.52	196.20	30.37	1.4221	0.687282
34.	TPB_25_100_25_p6	-110	25	0.60	281.69	248.82	24.32	2.0821	1.282925
35.	TPB_25_100_25_p65	-110	25	0.65	140.1	175.48	16.98	1.2974	0.842725
36.	TPB_25_100_30_p5	-110	30	0.50	288.51	251.8	43.1	1.8398	0.985668
37.	TPB_25_100_30_p55	-110	30	0.55	103.08	150.52	32.6	0.96	0.41748
38.	TPB_25_100_30_p6	-110	30	0.60	88.174	139.2	23.01	0.9262	0.501256
39.	TPB_25_100_30_p65	-110	30	0.65	99.974	148.23	21.22	1.394	0.685701
40.	TPB_25_100_25_p45	-100	25	0.45	378.78	291.57	44.96	2.198	1.147134
41.	TPB_25_100_25_p45	-120	25	0.45	112.36	183.92	41.29	0.9433	0.3
42.	TPB_25_100_25_p45	-90	25	0.35	794.34	422.23	69.84	3	1.4
43.	TPB_25_100_25_p35	-120	25	0.35	221.34	222.88	64.97	1.6104	0.516
44.	TPB_25_100_25_p35	-130	25	0.35	89.86	142	52.91	0.969	0.18323
45.	TPB_25_100_25_p35	-130	25	0.35	136.5	173.2	62.9	1.179	0.267
46.	TPB_25_100_25_p4	-80	25	0.40	49.83	105.75	32.49	0.669	0.159
47.	TPB_25_100_25_p4	-140	25	0.40	75.24	129.95	43.91	0.8576	0.198843
48.	TPB_25_100_25_p5	-80	25	0.50	475.78	326.78	37.99	2.2003	1.351173
49.	TPB_25_100_25_p5	-90	25	0.50	573.43	358.75	39.60	3.1886	2.1
50.	TPB_25_100_25_p5	-100	25	0.50	488.87	331.24	38.99	2.7198	1.62171
51.	TPB_25_100_25_p5	-140	25	0.50	68.972	124.42	32.89	0.7921	0.276
52.	TPB_25_100_25_p5	-80	25	0.50	733.38	401.47	40.36	3.5275	2.224668
53.	TPB_25_100_25_p5	-100	25	0.50	463.19	319.1	37.02	2.7447	1.71379
54.	TPB_25_100_25_p5	-100	25	0.50	518.09	337.44	38.69	2.8321	1.699799
55.	TPB_25_100_25_p55	-100	25	0.50	337.45	272.33	37.57	2.2173	1.271069

56.	TPB_25_100_25_p55	-120	25	0.50	129.34	168.6	34.97	1	0.431216
57.	TPB_25_100_25_p55	-130	25	0.50	54	108.94	28.94	0.693	0.239014
58.	TPB_25_100_25_p5	-100	25	0.55	218.37	221.38	28.83	1.612	0.929027
59.	TPB_25_100_25_p6	-120	25	0.55	119.91	164.05	29.42	0.9991	0.459387
60.	TPB_25_100_25_p55	-120	25	0.55	173.82	197.52	31.28	1.2736	0.6784
61.	TPB_25_100_25_p55	-130	25	0.55	81.425	135.18	30.17	0.7949	0.341126
62.	TPB_25_100_25_p55	-140	25	0.55	57.68	113.78	26.05	0.6562	0.2567
63.	TPB_25_100_25_p6	-100	25	0.60	417.87	306.25	26	2.6914	1.818475
64.	TPB_25_100_25_p6	-120	25	0.60	82.58	136.14	21.87	0.9087	0.433935
65.	TPB_25_100_25_p6	-130	25	0.60	73.34	128.3	23.78	0.75	0.378
66.	TPB_25_100_25_p6	-130	25	0.60	43.12	98.37	18.75	0.7434	0.2659
67.	TPB_25_100_25_p55	-140	25	0.60	37	91.128	11.74	0.6231	0.260609

2.7.1 Steps for calculation of T_0 for TPB specimen by single temperature method at test temperature -110°C

Step 1: At -110°C the J_{1C} [kJ/m^2] values from experiments are 167.9186, 171.525, 150.7126, 127.6622, 171.9148, 108.3349, 281.699, and 140.12 .These values must be converted to K_{1c} values with the help of the given formula

$$K_{1C} = \sqrt{\frac{J_{1c} x E}{1-\nu^2}} = \sqrt{\frac{167.916x10^3 x210x10^9}{1-0.3^2}} = 196849806.1 \quad Pa\sqrt{m}$$

The k_{1c} values are 196.85, 198.95, 186.493, 171.641, 199.179, 158.115, 248.8, and 175.4868

Step 2: The values of K_{1C} obtained from experiment should be censored with

$$K_{JC(Limit)} = \sqrt{\frac{E.b_0.\sigma_{YS}}{M(1-\nu^2)}} = \sqrt{\frac{210x10^9 x0.025x631.83x10^6}{30(1-0.3^2)}} = 348.577 Mpa\sqrt{m}$$

Step 3: To find K_0

$$K_0 = \left[\sum_{i=1}^{N} \frac{(K_{JC(i)} - K_{\min})^4}{N} \right]^{1/4} + K_{\min}$$

$$= [175.1884]^{1/4} + 20 = 195.1884 MPa\sqrt{m}$$

$$= [175.1884]^{1/4} + 20 = 195.1884 MPa\sqrt{m}$$

Step 4: To find Median Fracture Toughness $K_{JC(Median)}$

$$K_{JC(median)} = K_{\min} + (K_0 - K_{\min})(\ln 2)^{1/4} = 20 + (195.1884 - 20)(\ln 2)^{1/4} = 179.8 MPa\sqrt{m}$$

Step 5: To find reference temperature T_0

$$T_0 = T - \left(\frac{1}{0.019} \right) \ln \left[\frac{K_{JC(median)} - 30}{70} \right]$$

$$T_0 = -110 - \left(\frac{1}{0.019} \right) \ln \left[\frac{179.8 - 30}{70} \right] = -150°C$$

Therefore, for TPB specimen at test temperature T=-110°C; T_0= -150°C

All other T_0 calculations done in the subsequent discussions are in the same way as discussed above.

T_0 calculated from TPB specimen at test temperature T= -110ºC; gives T_0= -147ºC & T_0 calculated for CT specimen at test temperature T= -110ºC; gives T_0= -129ºC

2.7.2. Effect of test temperature on T_0

To study the effect of Test temperature on reference temperature (T_0) more than 6 test are performed on TPB specimen, as per ASTM E1921-02, at different test temperatures starting from -100° to -140°. The results are shown in Table 2.4.The variation of fracture toughness with test temperatures are shown in figure.2.7 and the respective Master curve are shown in Fig.2.8, 2.9 and 2.10. From the book of "An Introduction to the Development and Use of Master Curve Method" by Kim Wallin and his co-workers it is

clearly mentioned in the Chapter 10 "Determination of Reference temperature T_0" as per ASTM E 1921 that the limit of T_0 should be within ±50°C of the test temperature. At test temperatures above T_0 + 50° C problems can come from intrusion of R-curve effects. Weakest link size effects assumed in the use of size correction as given in Equation 1.6 will tend to vanish as both upper shelf and lower shelf test temperatures are approached. Therefore as T_0 calculated from test temperature -100°C gives value of -166°C which is more than the tolerance band of ±50°C , so the T_0 calculated from test temperature -100°C is considered as invalid.

Table: 2.4 *T_0* variations with test Temperature

Test Temp. ºC	T_0 ºC	Remarks
-100	-166	Invalid
-110	-150	Valid
-120	-155	Valid
-130	-160	Valid
-140	-143	Valid

From table 2.4 it is seen that at test temperature of -100 ºC *T_0* calculation is not valid as it violates the limit of T_0 within ±50 ºC of test temperature.

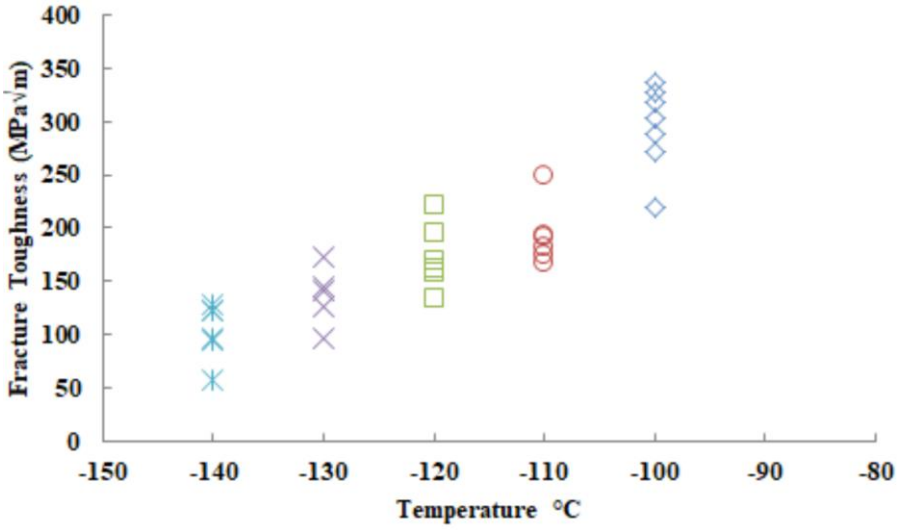

Fig.2.7 K_{JC} variation with Test Temperature

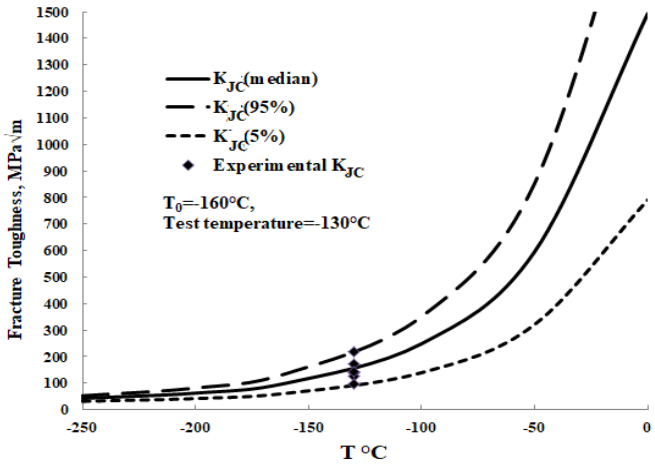

Fig.2.8. Master curve at-130^{0}C

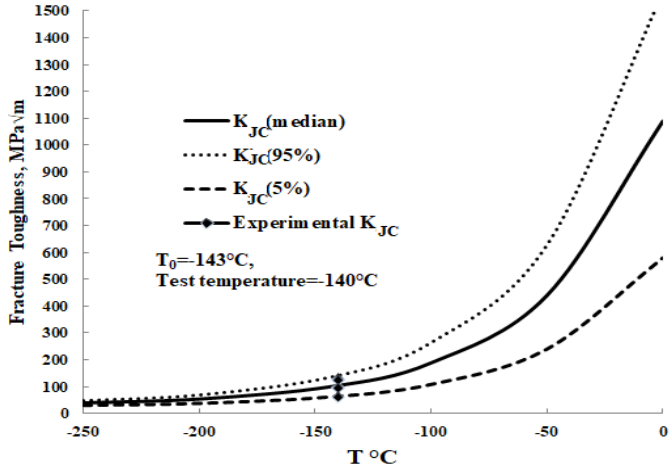

Fig.2.9. Master Curve at -140^{0}C

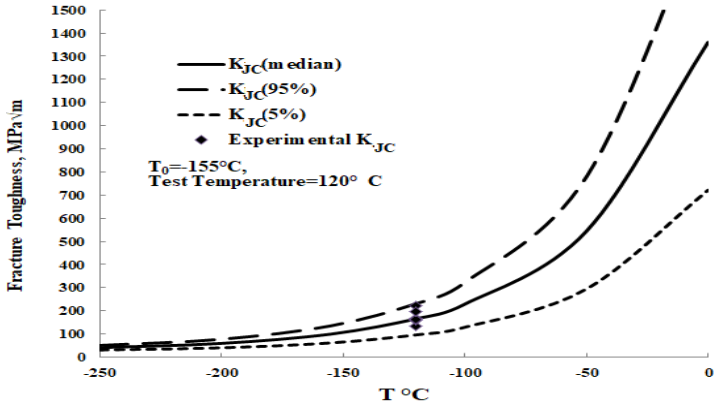

Fig.2.10. Master Curve at -120^{0}C

2.7.3. Effect a/W ratio and thickness of TPB specimen on T_0

Fracture toughness tests for J_{1c} are done on a huge variety of Three Point Bending (TPB) specimens at a fixed test temperature of -110ºC for different thickness of 8 mm, 10 mm, 15 mm, 20 mm, 25 mm, 30 mm, and varying a/w ratio of 0.35,0.4,0.5,0.55,0.6,0.65,0.7 to study the effect of thickness and a/W ratio on T_0 .The following table 2.5 gives the data of the entire test matrix which we have been completed to address the effect on T_0..

Table 2.5. J_{1c} values collected from experiment at a fixed temperature of -110^0C

a/W / ***Thickness***	**0.35**	**0.4**	**0.45**	**0.5**	**0.55**	**0.6**	**0.65**	**0.7**
8mm		151.33	617.24				187.69	
10mm		290.56 75.84	77.44 146.35	336.82	44.28			
12mm		449.283	153.257	199.90		65.55 105.08	92.7	
15mm	314.1	114.39	182.48	210	353.413	191.553	138.92	
20mm		78.39	282.12	224.58	206.71	170.28	518.69 153.7 121.38 429.52	118.33
25mm		171.9148	150.7126	167.9186	127.662	281.699	140.12	
30mm				288.51	103.083 254.54	88.174	99.974	71.94

2.8 Effect of thickness on T_0

For each thickness at least 6 tests of same thickness were performed according to ASTM E1921 to calculate T_0, and thickness correction is imposed to convert it into equivalent thickness of 25 mm. *Variation in* T_0 due to thickness is studied and shown in the following figure 2.11

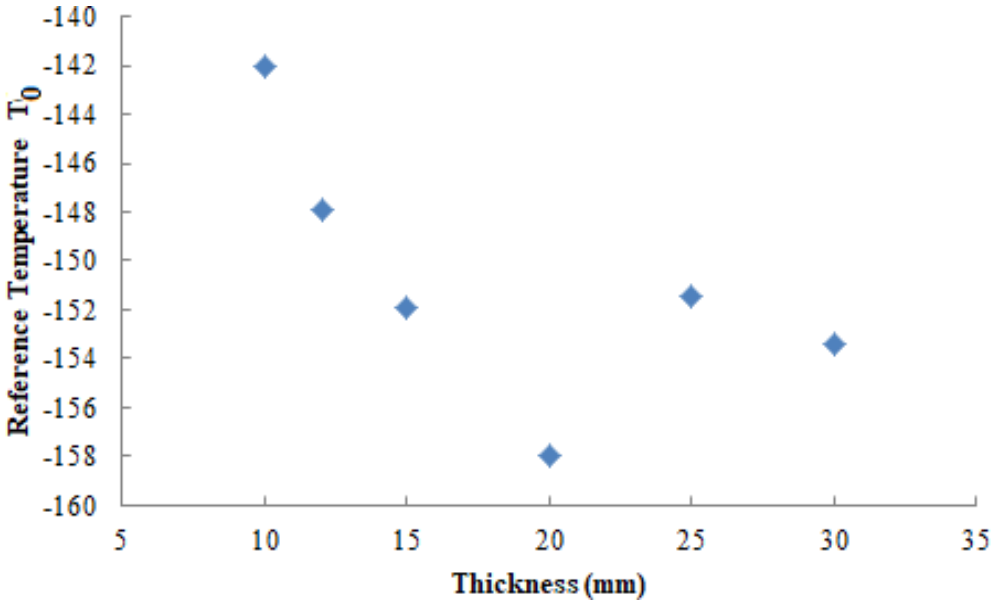

Fig.2.11: Variation of T_0 with Thickness

It is seen that from Fig: 2.11. T_0 varies with thickness even after implementing thickness correction on it.

The following figure 2.12 to 2.16 shows the Master Curve at -110^{0}C for different thickness of TPB specimen

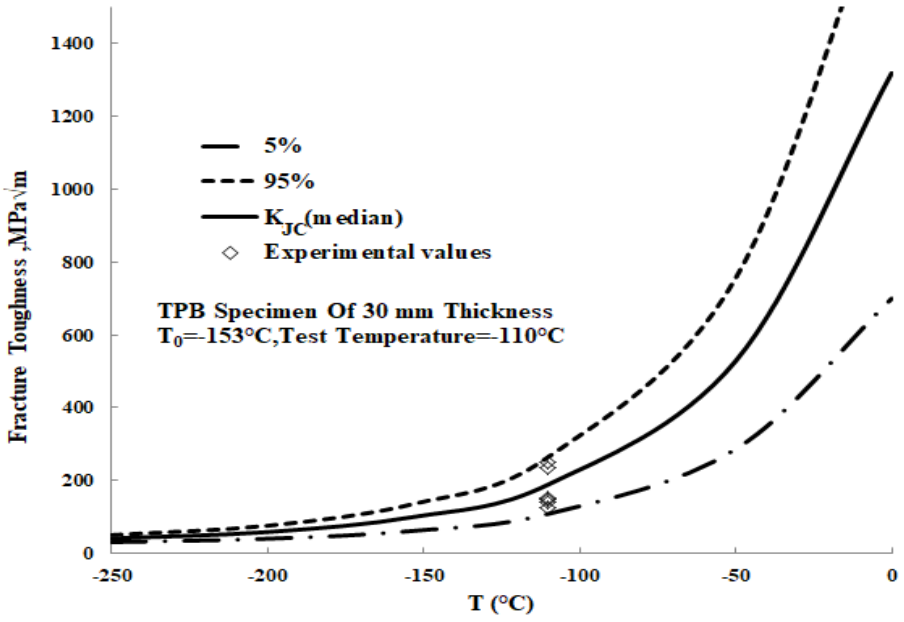

Fig.2.12. Master curve at -110^{0}C for specimen thickness 30 mm

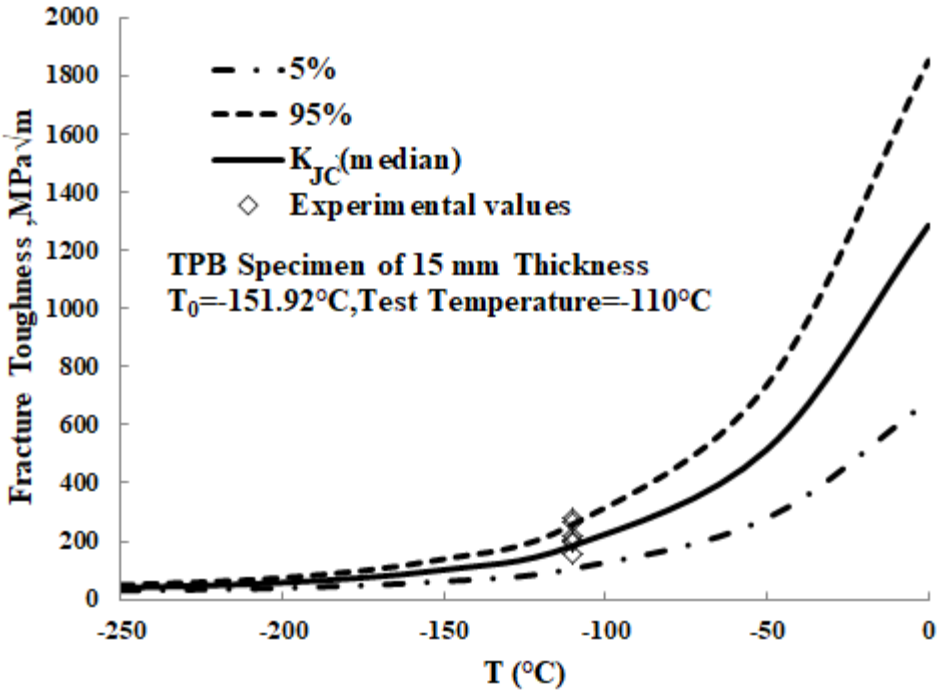

Fig2.13. Master curve at -110^{0}C for specimen thickness 15 mm

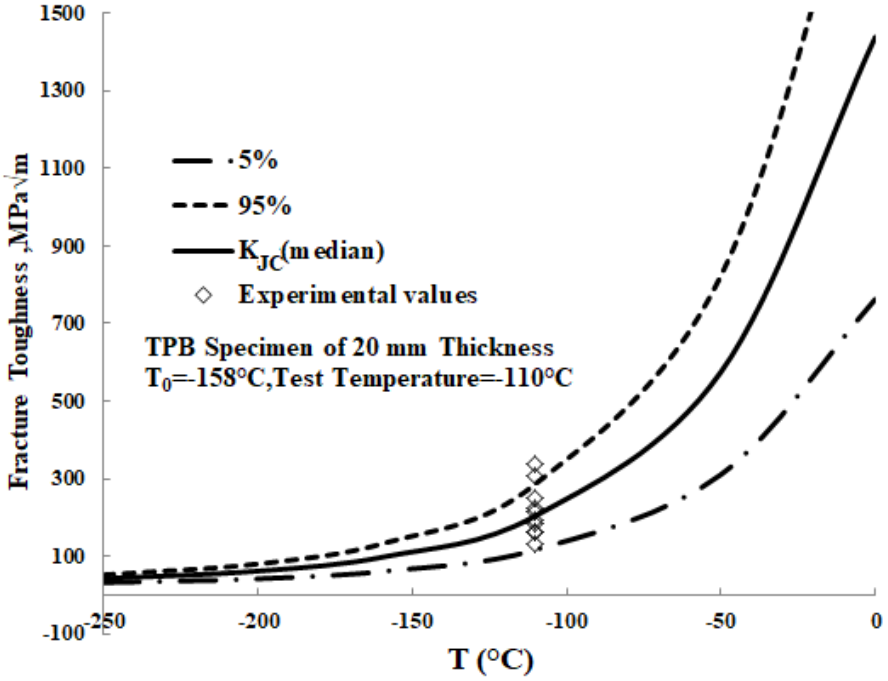

Fig.2.14. Master curve at -110^{0}C for specimen thickness 20 mm

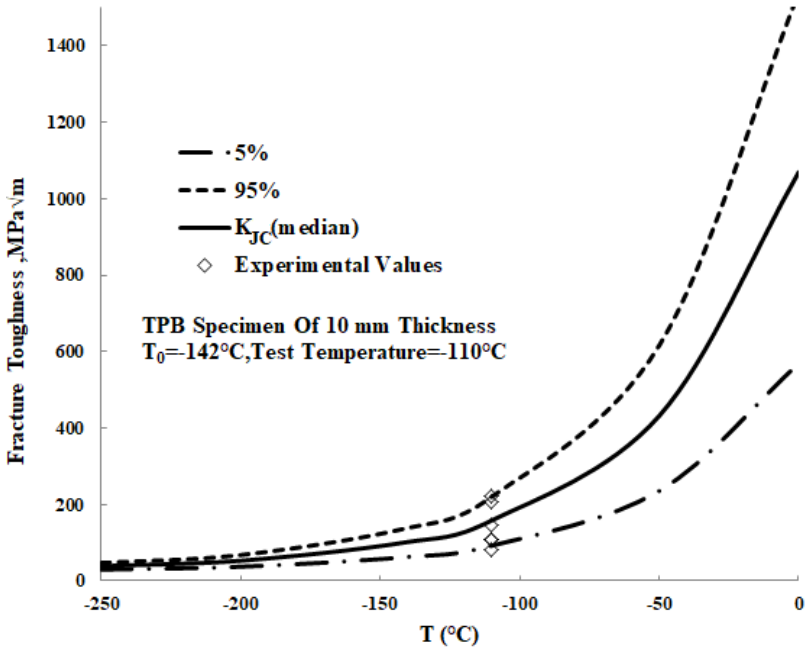

Fig.2.15. Master Curve at -110^{0}C for specimen thickness 10 mm

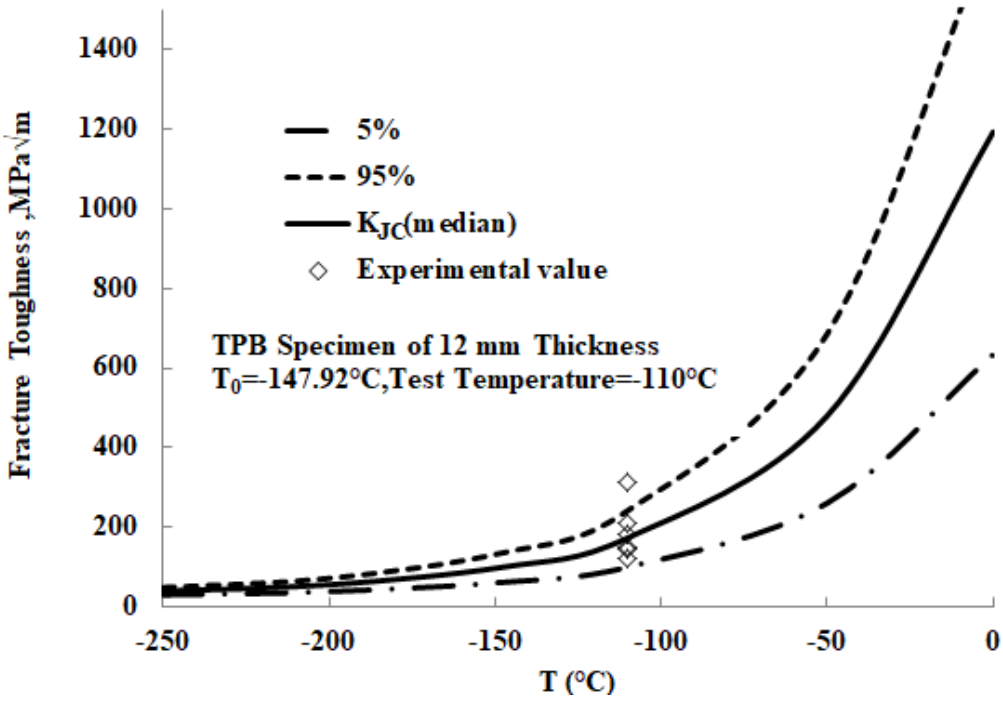

Fig.2.16. Master curve at -110^{0}C for specimen thickness 12 mm

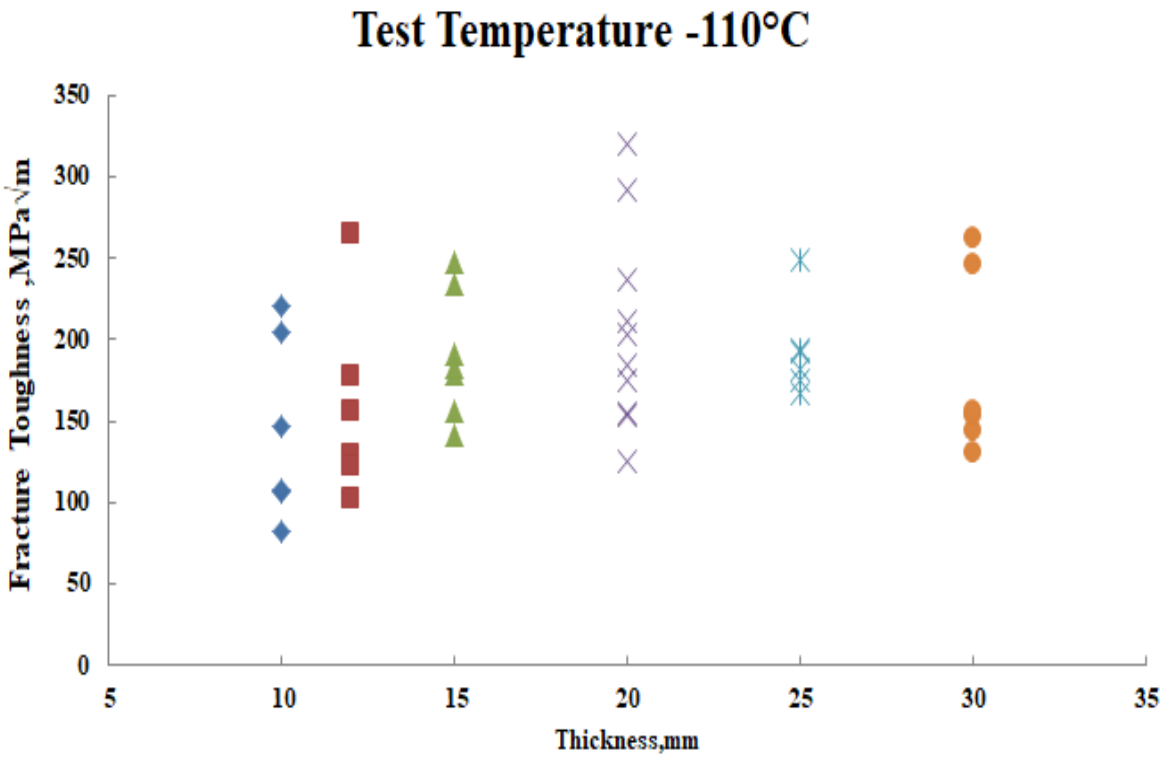

Fig.2.17.K_{1c} variation with thickness

K_{JC} variation with Thickness is shown in the figure 2.17. It is seen that as expected fracture toughness increases with decreasing thickness due to shift plain strain to plain stress condition , but this phenomenon continues only up to 20 mm. After that it is seen that the fracture toughness falls with decreasing thickness and this trend is also described by T.LAnderson while studying the Effect of Thickness on Apparent Fracture Toughness in his Third Edition of Fracture Mechanics, Fundamental and Applications.

2.8.1. Effect of a/W ratio on T_0

For each a/W ratio of TPB specimen at least 6 tests were performed according to ASTM E1921 to calculate T_0,.Effect of T_0 due to variation in a/W is studied and shown in the following diagram 2.18 **.**The master curves are drawn for different a/W ratios, at the Test of -110 ºC and at an equivalent thickness of 25 mm as shown in figure 2.19 to2.23.

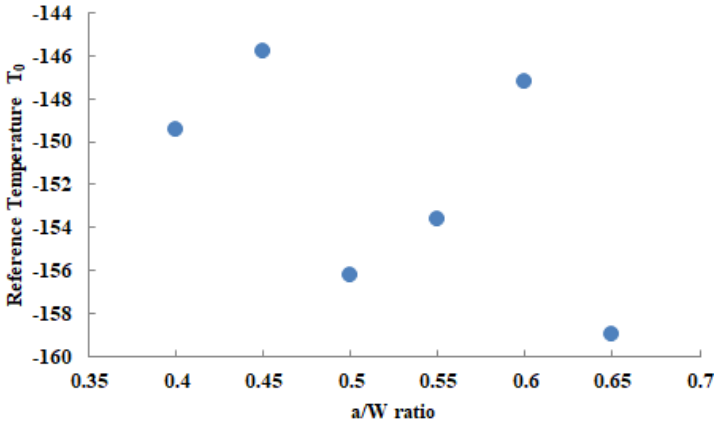

Fig: 2.18 The variation of T_0 with a/w at affixed Test Temperature of -110 ºC

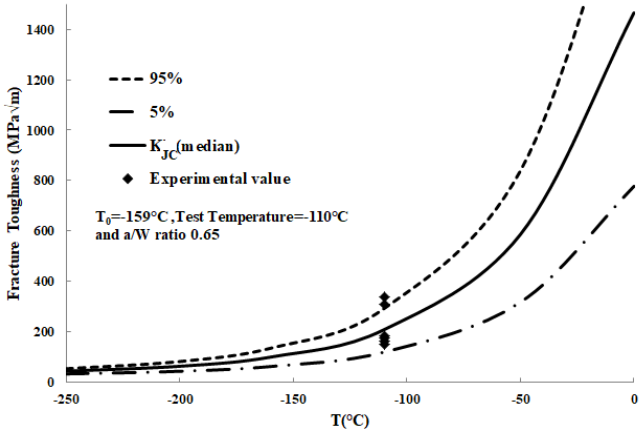

Fig.2.19. Master curve at -110^{0}C for specimen with a/w =0.65 and equivalent thickness of 25 mm

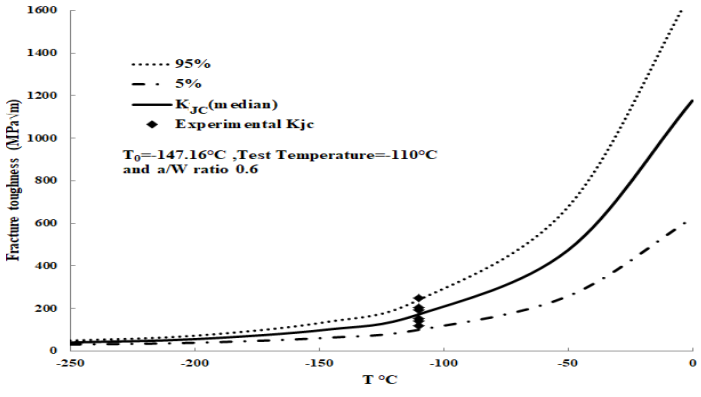

Fig.2.20. Master curve at -110^{0}C for specimen with a/w =0.6 and equivalent thickness of 25 mm

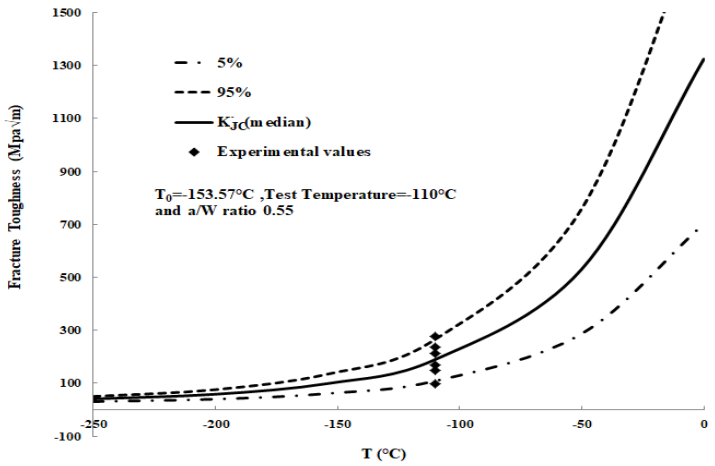

Fig.2.21. Master curve at -110^{0}C for specimen with a/w =0.55 and equivalent thickness of 25 mm

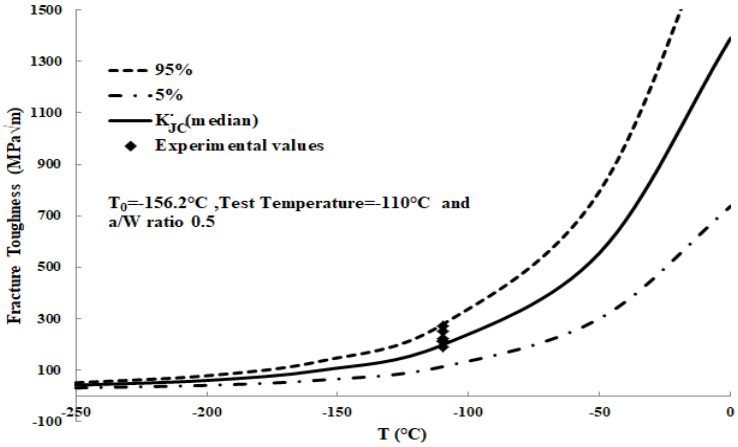

Fig.2.22. Master curve at -110^{0}C for specimen with a/w =0.5 and equivalent thickness of 25 mm

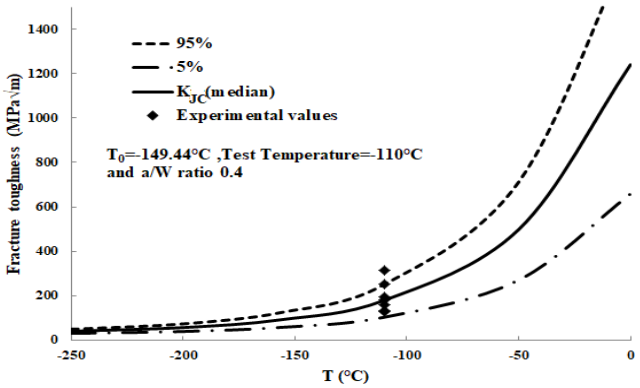

Fig.2.23. Master curve at -110^{0}C for specimen with a/w =0.4 and equivalent thickness of 25 mm

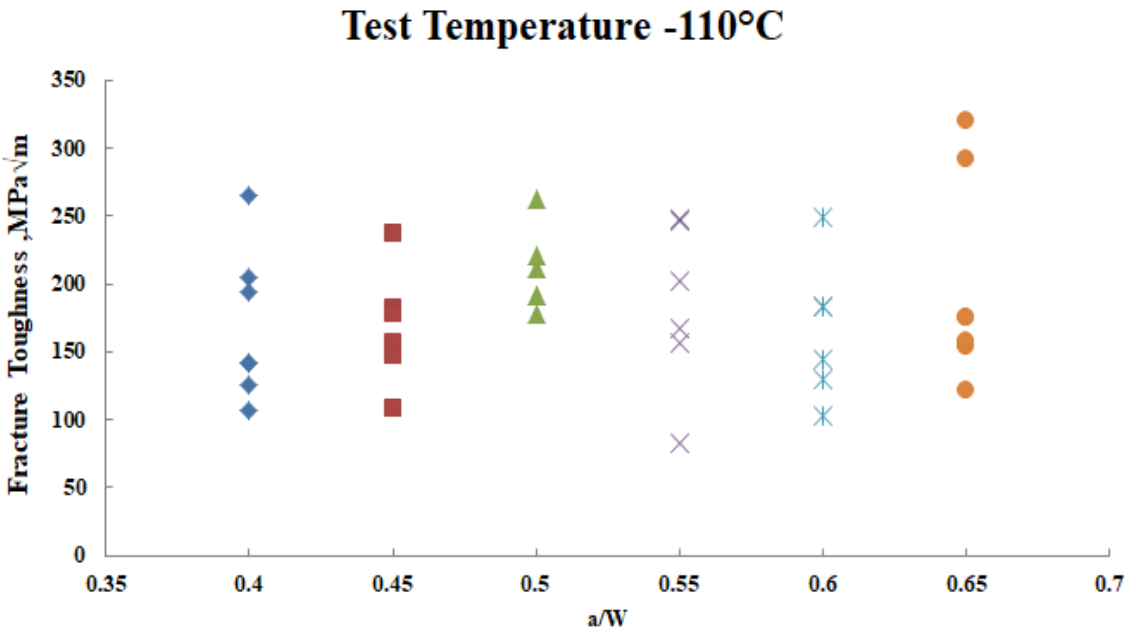

Fig.2.24 K_{JC} variation with a/w ratio from experiment

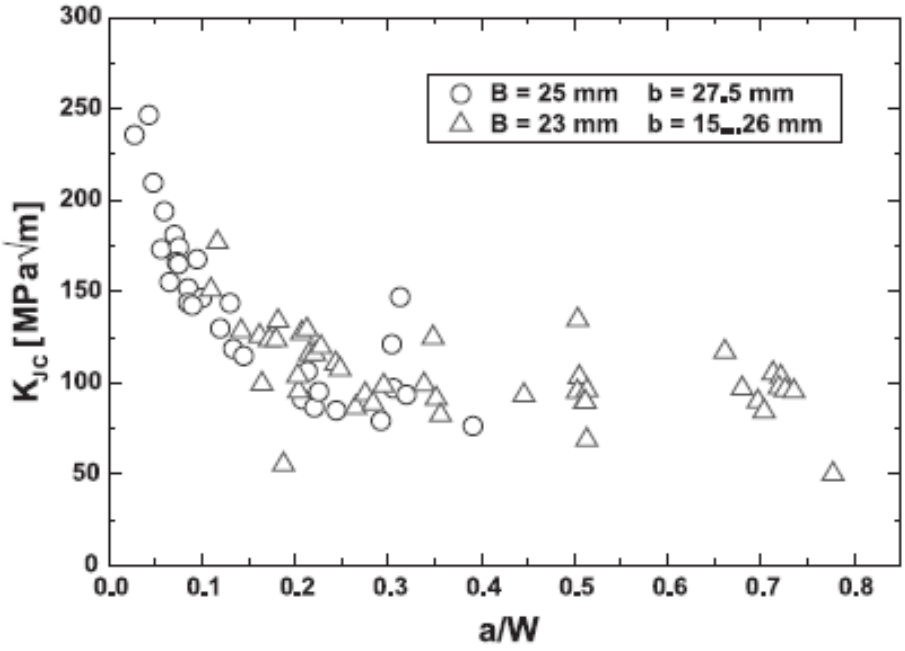

Fig.2.25 K_{JC} variation with a/w ratio from Kim Wallin's paper[45]

K_{JC} variation with a/w ratio is shown in figure 2.24. It is seen from Kim Wallin's paper**[**45] as shown in figure 2.25,that for the material which he used in case of TPB specimen fracture toughness remains practically constant for crack size above a/w=0.3, and for a/w less than 0.3 fracture toughness increases with decreasing crack depth.

For 20MNMONI55 steel (the material used in this thesis) it is observed that in case of TPB specimen fracture toughness remains practically constant for crack size above a/W=0.4, and for a/W less than0.4 fracture toughness increases with decreasing crack depth.

Table 2.6. The statistical mean average and standard deviation of T_0 determined with varying thickness and *a/W* ratio

Thickness (mm)	***T_0***	***Average (Mean)***	***Standard Deviation***	***a/W***	***T_0***	***Average (Mean)***	***Standard Deviation***
10	-142	-150.78	4.93	0.4	-149.44	-151.86	4.78
12	-147.92			0.45	-145.8		
15	-151.92			0.5	-156.2		
20	-158			0.55	-153.57		
25	-151.49			0.6	-147.16		
30	*-153.36*			0.65	-159		

2.8.2 Discussion on the effect of a/W ratio and thickness of the specimen on Reference Temperature T_0

As observed in the preceding study, that the variation in T_0 with *a/W* ratio and thickness are scattered and did not reflect any remarkable pattern. But the study focuses on the fact that the variation in T_0 with thickness and *a/W* lies within a tolerance band of ±8° which is at per with ASTM E 1921 as reflected in the Table 2.6

As explained by T.L. Anderson in his book Fracture Mechanics Fundamental and Applications (edition:) it is clearly shown in the graph (Figure 2.43) that for ductile failure as thickness increases at first fracture toughness increases and then it decreases with increase in thickness (which is explained as the phenomenon for transition from plane stress to plain strain condition) until a plateau is reached after which the toughness remains insensitive to further increase in thickness. Again it is referred that cleavage fracture toughness exhibits a slight effect of thickness-dependent due to weakest link sampling effect which also endorses the decrease of fracture toughness with increase in thickness. With this understanding we have done tests in lower DBT temperature range but the observation from the test results found to be different from above understanding. In our case the effect of thickness is shown for a fixed temperature of -110°C where the fracture mechanism is entirely cleavage fracture and the variation with thickness does not reflect any remarkable pattern only a scattered effect in fracture toughness variation with increase in thickness is observed As the deviation in T_0 calculated from fracture toughness results lies within a close tolerance band of ±8° with the variation in thickness which is conforming with ASTM E 1921 results are accepted to be valid. The motivation of further exploration of the fracture mechanism in DBT range and thickness dependence of fracture toughness is inspired from this apparently inexplainable results. The deviation observed in the results is conceptuated to be splitted in two parts as bias and random uncertainty, The bias part is influenced by weakest link in two ways. One, the probability of presence of nucleation sites which increases with thickness and hence fracture toughness is decreased but the load level or plasticity level at crack tip at failure also influences the fracture toughness which do not follow the same trend. Hence the combined bias may appear to be fluctuating instead of a specific trend as expected. The propensity of this idea is thoroughly attempted to verify by further experiment and analysis.

In first part ductile parameters to represent stress state at crack tips are used at upper DBT range to calibrate the effect of geometry on T_0 (Chapter 3) and for lower DBT range Weibull stress is used for the same purpose (Chapter 4 & 5).

2.9. Comparison of T_0 Values obtained from CT and TPB specimen to study the effect of geometry on T_0 .

As discussed in the preceding articles due to different loading conditions in CT and TPB specimen, the constraint effects are different at the crack tip area of both this specimens. So the T_0 value is also different though they are of the same size. A correction formulation has been described to adjust the T_0 obtained from TPB specimen to that of 1T CT specimen as per the IAEA-TECDOC-717 GUIDELINES as shown in Table 2.6.The experiment and the results for Compact Tension Specimen (CT) are performed by the previous researchers in our laboratory[8,9]. This results matches well with IAEA-TECDOC-717 GUIDELINES.

Two equations are used to adjust the T_0 obtained from three-point bend specimens to that of a 1T C(T) specimen as per "IAEATECHDOC-717 GUIDELINES" which are as follows

SE(B), B × 2B: K-SE(B)/K-C(T) = 1.10 + 0.00053 [175 – M-SE(B)]

SE(B), B × B: K-SE(B)/K-C(T) = 1.19 + 0.00180 [120 – M-SE(B)]

where K-SE(B) is measured K_{JC} for the Three point bend specimen, K-C(T) is K_{JC} for the 1TC(T) specimen, and M is the constraint adjusting parameter given in the following equation.

$M_{lim} > b\ \sigma_{ys}\ E/K^2Jc(1-\nu^2)$

Where b is the specimen remaining ligament, σ_{ys} is the material yield strength, E is Young's modulus, K_{Jc} is the measured cleavage fracture toughness, and ν is Poisson's ratio. The M_{lim} specified in E1921 is 30 and is the same for compact and three-point bend specimens. Various analytical studies have concluded the need for M_{lim} values from 30 to 200, with the compact specimen geometry requiring a lower M_{lim} than that for the three-point bend. The effect of Censor Parameter (M) on the Reference Temperature is studied in details immediately after this part of discussion.

Table: 2.6. Adjusted value of TPB specimen from Experimental Results

Specimen type	T_0	T_0(adjusted)	T_0-T_0(adjusted)ºC
TPB (25x25)	-150	-148.69	-1.31

Table: 2.7. Comparison of T_0 for CT and TPB specimen for different test temperature

Test temperature	T_0(CT)	T_0(TPB)	T_0(TPB Adjusted)
-100	-123	-166.433	-134
-110	-129.39	-150	-148.69

Table: 2.8. Comparison of T_0 values for **CT** and **TPB** specimen by **Multiple Temperature method**.

T_0(CT)	T_0(TPB)	T_0(TPB Adjusted)
-129	-150	-147

Table: 2.9. Comparison of T_0 values for CT and TPB specimen at different a/w ratios

a/W	T_0(CT)	T_0(TPB)
0.45	-134	-145.8
0.5	-131	-156.2
0.55	-131.538	-153.57

Table: 2.10. Comparison of T_0 values for CT and TPB specimen at different thickness (after imposing the thickness correction)

Thickness (mm)	T_0(CT)	T_0(TPB)
25	-129.39	-150
12.5	-136	-147.92

Table 2.7 to Table 2.10 gives the detailed view of comparison between CT and TPB specimen in different ways.

2.10. To Study the effect of Censor Parameter (M) on the Reference Temperature

As $K_{JC(Limit)}$ represents the higher bound of acceptability of fracture toughness, increasing (M) reduces the value of limit and censors some of the previously accepted values thus the value of T_0 is computed from a modified data sheet and thus T_0 value is changed.Thus

the effect of Censor Parameter (M) on the Reference Temperature is pronounced and studied vividly in this part of the work.

We know that limiting value of K_{JC} can be found out from the

$$K_{JC(Limit)} = \sqrt{\frac{E.b_0.\sigma_{ys}}{M\left(1-\nu^2\right)}} \qquad (2.9)$$

Where,

E= Young's Modulus of the Material,

b_0=Ligament length

σ_{YS} =Yield strength of the material

ν =Poisson's ratio and

M= Censor parameter

T_0 variation with M for TPB specimens are plotted in the following figure 2.32 for different a/W ratio 0.5, 0.55, 0.6.The results are also provided in the table 2.11 for better understanding of the effect of M on T_0.

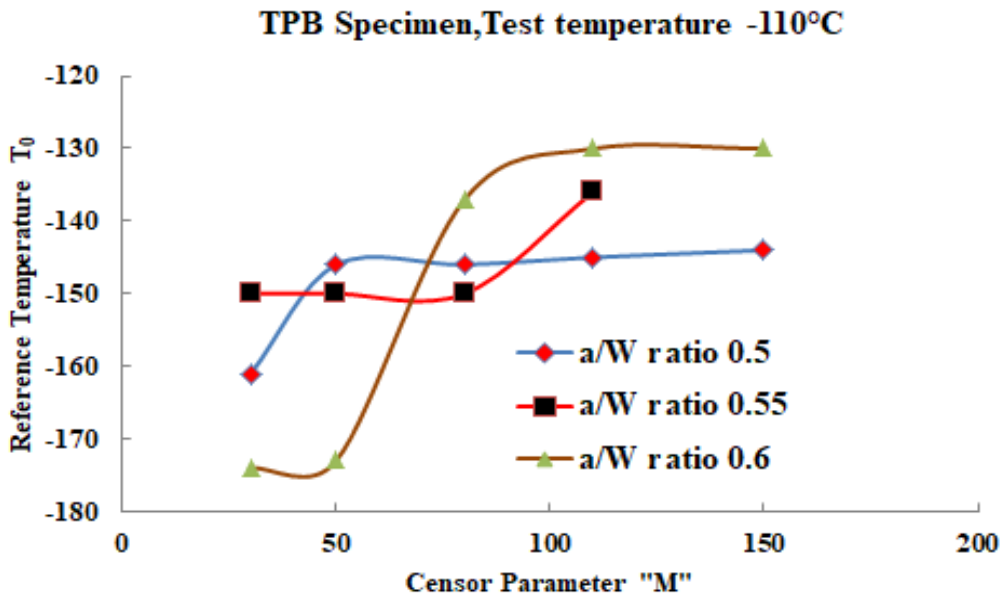

Fig.2.26.T_0 variation with M for TPB specimens

Table: 2.11. Variation of M for different a/W ratio of TPB specimen.

TPB a/W	M	T_0	K_{JC}(limit)
TPB a/w = 0.50	30	-161	348.577
	50	-146	270.000
	80	-146	213.000
	110	-145	182.000
	150	-144	156.000
TPB a/W = 0.55	30	-150	348.577
	50	-150	270.000
	80	-150	213.000
	110	-136	182.000
	150	-	156.000
TPB a/W = 0.60	30	-174	348.577
	50	-173	270.000
	80	-137	213.000
	110	-130	182.000
	150	-130	156.000

variation with M for TPB and CT specimens are given together for a/W ratio 0.5 in the figure 2.27 and also for better understanding provided in the table 2.12 is provide.

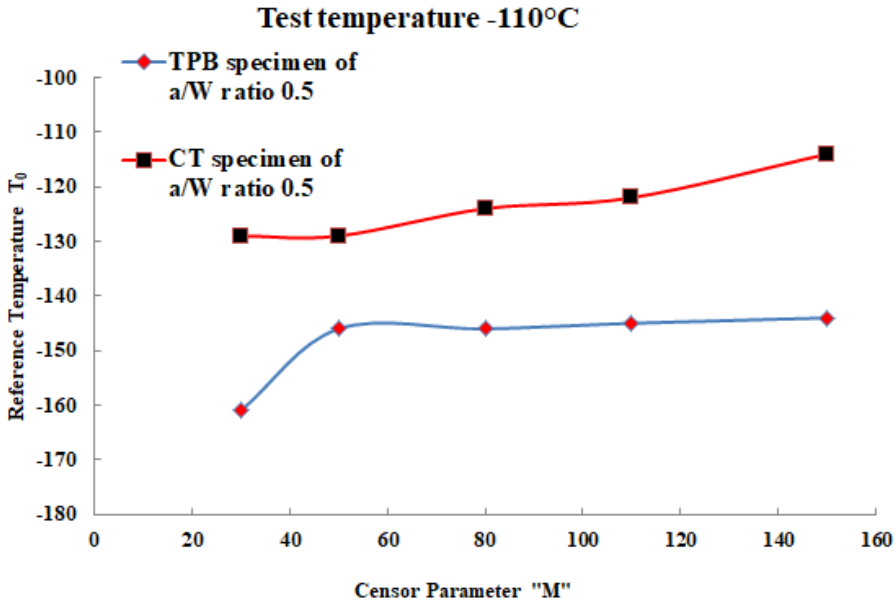

Fig.2.27. T_0 variation with M for TPB and CT specimens

Table: 2.12. Variation of M for TPB specimen and CT specimen for fixed a/W ratio of 0.5

	M	T_0	$K_{JC(limit)}$
TPB a/w = 0.50	30	-161	348.577
	50	-146	270
	80	-146	213
	110	-145	182
	150	-144	156
CT a/w = 0.50	30	-129	348.577
	50	-129	270
	80	-124	213
	110	-122	182
	150	-114	156

The value of T_0 for TPB specimen is found to be lower than that of CT specimen consistently in all cases. The loading type is different and the constraint level is lower in case of TPB specimen compared to CT specimens and yields higher fracture toughness. This observation is in parity with the results shown in CRP report[2].The fracture toughness for TPB specimen of same geometry will be higher compared to CT specimen, hence limiting value of fracture toughness for TPB specimen should be computed with some higher value of M to avoid specimen with excessive ductile stretch. From the experimental results it is observed that the value of M may be taken as 50 for TPB specimen instead of 30 as is taken for CT specimen

Conclusions

- The propositions related to master curve methodology is well applicable for this particular RPV steel to characterize the fracture behavior in DBT region.

- The reference temperature (T_0) is found to be influenced by geometry and also by the loading condition while comparing the CT results with the TPB results.

- The value of T_0 obtained by Single Temperature at -110^0C matches with the multi temperature value. For the other Temperatures T_0 obtained by Single Temperature at -120^0C,-130^0C and -140^0C lies within a range of $\pm 10^0$C.

- According to this study we observe that even after incorporating thickness correction on TPB specimens, T_0 is mildly dependent on the thickness of the specimen.

- It is observed for the material 20MnMoNi55 that, fracture toughness remains practically constant for a/w above 0.4, which matches with the result of Kim Wallin's observation on quantifying T_{stress} controlled constraint by the master curve transition temperature T_0,[7].

- While studying on Censor Parameter it is observed that the optimum value of censor parameter (M) could be taken 50 for TPB specimen instead of 30 as is taken for CT specimen., because it is seen that increasing the value of M beyond 50 has insignificant effect on reference temperature (T_0).

***The content of this chapter is published in Procedia Engineering 86 (2014) 264 – 271. Science Direct (Elsevier) with the title Study of Constraint Effect on Reference Temperature (T0) of Reactor Pressure Vessel Material (20mnmoni55 Steel) in the Ductile to Brittle Transition Region*.**

Chapter 3

To Study the Effect of Loss of Constraint on Reference Temperature (T_0) With the Help of Q-Stress, Triaxiality Ratio and T-Stress

Outline of the chapter

A series of experiments are performed in the ductile to brittle region on TPB specimens with different thickness and a/W ratio and a variation of T_0 is obtained, which indicates constraint dependence of T_0. An attempt is made to correlate T_0 with Q-stress, T-stress and Triaxiality ratio to count for the constraint loss compared to a standard specimen of 25 mm thick and a/W ratio as 0.5. Both the average value and also the maximum value of the crack tip stresses are considered to predict T_0 at different constraint level and compared with the experimental results.

3.1. Introduction

The effect of Constraint level at the crack tip due to variation in thickness or a/W ratio on Master Curve and T_0 are shown in the chapter 2. But no functional correlation is established between T_0 and the loss of constraints to quantify the effect. The application of T_0 to assess the degree of embrittlement for components require relationship between T_0 and crack tip stress parameters. This idea encouraged to develop correlation which takes care of the constraint effect on the Master Curve. The fracture mechanism is probabilistic in DBTT region. At upper shelf ductile fracture is predominant but with the fall of temperature most of the failure though initiated by ductile stretch but terminated with brittle fracture and beyond Nil Ductility Temperature (NDT) the failure is completely brittle. Hence in the upper shelf of DBTT the fracture toughness value is related to amount of ductile stretch before initiation of brittle fracture. Hence a stress

related parameter which can represent the triaxiality level at the crack tip at failure point must have influence on the value of fracture toughness and hence on T_0. Based on this idea it is attempted to consider different triaxiality parameters like Q-Stress, Triaxiality Ratio and T-Stress to correlate the constraint effect with the Master Curve. 1T (25mm thick) specimen with a/w ratio as 0.5 is assumed to be reference specimen and the value of T_0 obtained for this specimen is assumed to be reference $T_{0.}$ In this work, Finite Element Analysis is done using ductile material model to calculate Q-Stress, Triaxiality Ratio and T-Stress of each fracture specimen at failure point. A functional relationship is proposed between the stress parameter (constraint level) near the crack tip of a reference specimen and correlated with the stress pattern of any other specimen of different thickness and *a/W* ratio. The functional relationship is then used to predict the Reference Temperature (T_0) of different thickness and *a/W* ratio by correlating the Reference Temperature (T_0) of a standard specimen. The same functional relationship is applied to predict the reference temperature T_0 of specimen of any thickness and *a/W* ratio from reference temperature T_0 of reference specimen and compared with experimental results. Both the average value and the maximum value of the stress parameters are considered to predict T_0 at different constraint level and compared with the experimental results.

3.2. Constraint effect on T_0

The variation of T_0 with thickness of TPB specimen is shown in the Fig.2.11 ,the Master Curve for 25 mm thickness (with different a/W ratio) are shown in figures. 2.12 to 2.16 respectively. The variation of T_0 with a/W ratio is shown in the Fig.2.18, the Master Curve for constant a/W ratio 0.5(with different thickness) are shown in figures 2.19 to 2.23.

3.3. Finite Element Analysis

For the evaluation of constraint parameters T-stress, Q parameter or Triaxiality ratio elastic-plastic finite element analysis is performed for each TPB specimen taking plastic strain verses stress data from tensile test performed at -110° C in Universal Testing Machine (Instron 8801) as shown in Fig.3.1. The Von Misses stress distribution of quarter TPB specimen is shown in Fig.3.2, Fig.3.3 & 3.4 show a comparison of Load vs.

LLD curve and J Integral vs. LLD curve respectively obtained from experiment and FE simulation.

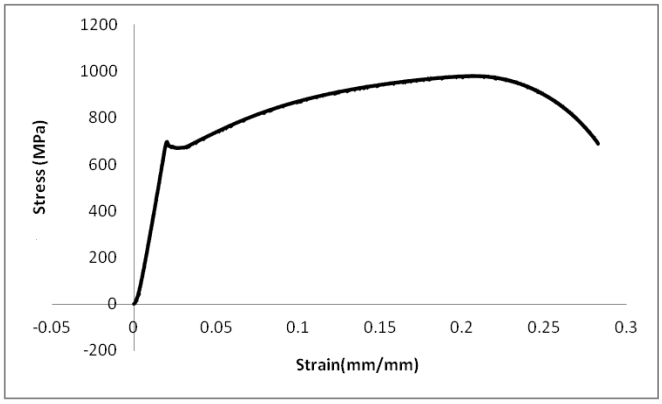

Fig.3.1. Stress vs strain curve at a temperature of.-110 °C for the material 20MnMoNi55 Steel.

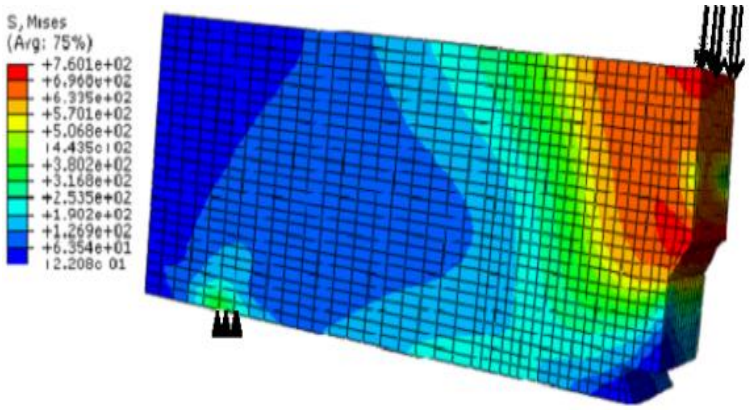

Fig.3.2. Quarter model of TPB specimen showing the Von misses stress distribution at failure displacement.

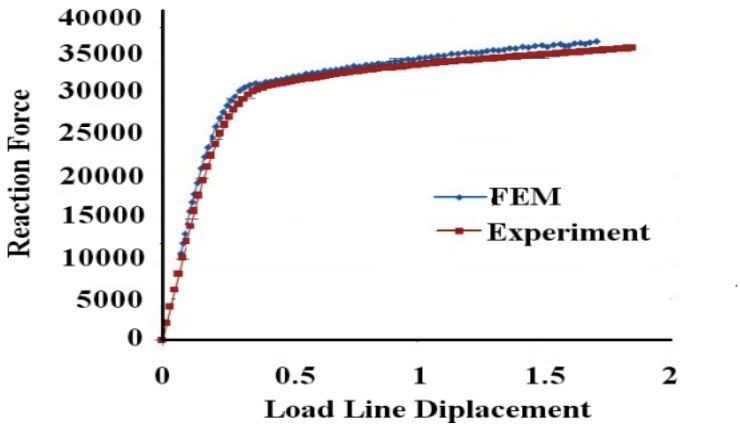

Fig.3.3. Comparison of load vs. Load Line Displacement (LLD)-110 °C

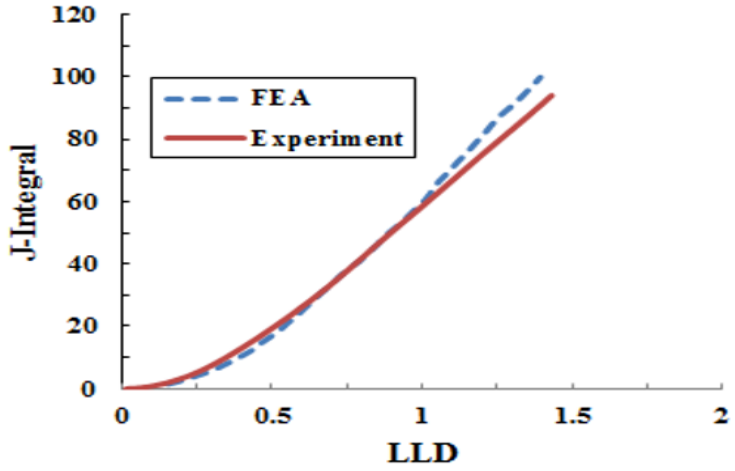

Fig.3.4.Comparison of J-Integral vs. Load Line Displacement (LLD) -110 °C.

3.4. Stress based parameters to represent constraint level used to correlate the constraint effect on Master Curve and Reference Temperature (T_0)

3.4.1.T-Stress as parameter capturing loss of constraint :

Williams described in his work [81] that the crack-tip stress fields in an isotropic elastic material can be expressed as an infinite power series, where the leading term exhibits a $1/\sqrt{r}$ singularity, the second term is constant with *r*, the third term is proportional to $\sqrt{r}$, and so on. According to the Classical fracture mechanics theory normally all the terms except the singular term are neglected leading to a single-parameter description of the

near-tip stress field. Because of a positive exponents on r the third and higher terms in the Williams solution, vanish at the crack tip, the second (uniform) term remains finite. It turns out that this second term can have a profound effect on the plastic zone shape and the stresses deep inside the plastic zone. Hence fracture parameter may have dependence geometries like thickness or a/W ratio which can be verified by evaluating the second term for the specific geometry.

For a crack in an isotropic elastic material subject to plane strain Mode I loading, the first two terms of the Williams solution are shown in equation 3.1

$$\sigma_{ij} = \frac{K_I}{\sqrt{2\pi r}} f_{ij}(\theta) + \begin{bmatrix} T & 0 & 0 \\ 0 & 0 & 0 \\ 0 & 0 & \sqrt{T} \end{bmatrix} \qquad (3.1)$$

Where T is a uniform stress in the x direction (which induces a stress υT in the z direction in plane strain). The limitation of using T stress is that evaluation of T stress is based on elastic analysis.

3.4.2. Mode of T-stress calculation [44]

T-stress is defined by

$$\mathbf{T} = \left[\frac{\mathbf{u_y(y) - u_y(0)}}{\mathbf{y}} \right] \mathbf{E} \qquad (3.2)$$

Where,

$u_y(0)$= Displacement in the Y-direction at the crack tip

$u_y(y)$= Displacement in the Y-direction at the end point

y=distance between this two points.

E=Young's Modulus of the material

T-stress is calculated from 2D analysis as shown in figure 3.5 with plain strain condition

according to equation 3.2 for each of the TPB specimens of different thickness and a/W ratio The failure load line displacement obtained from the experimental fractured specimen is the limit upto which the FEA is performed.Calculation of T-stress is performed in accordance with the equation 3.2.Once T-stress is calculated for a specimen at the failure load an attempt is taken to corelate it with the Reference Temperature T_0 obtained from the identical specimen.Based on this corelation prediction of T_0 for any a/W ratio is done ,with respect to a standard TPB specimen of a/W ratio 0.5 and thickness 25 mm, with the help of equation 3.3 and compared with the experimentally obtained values as shown in figure 3.6 . Then prediction of T_0 for any thickness is done ,with respect to a standard TPB specimen of a/W ratio 0.5 and thickness 25 mm, with the help of equation 3.4 and compared with the experimentally obtained values as shown in figure 3.7.

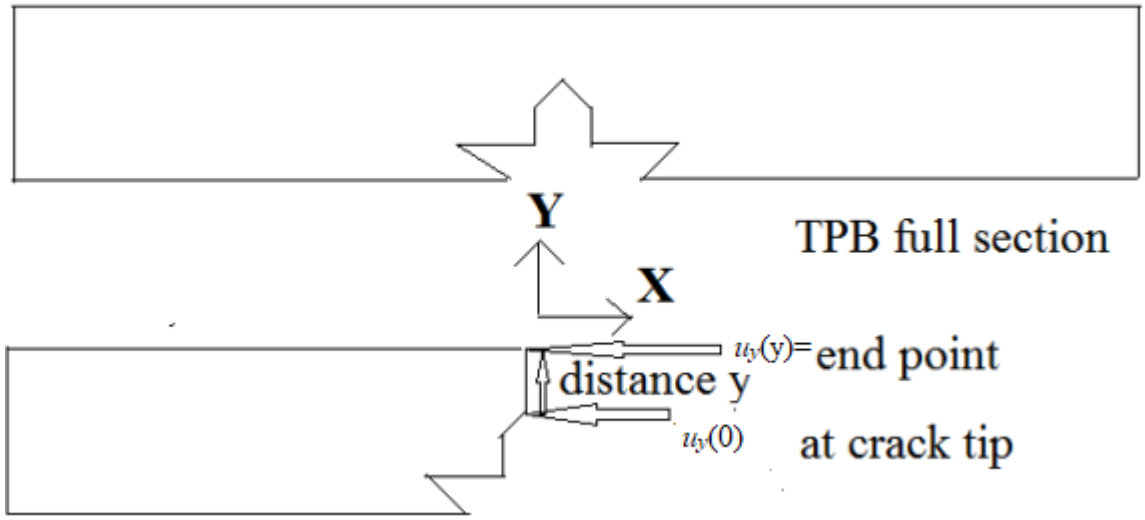

Fig. 3.5. TBP half section

$$T_{0(xx)} = \left[\left\{ \left(T\_Stress_{(xx)} - T\_Stress_{(0.5)} \right) * (-50) \right\} - 0.5 \right] + T_{0(0.5)} \qquad (3.3)$$

Where,

$T_{0(xx)}$ = reference temperature (T_0) of any a/W ratio.

$T_{0(0.5)}$ = reference temperature (T_0) of a/W ratio 0.5, as specimen with thickness 25 mm and a/W ratio 0.5 is taken as reference for calculation.

$$T_{0(xx)} = \left[\left\{\left(T\_Stress_{(xx)} - T\_Stress_{(25)}\right)*(-5)\right\} - 0.1\right] + T_{0(25)} \qquad (3.4)$$

Where,

$T_{0(xx)}$ = reference temperature (T_0) of any thickness

$T_{0(0.5)}$ = reference temperature (T_0) of a/W ratio 0.5, as specimen with thickness 25 mm and a/W ratio 0.5 is taken as reference for calculation

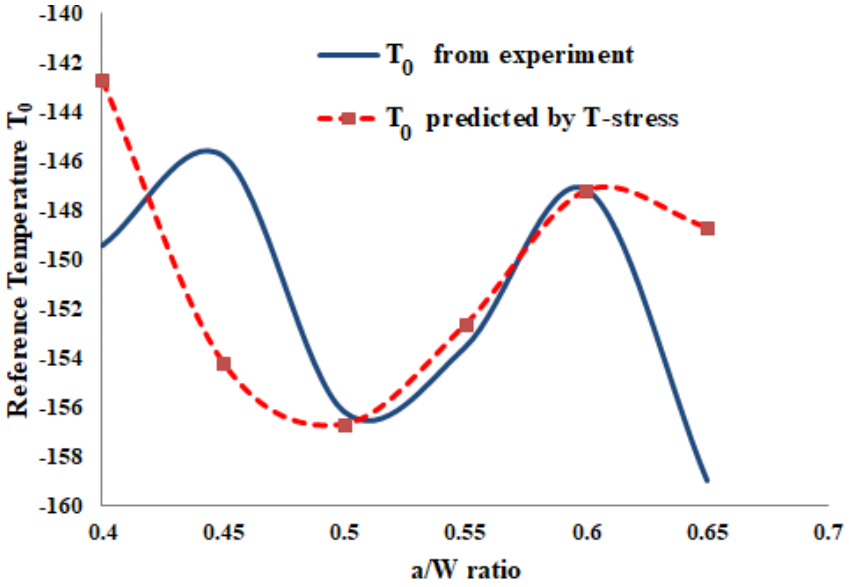

Fig.3.6.T_0 predicted both by T-Stress for different a/W ratio

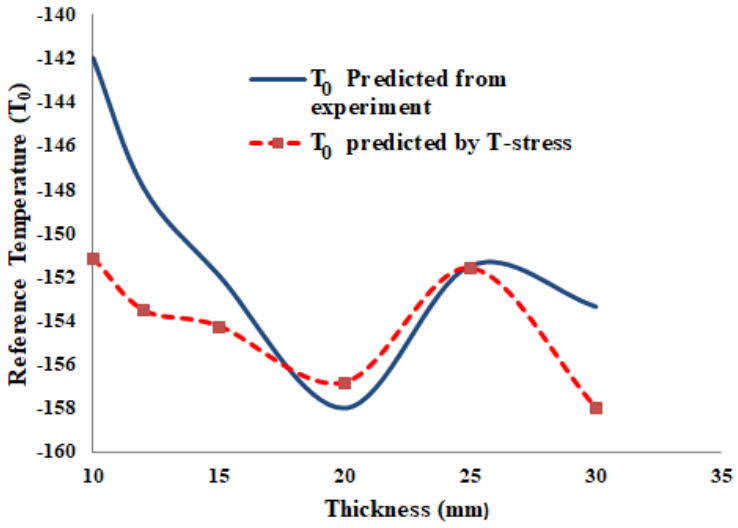

Fig.3.7.T_0 predicted both by T-Stress for different thickness

3.4.3.Q-Stress as parameter capturing loss of constraint :

Q is another second parameter like T stress to represent crack tip constraint. The two parameters, J and Q, have distinct roles: J sets the size scale of the process zone over which large stresses and strains develop, while Q scales the near-tip stress distribution relative to a high triaxiality reference stress state. An immediate consequence of the theory is this: it is the toughness values over a range of crack tip constraint that fully characterize the material's fracture resistance. It is shown that Q provides a common scale for interpreting cleavage fracture and ductile tearing data thus allowing both failure modes to be incorporated in a single toughness locus. The evolution of Q, as plasticity progresses from small scale yielding to fully yielded conditions, has been quantified for several crack. Q is used as a field parameter and as a point wise measure of stress level is discussed. Q is effectively independent of distance. In words, Q is the difference between the actual hoop stress and the corresponding HRR stress component at $r = 2J/\sigma_0$

3.4.4. Mode of Q-Stress calculation [82,41,15]

Q-stress are taken along the crack face as shown in Fig.3.8.a and its distribution along thickness is shown in Fig 3.8(b).Its distribution along the width of the specimen is Fig.3.8(c)& 3.8.(d). Calculation of Q-stress is performed in accordance with the equation 3.5,3.6 and 3.7.Once Q-stress is calculated for a specimen at the failure load an attempt is taken to corelate it with the Reference Temperature T_0 obtained from the identical specimen.Based on this corelation prediction of T_0 for any a/W ratio is done ,with respect to a standard TPB specimen of a/W ratio 0.5 and thickness 25 mm, with the help of equation 3. 8 and compared with the experimentally obtained values as shown in figure 3.9(a) and Prediction of T_0 for any thickness is done ,with respect to a standard TPB specimen of a/W ratio 0.5 and thickness 25 mm, with the help of equation 3.9 and compared with the experimentally obtained values as shown in figure 3.9(b)

$$Q = \frac{(\sigma_{\theta\theta})_{Hydrostatic} - (\sigma_{\theta\theta})_{HRR}}{\sigma_0} \qquad (3.5)$$

$$\text{At,} \quad \theta = 0,\ r = \frac{2J}{\sigma_0} \tag{3.6}$$

Where,
$$(\sigma_{\theta\theta})_{HRR} = \sqrt{\frac{J_c}{r}} \tag{3.7}$$

And σ_0 = Yield stress.

As for determining reference temperature (T_0) at least 6 tests were required, so for the calculation of $(\sigma_{\theta\theta})_{HRR}$ J_C median value is taken

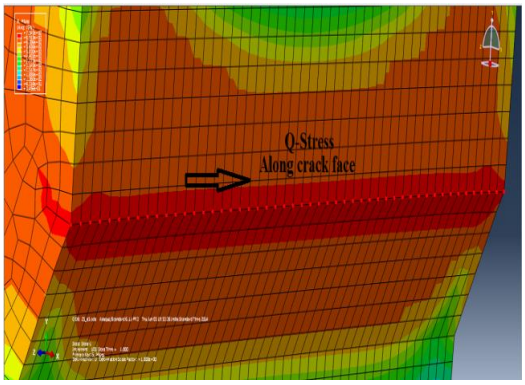

Fig.3.8(a) Q-Stress distribution along crack face

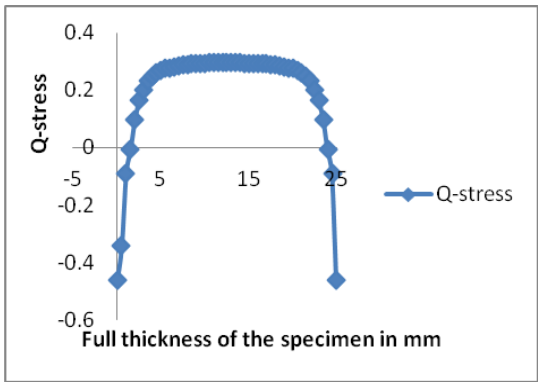

Fig.3.8(b) Q-Stress variation with thickness of the specimen

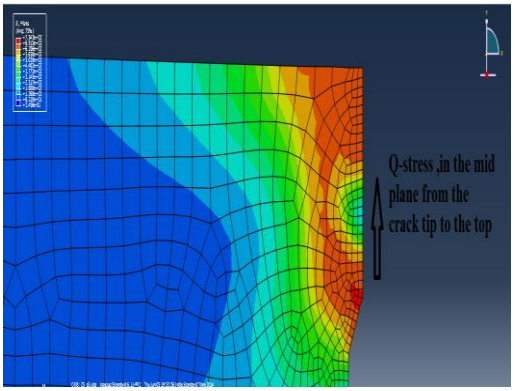

Fig.3.8(c) Stress variation along width of the specimen

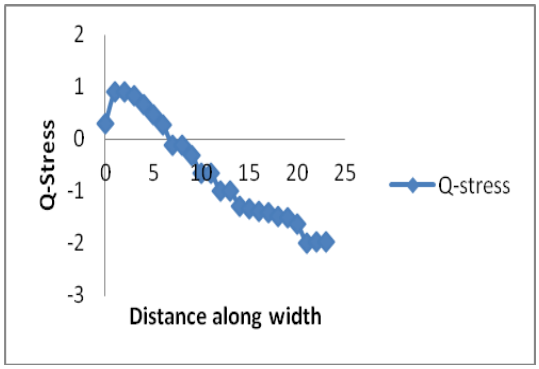

Fig.3.8(d) Graphical representation of Q-Stress variation along width of the specimen

$$T_{0(xx)} = \left[\left\{ \left(Q\_Stress_{(xx)} - Q\_Stress_{(0.5)} \right) * (-100) \right\} + 0.1 \right] + T_{0(0.5)} \qquad (3.8)$$

Where,

$T_{0(xx)}$ = reference temperature (T_0) of any a/W ratio.

$T_{0(0.5)}$ = reference temperature (T_0) of a/W ratio 0.5, as specimen with thickness 25 mm and a/W ratio 0.5 is taken as reference for calculation.

$$T_{0(xx)} = \left[\left\{ \left(Q\_Stress_{(xx)} - Q\_Stress_{(25)} \right) * (-20) \right\} - 0.1 \right] + T_{0(25)} \qquad (3.9)$$

Where,

$T_{0(xx)}$ = reference temperature (T_0) of any thickness

$T_{0(0.5)}$ = reference temperature (T_0) of a/W ratio 0.5, as specimen with thickness 25 mm and a/W ratio 0.5 is taken as reference for calculation

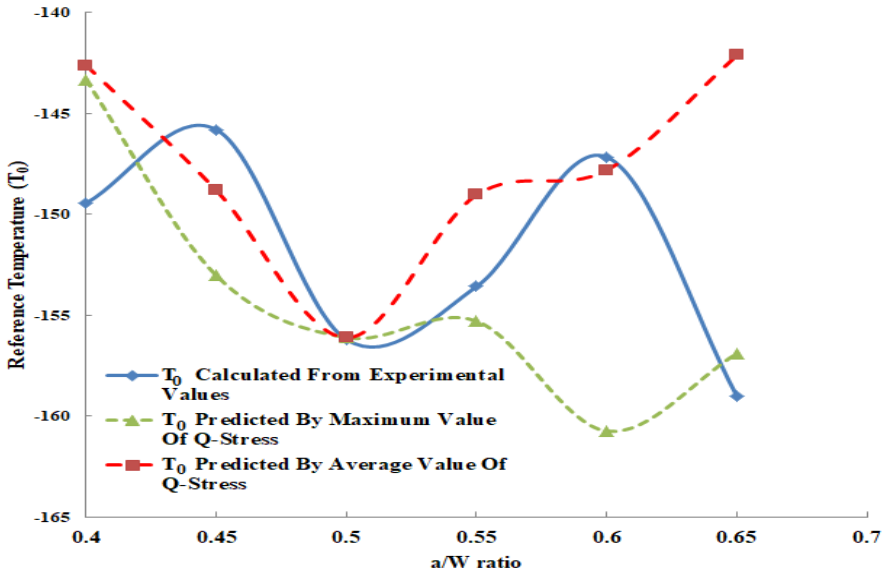

Fig.3.9.(a) T_0 predicted both by Avgerage and Maximum values of Q-stress with respect to a/W ratio

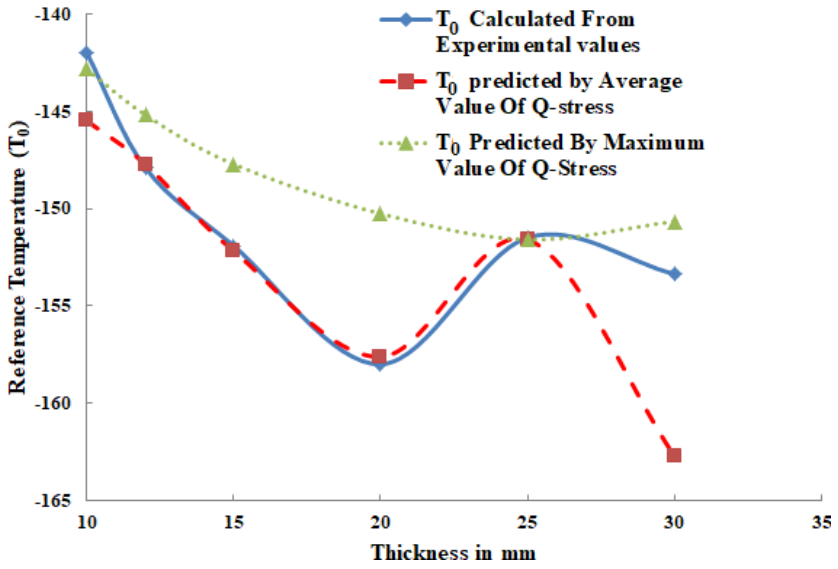

Fig.3.9.(b).*T_0* predicted both by Avgerage and Maximum value of Q-stress with respect to thickness

3.4.5. Triaxiality Ratio as parameter capturing loss of constraint :

It is defined as the ratio of Hydrostatic stress to Von Misses Equivalent stress. The stress triaxiality ratio strongly affects the fracture behaviour of materials. The fracture of ductile metals is strongly dependent on hydrostatic stress due to growth of long cylindrical voids and spherical voids. Also the criteria for fracture initiation depend on hydrostatic stress, and the mechanism of fracture is dependent on the amount of triaxiality [83,84].For large triaxialities, void growth is the dominant failure mode, while at low stress triaxialities, fracture may develop as a combination of shear and void growth modes. In order to simulate crack formation and propagation, a criterion for void coalescence is required. After the onset of void coalescence, material loses load carrying capacity rapidly [85]. Many engineering structures of ferritic steels operate near the DBT region where unstable fracture occurs by transgranular cleavage after small amount of ductile crack growth. Statistical models have been developed to describe the DBT behavior. Some indicated that for a stationary crack the constraint ahead of crack tip depends on both specimen configuration and initial crack length [86, 87]. Therefore, the stress triaxiality factor (TF) determined from the FE analysis can be used as an intermediate alternative parameter to

predict the fracture behavior of the material and the effect of different fracture parameters with different damage and crack propagation models.

3.4.6. Calculation of triaxiality parameters:

The method of triaxiality ratio calculation of TPB specimen of different thickness and a/W ratio are shown in Equation 3.10, 3.11, 3.12.

$$Triaxiality\ Ratio = \frac{\sigma_{Hydrostatic}}{\sigma_{Equivalent}} \tag{3.10}$$

$$\sigma_{hydrostatic} = \frac{\sigma_{xx} + \sigma_{yy} + \sigma_{zz}}{3} \tag{3.11}$$

$$\sigma_{equivalent} = \frac{1}{\sqrt{2}} \sqrt{\left[\left(\sigma_{xx} - \sigma_{yy}\right)^2 + \left(\sigma_{yy} - \sigma_{zz}\right)^2 + \left(\sigma_{zz} - \sigma_{xx}\right)^2 \right]} \tag{3.12}$$

Fig.3.10.(a) shows the crack face direction on which triaxiality is calculated and fig.3.10(b) shows triaxiality variation with thickness of the specimen, the maximum triaxiality is shown in Fig.3.10.(c). Average triaxiality is calculated from all nodal values. Maximum tri axiality occurs at a distance of 2mm from the crack tip measured along the width of the specimen. Plot of triaxiality verses width of specimen is shown in Fig.3.10(d).

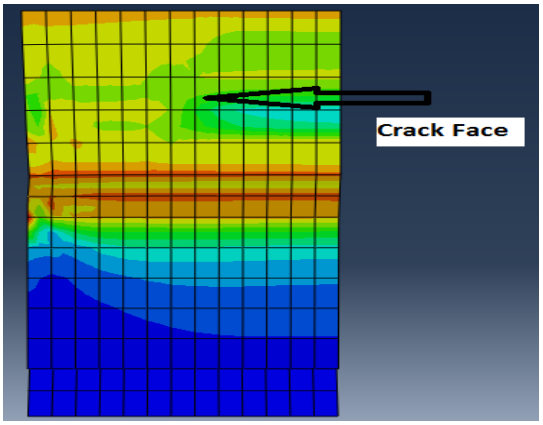

Fig 3.10.(a) FE model of 1T TPB and for half thickness & a/w=0.6

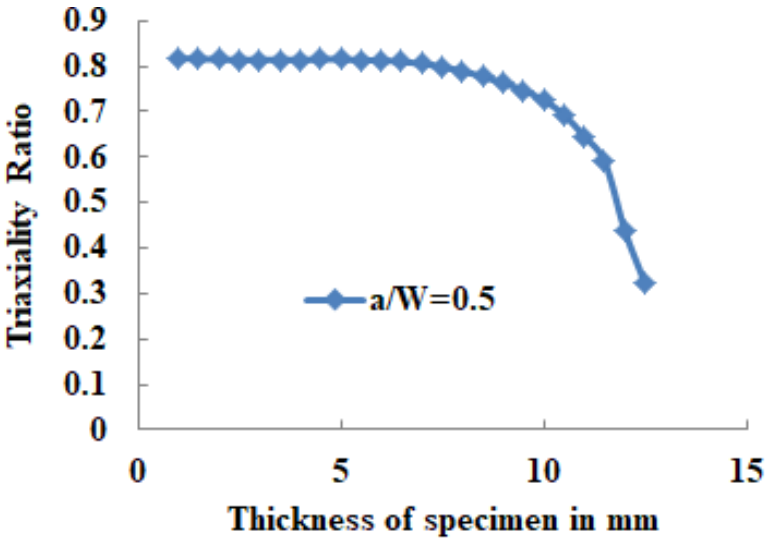

Fig.3.10(b) Triaxiality ratios vs. Distance at the crack face.

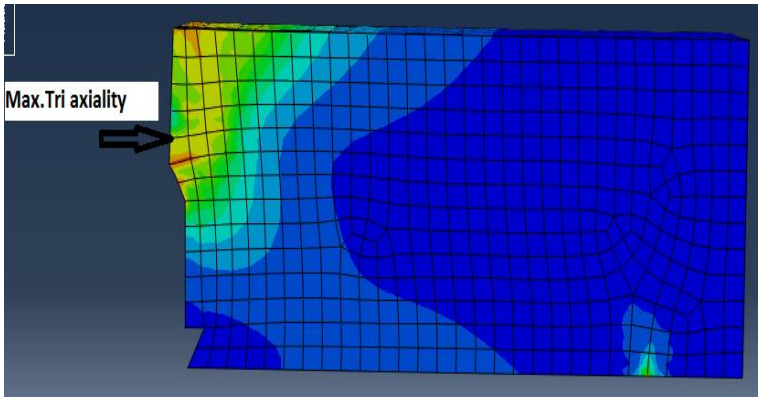

Fig.3.10. (c) Showing MaximumTri for 1T TPB

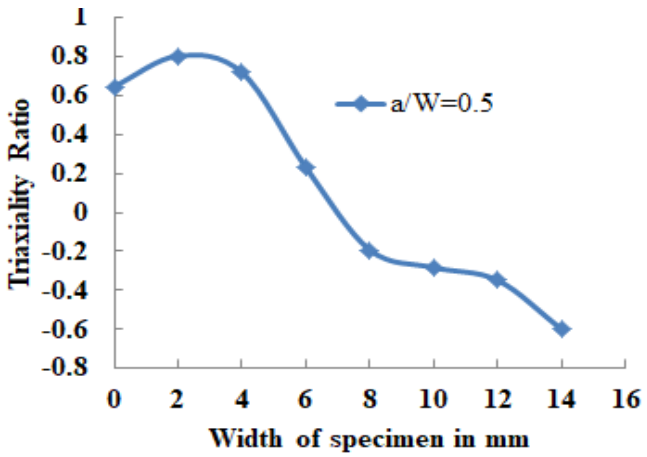

Fig.3.10.(d) Showing Triaxiality variation along width of specimen.

Calculation of Triaxiality ratio is performed in accordance with the equation 3.10,3.11 and 3.12.Once Triaxiality ratio is calculated for a specimen at the failure load, an attempt is taken to corelate it with the Reference Temperature T_0 obtained from the identical specimen.Based on this corelation prediction of T_0 for any a/W ratio is done ,with respect to a standard TPB specimen of a/W ratio 0.5 and thickness 25 mm, with the help of equation 3.13 and compared with the experimentally obtained values as shown in figure 3.11(a) and Prediction of T_0 for any thickness is done ,with respect to a standard TPB specimen of a/W ratio 0.5 and thickness 25 mm, with the help of equation 3.14 and compared with the experimentally obtained values as shown in figure 3.11(b)

$$T_{0(xx)} = \left[\left\{\left(TriaxialityRatio_{(xx)} - TriaxialityRatio_{(0.5)}\right)*(-100)\right\} - 0.1\right] + T_{0(0.5)} \quad (3.13)$$

$T_{0(xx)}$ = reference temperature (T_0) of any a/W ratio.

$T_{0(0.5)}$ = reference temperature (T_0) of a/W ratio 0.5, as specimen with thickness 25 mm and a/W ratio 0.5 is taken as reference for calculation.

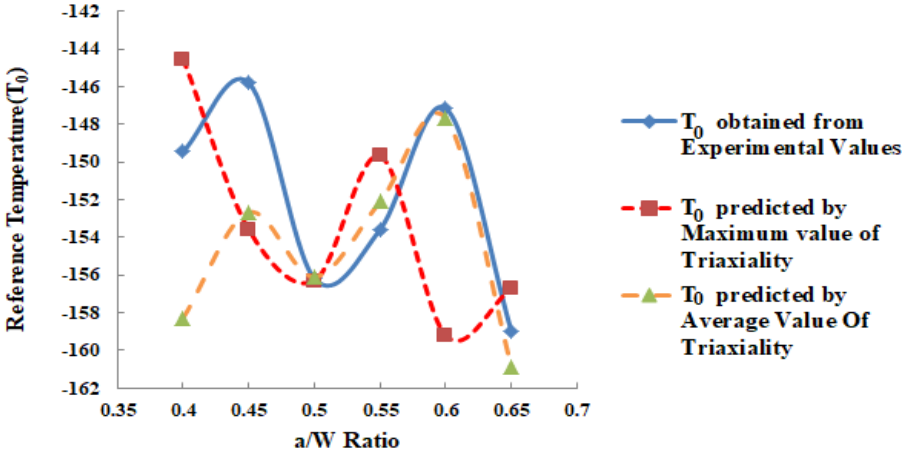

Fig. 3.11(a) T_0 predicted both by Average and Maximum value of Triaxiality variation in a/W ratio.

$$T_{0(xx)} = \left[\left\{\left(TriaxialityRatio_{(xx)} - TriaxialityRatio_{(25)}\right)*(-20)\right\} - 0.5\right] + T_{0(25)} \quad (3.14)$$

$T_{0(xx)}$ = reference temperature (T_0) of any thickness

$T_{0(0.5)}$ = reference temperature (T_0) of a/W ratio 0.5, as specimen with thickness 25 mm and a/W ratio 0.5 is taken as reference for calculation.

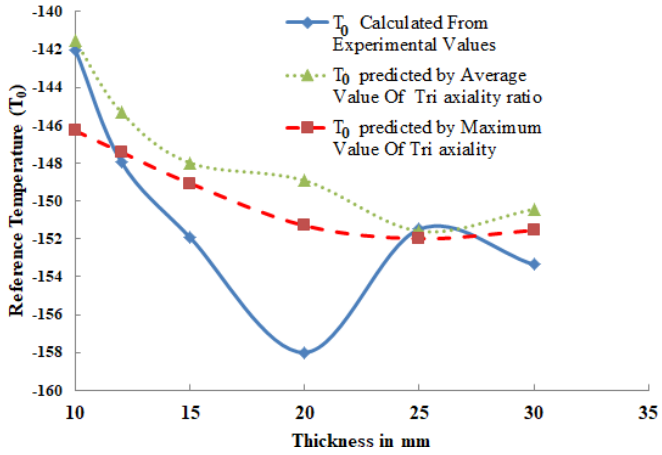

Fig.3.11. (b) T_0 predicted both by Average and Maximum value of Triaxiality with variation in thickness.

3.5. Prediction of T_0 from Triaxiality ratio ,Q-stress and T-Stress.

Prediction of T_0 with respect to a/W ratio 0.5 with different parameters Tri axiality ratio, Q-Stress, T-Stress are shown and compared with experimental results together and shown in figure 3.12

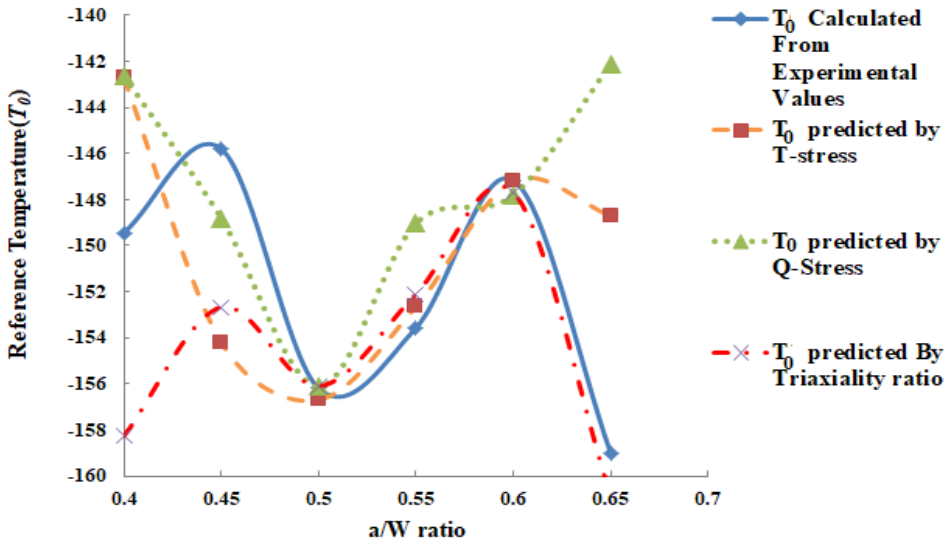

Fig.3.12. Predicted variation of T_0 from Triaxiality ratio, T-Stress and Q-stress with a/W ratio of the specimen

Once the reference temperature T_0 is calculated from experiment for a standard specimen of a/W ratio 0.5 and thickness 25 mm T_0 could be predicted for any specimen of different a/W ratio having fixed thickness of 25 mm by calculating Tri axiality ratio, Q-Stress$_{(xx)}$, T-Stress$_{(xx)}$ from FEA and utilising the above described equations.

Prediction of T_0 with respect to thickness of 25 mm with different parameters Tri axiality ratio, Q-Stress, T-Stress are shown and compared with experimental results together and shown in Fig 3.13. Once the reference temperature T_0 is calculated from experiment for a standard specimen of a/W ratio 0.5 and thickness 25 mm T_0 could be predicted for any specimen of different thickness having fixed a/W ratio by calculating Tri axiality ratio, Q-Stress$_{(xx)}$, T-Stress$_{(xx)}$ from FEA and utilising the above described equations

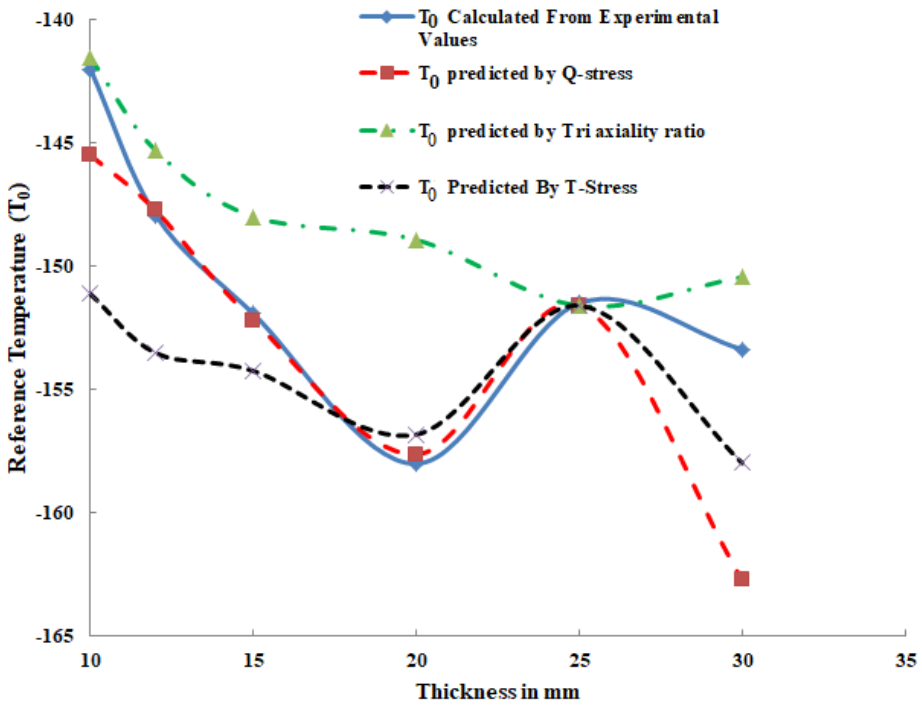

Fig.3.13 Predicted variation of T_0 from Triaxiality ratio, T-Stress and Q-stress with thickness of the specimen

The functional form correlating constraint parameters to T_0 for different *a/W* ratio and thickness are similar for all T-stress, Q-stress and Triaxiality parameter and the correlation is linear.

Conclusions

- Variation of reference temperature (T_0) with a/W ratio and thickness of the specimen are observed from experimental results.

- T stress, Q-stress and triaxiality ratio are calculated from FE analysis for each specimen.

- T_0 for different thickness and a/w ratio are predicted using these parameters as capturing constraints at each specimen comparing with respect to a generally accepted a/W ratio 0.5 and thickness of 25 mm. .

- Predicted T_0 provides a qualitative and quantitative matching with the experimental results for all the parameters. The predicted T_0 by the constraint parameter T_0 correlation for all three parameters with a/W ratio and thickness agrees well with experimental values within ±10° C. This is well within experimental error.

- From table no.2.5 page no.49 it is apparent that, the fracture toughness are obtained for TPB specimen of a fixed a/W ratio from widely different thickness of the specimen. Though thickness correction is imposed and the fracture toughness are converted to a standard thickness of 25 mm or 1T but this consideration may infer the cause for the variation for T_0 calculated from a/W=0.65.The fracture toughness are determined from different thickness of the specimen in order to study the effect of both a/W ratio and thickness on reference temperature T_0 from a single test matrix.

- The matching is found to be not good when the test results at lower transition temperatures are used.

- From this study it can be concluded that Q-stress can be used as parameter to capture effect of constraint on T_0 in the upper shelf of DBTT.

Chapter 4

Calibration Of Beremin Parameters FOR 20mnmoni55 Steel And Prediction Of Reference Temperature (T_0) For Different Thickness And a/W Ratio

Outline of the Chapter

Master curve and reference temperature (T_0) from three-point bending specimens of 20MnMoNi55 steel for different thicknesses and a/W ratios are determined using Kim Wallin's master curve methodology (ASTME1921-02) to study the effect of variation in thickness and a/W ratio at reference temperature (T_0). For upper shelf region of DBTT, ductile stress parameters like T-stress, Q-stress and Triaxiality ratio are used to correlate dependence of T_0 on thickness and a/W ratio are described in last chapter. But in transition and lower transition failure mechanism is mainly brittle in nature and use of ductile stress parameters will not yield good results. Hence Beremin's material model for brittle fracture is used to estimate the dependence of T_0 on constraint in terms of Weibull stress. Weibull stress at the crack tip is calculated from FE analysis of each fracture test using FE software ABAQUS. Calibration of Beremin parameters, like Weibull modulus (m) and scaling parameter σ_u and $C_{m,n}$ are done using linear regression analysis of a large number of fracture test data at single test temperature of -110°C. T_0 for different thicknesses and a/W ratios are also evaluated from corresponding Weibull stress based on Beremin model using calibrated m, σ_u and $C_{m,n}$ which are compared with experimental results and case-specific good matching is obtained. The same calibrated values of Beremin parameters and $C_{m,n}$ are also used to evaluate T_0 for CT specimen of the same material using Beremin model, and an excellent matching with the experimental result is found. Then we proceed to calibrate the parameters for -100°C and -130°C in

order to study the variation of Weibull Modulus (m) & Weibull Scalar Parameter (σu) with temperature, for the Brittle dominated portion of DBT region.

4.1. Introduction

The reference temperature, T_0 is a measure of degree of embrittlement and useful for comparison of materials. But the T_0 obtained from E1921 is questionable when applied for assessments of structural defects. Structures most often have shallow, surface-breaking or embedded defects and are loaded predominantly in tension not bending, and the local J values vary strongly along the crack fronts. The ‘‘applicability’’ of T_0 values obtained from high-constraint, straight through-cracks to real applications requires additional models that accommodate effect of constraint differences and variations in local J values. Micromechanical models for brittle fracture offer the most promising approach at present to understand toughness transferability issues and to develop quantitative frameworks. In order to relate the variation in reference temperature (T_0) with thickness and a/W ratio in terms of constraint, it is required to investigate the stress scenario at failure near the crack tip. Many researchers used different finite element parameters like Q-Stress[45], Triaxiality ratio, T-stress[2], to study the effect of constraints on reference temperature (T_0) but appeared to have limitations to predict cleavage fracture. Characterization of cleavage fracture in DBTT requires local approaches which deal with the micromechanics of the failure mechanism along with the macroscopic fracture toughness namely, Jc, K_{JC}, CTOD. Beremin [17] proposed a relationship between the micro mechanism of fracture and macroscopic fracture parameters (such as the J-integral) by introducing the Weibull stress (σ_w). The model is based on statistical distribution of micro cracks present in small, statistically independent volumes of material. Each small volume experiences loading from the macroscopic (continuum) stress field described, for example, by a local value of maximum (tensile) principal stress. Beremin proposed Weibull stress σ_w as a scalar measure of the crack-front loading computed based on average of the cumulative failure probability taken over a critical volumes ahead of a crack front. A relatively simple expression for macroscopic failure probability is developed involving Weibull stress, σ_w; a Weibull modulus, (m) that characterizes the size distribution of micro cracks; a Weibull scale parameter, σ_u, that

represents the aggregate micro-crack toughness. From two parameter Weibull distribution the cumulative failure probability as a function of Weibull stress is represented by the following equation $\mathbf{P_f(\sigma_w) = 1 - exp\left[-\left(\frac{\sigma_w}{\sigma_u}\right)^m\right]}$ where 'm' denotes the Weibull modulus (shape parameter) which quantifies the statistical scatter ,and σ_u is a scale parameter which sets the value of σ_w at 63.2% failure probability. The physical significance is that the Weibull modulus, m, characterizes the size distribution of microcrack present in volume V_0. The stressed volume is assumed to be divided in smaller volumes V_0. V_0 must be large enough so that the probability of finding a microcrack of reasonable length will not be vanishingly small and that the statistical independence of neighboring volumes V_0 may be assumed. In other words, V_0 must include a certain number of grains. While the Weibull scale parameter, σ_u, represents the aggregate microcrack toughness of all this smaller volumes V_0. In the Weibull stress framework, these two coupled parameters describe material features invariant of crack-front constraint, crack-front length, etc.

The transferability models of elastic-plastic fracture toughness values rely on the notion of the Weibull stress as a crack-tip driving force [49]. This is based on the idea that unstable crack propagation (cleavage) occurs at a critical value of the Weibull stress; corresponding to a remote loading (as measured by J). The variation in the Weibull stress, due to difference in thickness and a/W ratio of the specimen, reflects the dependence of Weibull stress on near-tip stress fields. Weibull modulus, (m) plays a major role in the process to correlate effects of constraint loss for varying crack configurations and loading modes. Calibration of Weibull parameters (m, σ_u) for a given material is a key element in fracture assessment procedures based upon σ_w. Once calibrated for a material, the Weibull stress approach enables application of quantitative ''toughness scaling'' models to transfer (or scale) the measured, stochastic distributions of macroscopic toughness (K_{JC} values) from one constraint and crack-front length configuration to another based on the simple equivalence of equal cumulative fracture probabilities.[88,18].

Claudio Ruggieri and his co-workers have studied the effect of constraint loss on reference temperature (T_0) [19] using Weibull Stress as a local fracture parameter for transgranular cleavage failure. Monte Carlo procedure is used to generate trial sets of small scale yielding (SSY) fracture toughness data which follows three parameter Weibull distribution to determine T_0. Claudio Ruggieri also proposed a new procedure [89] to calibrate the Weibull stress modulus, m, which employs SSY values for cleavage fracture toughness measured in the DBT region. W.J. McAfee et al.[28] studied the effect of shallow flaw (a/w=0.1) and deep flaw (a/w=0.5) on reference temperature (T_0) for a highly-characterized A533B plate material. Due to constraint loss in the shallow-flaw specimens resulted in a -26.8 °C shift in transition temperature relative to the deep-flaw constraint condition. While both the shallow and deep-flaw data were constraint-adjusted to small-scale yielding (SSY), the shifts in T_0 were -35.5 °C and -8.1 °C, respectively. Guian Qian **[**90**]** calibrated Beremin parameters (m & σ_u) on the basis of linear regression analysis, based on a modified Weibull stress calculation strategy.

Once the parameters are calibrated, the next area of debate put forward by different researchers for the last 20 years is the sensitivity or dependence of the parameters with temperatures.

Hojo et al.[73] Calibrated distribution of Weibull stress in the brittle fracture region using notched round bar specimens and CT specimen for A533B steel and showed that m & σ_u are insensitive to temperature at least in the lower self-portion of DBT region.

Gao et al. [74] also showed in their work that m does not vary with temperature for A508 steel in the transition region. They used a 3-parameter Weibull Distribution model where the first parameter m remains constant with temperature while the Second parameter σ_u increases with temperature and third parameter the threshold value Weibull stress $\sigma_{w\text{-}min}$(below which cleavage fracture does not occur) decreases with temperature.

Bogdan Wasiluk et al.[75] studied the variation of Beremin parameters on 22Ni–MoCr37 steel similar to ASTM A508 Cl.3. They also used a 3-parameter Weibull Distribution model where the first parameter is “m” the Second parameter “σ_u” and third parameter the threshold value Weibull stress $\sigma_{w\text{-}min}$(below which cleavage fracture does not

occur).They have calibrated the parameters at two extreme temperatures of DBT region that is at -40°C & at -110°C.From the results they have concluded that "m" remains practically insensitive to temperatures,(m=20 at -40°C &m=18 at -110°C) while "σ_u" & $\sigma_{w\text{-}min}$ shows a marked increases with temperature.

Petti and Dodds [51] proposed from their study on A533B and A508 steels that, "σ_u", increases with temperature, while they assumed "m" remains invariant with temperature. They have also proposed a calibration scheme of "σ_u" with variation in temperature, by employing the Master Curve methodology.

But the work done by C.S. Wiesner and M.R. Goldthorpe [77] reveals a different trend. They studied on three types of specimen ,notched tensile specimen , notched (Charpy-type) four point bend and fracture mechanics specimens of BS 4360 Grade 50D structural steel at different temperatures. The results reveals that the parameters remains invariant with temperature for notched tensile specimen but for other two specimens notched bend and fracture mechanics specimens, the parameters shows clear dependence on temperature.

4.2. Scope of this chapter

Large number of fracture tests (38 in number) are already performed at (-110^0 C) on a variety of TPB specimens to determine the effect of thickness and a/W ratio on Reference temperature T_0. FE simulations of all the fracture tests are done and Weibull stresses are computed at failure load with an assumed Weibull modulus (*m*). Then Weibull modulus (m) and Scaling parameter (σ_u) and C_{mn} are finalized iteratively using linear regression analysis between failure probability measured from experimental results and Weibull stress obtained from FE analysis for the same experiment. Fracture test results of 38 TPB specimens of different thickness and a/w ratio at a fixed temperature of -110^0C have been used in regression analysis to capture the probabilistic nature of the failure process and to extract the material parameters valid over a wide range of thickness and a/w ratio. The value of Beremin coefficient $C_{m,n}$ is also determined from fracture test results using Beremin formulation. $C_{m,n}$ [56] is actually a function of Weibull modulus (*m*) and Power Law Hardening (n) for a given material.

From the value of the Weibull stress at failure load of each specimen obtained from FE simulation, the value of probability of failure and hence the fracture toughness are calculated using Beremin model with calibrated *m* and σ_u and $C_{m,n}$. Using the value of fracture toughness obtained by the application of Beremin model for a set of specimens with fixed thickness or a/w ratio, the corresponding value of T_0 can be calculated. Variation of Reference Temperature (T_0) obtained from Beremin model for variation in both thickness and a/W ratio is studied and compared with the variation of Reference Temperature (T_0) obtained from direct experiment (ASTM E1921-02). The same values of Beremin parameters *m* and σ_u and $C_{m,n}$. are used to predict T_0 from FE analysis for CT specimen of the same material of different a/w ratio and compared with experimental results. Then an attempt is taken to calculate the values of Beremin parameters m , σ_u and $C_{m,n}$ for -100°C and -130°C in order to study the variation of Weibull Modulus (m) & Weibull Scalar Parameter (σ_u) with temperature, for the Brittle dominated portion of DBT region using the values for -110°C.

$$\ln\left[\frac{1}{1-P_f}\right] = \frac{\sigma_0^{m-4} K_{1C}^4 B C_{m,n}}{V_0 \sigma_u^m}$$

Where,
P_f= Probability of failure
σ_0= Yield stress of the material for a specific temperature
K_{1C}=Fracture Toughness
B=Width of the material
V_0=controlled volume
σ_u= Weibull scale parameter
m= Weibull modulus
$C_{m,n}$= Function of Weibull modulus (m) and Power Law Hardening (n) for a given material.

Calculating P_f with the help of Weibull stress and using the parameters in the above equation K_{1C} can be calculated. This K_{1C} is the predicted value from Beremin model.

4.3 Reference Temperature (T_0) for different a/W ratio and thickness.

T_0 are calculated by single temperature methods (ASTM-1920) for TPB specimen of different thickness and *a/W* ratio for the material 20MnMoNi55 steel at a fixed temperature of -110^0C. Master curves for *a/W* ratio of 0.5 and 0.6 are shown in Figs.2.22

and 2.20. At least six numbers of valid K_{JC} values of each thickness or *a/W* ratio are considered for evaluation of respective T_0 .

The variation of T_0 with *a/W* ratio and thickness of specimen are shown in the Table 4.1. It is seen that value of T_0 decreases up to *a/W* ratio of 0.5 and then increases with increase in the value of *a/W* ratio. The values of T_0 for different *a/W* ratio lies within a variation of 10.8 The variation observed is without any specific trend and the maximum variation observed (14^0C) is nearly 10%.The effect of thickness on T_0 is studied and shown in the Table.4.1 and the Master Curve for the respective thickness is shown in Fig. 2.12 to 2.15 It is seen that, T_0 decreases with increase in thickness and reaches a minimum value at 20 mm thickness and then the value again increases with increase in thickness and gets saturated.

Table4.1: Reference Temperature T_0 obtained from Experiment for different *a/W* ratio and Thickness of the TPB specimen.

a/W	***T_0***	**Thickness(mm)**	***T_0***
0.4	-149.44	30	-153.36
0.45	-145.8	25	-150.77
0.5	-156.2	20	-148.4
0.55	-153.57	15	-147.9
0.6	-147.16	12	-147.92
0.65	-159	10	-141.9

4.4. Variation of T_0 with thickness and a/W ratio.

Variation of T_0 with a/W ratio or thickness are found to be within 10% and no specific trend is observed. This variation is accepted in ASTM E 1920 as measurement uncertainty. The amount of uncertainty comprises of bias and random components. In reality the value of T_0 for a sample depends on K_{JC} values which depend on failure points. The failure point in transition zone is governed by random distribution of nucleation sites and can be captured by Weibull parameters. But the plasticity level at failure point influence K_{JC} values and so T_0. Though the plastic zone size depends on failure load level it is also dependent on constraint level of the specimen related to specific a/w ratio or thickness. In ASTM E 1920 the evaluation of T_0 does not take care of the stress state at the crack tip of the specimen and it proposes a value of T_0 independent of a/W ratio or

thickness. The variation in T_0 may be contributed partly due to variation in stress level at crack tip because of variation in a/w ratio and thickness and partly by randomness in failure point governed by randomly distributed nucleation sites. A better case specific prediction of T_0 for a sample of given thickness and a/W ratio may be possible if the effect of stress level at failure load at that thickness and a/W ratio is considered while evaluation of T_0 using the material parameters related to randomness in failure. This consideration of constraints in evaluation of T_0 may improve the uncertainty band by eliminating the bias due to constraint level.

4.5. F.M. Beremin Model.[17]

To consider the effect of stress level on T_0, it is preferred to derive that stress criteria from a micro mechanistically based model which can describe the physical process of fracture at low temperature. In the present study Weibull Stress to be derived from Beremin model is considered as local stress based criteria to predict probability of cleavage failure. Before application of Weibull Stress it is quite essential to calibrate the values of Weibull modulus (m) and Scaling parameter σ_u for the referred material at the temperature of interest, for its flawless application.

The model proposed by Beremin had two main assumptions in the method:

- The failure probability inside a small uniformly stressed volume can be expressed by the stress level and the distribution of micro cracks in this volume.
- The total failure probability of the whole component follows a weakest link mechanism, and failure in one part of the component results in final failure of the whole component.

Based on these assumptions a relatively simple expression for macroscopic failure probability is developed involving Weibull stress, σ_w; a Weibull modulus, (m) that characterizes the size distribution of micro cracks; a Weibull scale parameter, σ_u, that represents the aggregate micro-crack toughness.

According to Beremin model, the probability of failure is given as,

$$P_f = 1 - \exp\left(-\left(\frac{\sigma_w}{\sigma_u}\right)^m\right) \qquad (4.1)$$

$$\sigma_w = \sqrt[m]{\left(\sum_{j=1}^{n} \sigma_1^j\right)^m \frac{V_j}{V_0}} \qquad (4.2)$$

n is the number of volumes *Vj*, or elements in a FEM calculation and σ_1^j the maximal principle stress of the element j and V_j/V_0 is just a scaling based on the assumption that the probability scales with the volume.

4.6. Finite Element Analysis for Computing Weibull Stress at Failure Point for TPB Specimen

Elastic-plastic finite element analysis for all the fracture tests is performed using ABAQUS 6.13. The material constitutive properties are defined by the Young's modulus E , Poisson's ratio ν , and Yield stress versus plastic strain obtained from tensile test data performed at -100°C, -110°C ,-120°C -130°C, -140°C ,in Universal Testing Machine (Instron 8801) [36,37].Figure 4.1 shows the stress versus plastic strain diagram at different temperatures and Table 4.2 gives the Yield Stress and Ultimate Stress verses Temperature for 20MnMoNi55 steel at different temperatures in the Brittle Dominated DBT region which is used as material input parameter for Elasto plastic finite element analysis. Isotropic elastic and isotropic hardening plastic material behaviour are considered for the material used.

3-D finite element modelling is done for quarter TPB specimen of respective *a/W* ratio and thickness to calculate the Weibull stress for the specimen and hence to calculate T_0 from Beremin model. The FE model was meshed with 8-node isoparametric hexahedral elements with 8 Gauss points taken for all calculations as referred by IAEA-TECDOC-1631[78]**.** Reduced integration with full Newtonian non-linear analysis computation is carried out for all the specimens. In the region ahead of crack tip the mesh was refined with element volume of 0.05 X0.05 X 0.05 mm^3 .In order to facilitate in the calculation

of Vj the element size is kept constant near the crack tip.[78,91] Since large strain is expected in the crack tip field, a finite strain (large deformation theory) method is used.

As the crack extension during the experiment is found to be very small, the crack growth is not simulated in this FE analysis. The boundary condition of application of load and extraction of load and displacement was done by following guidelines of IAEA-TECDOC-1631project finite element round robin program. The rollers are defined as analytically rigid bodies.

The boundary conditions and the mesh for TPB specimen are shown in figure 4.2.(a) .and the maximum principal stress distribution at -110°C where the stress has exceeded twice the yield stress at that temperature, known as fracture process zone shown in Fig.4.2.(b) which is required to calculate Weibull stress (σ_W) .

The boundary conditions and the mesh for Compact Tension (CT) specimen are shown in figure 4.3.(a) .and the maximum principal stress distribution at -110°C where the stress has exceeded twice the yield stress at that temperature, known as fracture process zone shown in Fig.4.3.(b) which is required to calculate Weibull stress (σ_W) .

Table4.2: Yield Stress and Ultimate Stress verses Temperature for 20MnMoNi55 steel at different temperatures in the Brittle Dominated DBT region

Temperature (^{0}C)	**Yield Strength (MPa)**	**Ultimate Strength (MPa)**
-100	593.43	760.49
-110	630.43	786.56
-120	667.06	813.66
-130	701.451	825.054
-140	723.47	856.84

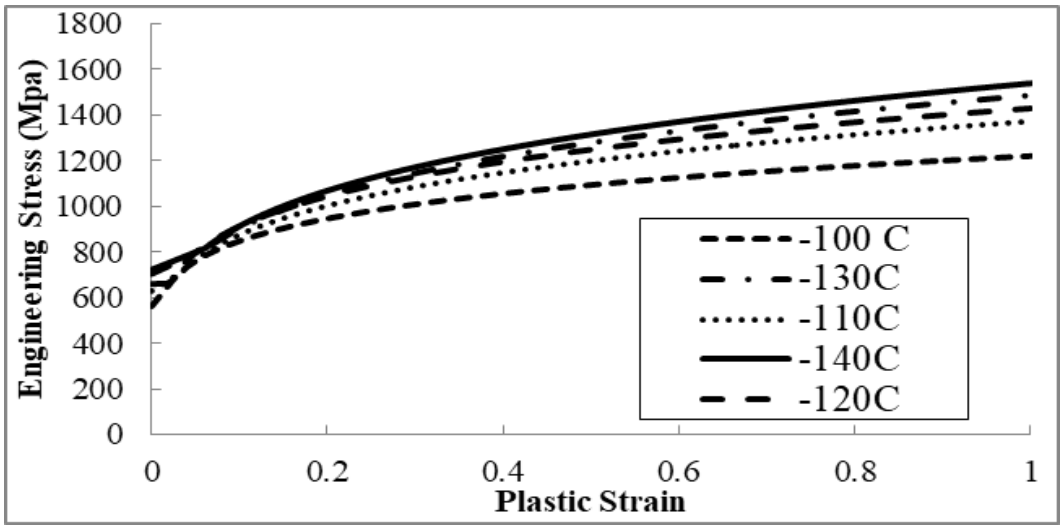

Fig.4.1.Engineering Stress verses Plastic strain for 20MnMoNi55 steel at different temperatures in the Brittle Dominated DBT region

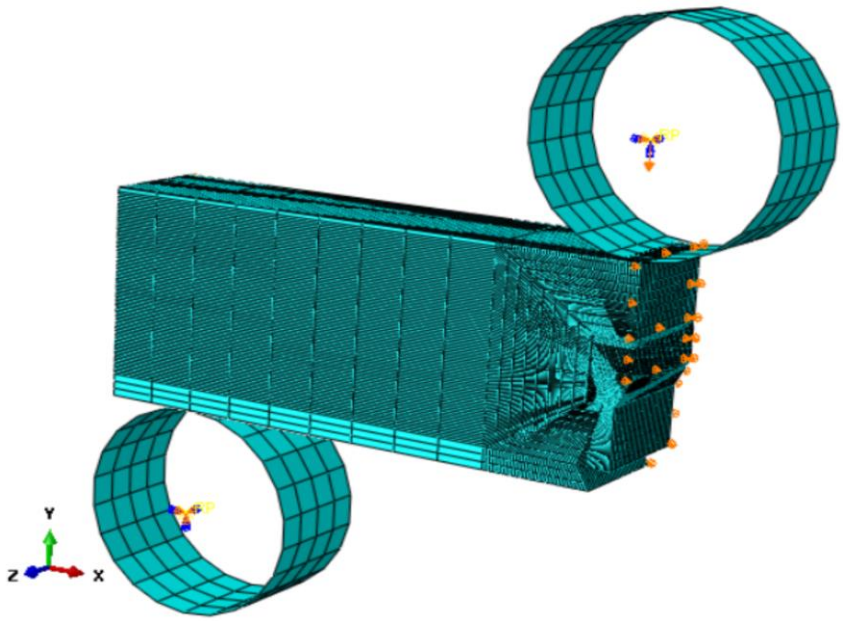

Fig. 4.2.(a) Quarter TPB specimen model along with boundary conditions

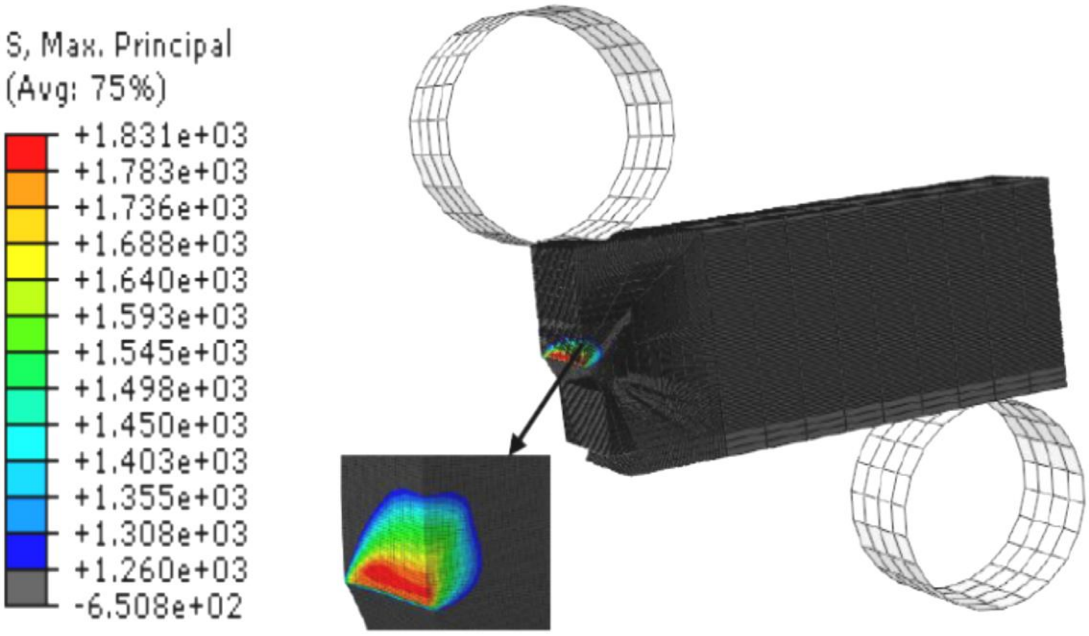

Fig.4.2(b). Maximum principal stress (MPa) distribution in the fracture process zone**.**

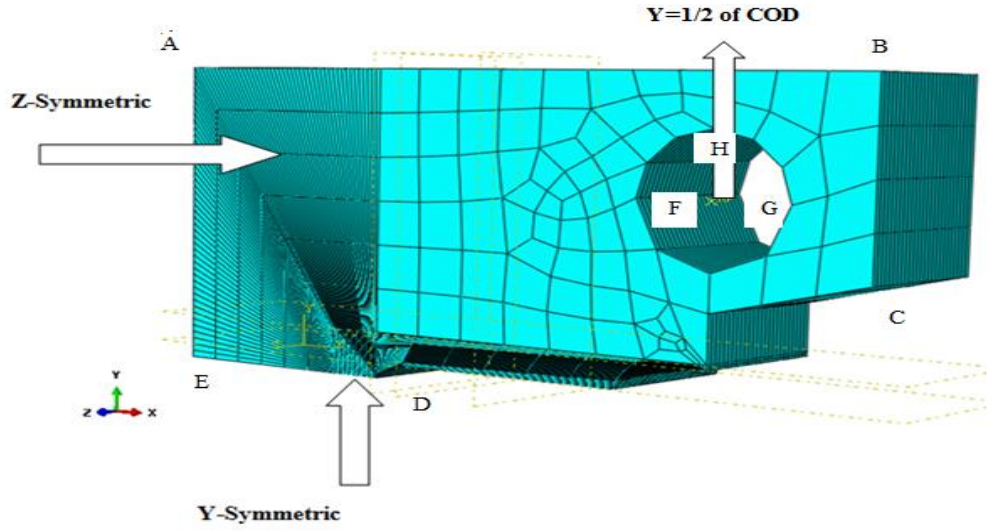

Y-Symmetric along ED through thickness. (Symmetric Boundary condition is imposed on the plane along ED through thickness)
Z-Symmetric along plane ABCDE. (Symmetric Boundary condition is imposed on the plane ABCDE)
Displacement equal to half of Crack Tip Opening displacement is applied along the Y-Direction as shown, throughout the thickness of the specimen along the semicircle FHG.

Fig 4.3.(a). Showing Boundary Condition and mesh distribution on CT Specimen of a/W=0.

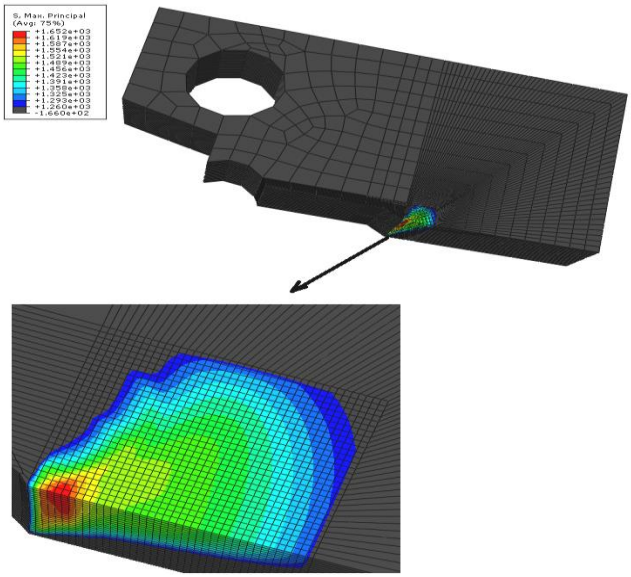

Fig. 4.3(b). Quarter model of Compact Tension (CT) specimen showing Maximum Principal Stress distribution in the fracture process zone (FPZ) region

4.7. Validation of the FE model and material properties

Fig.4.4.a., 4.4.b and 4.4.c gives a comparison between experimental load verses Load Line Displacement (LLD) of TPB specimen with FE simulated results from Abaqus 6.13 at the -100°C,-110°C and -130°C temperatures Fig.4.4.d presents comparison of J-Integral vs. Load Line Displacement (LLD) of experiment and FEA of TPB specimen at the same test temperature (-110°C). The crack is assigned in the TPB model using contour integral and the crack extension direction is shown through q-vector method. Q-vector method is used for virtual crack extension direction. The direction of virtual crack extension at each crack tip in two dimensions or at each node along the crack line in three dimensions can be provided by specifying either the normal to the crack plane, $\mathbf{n}$, or the virtual crack extension direction, $\mathbf{q}$. In this case ABAQUS/Standard will calculate a virtual crack extension direction, $\mathbf{q}$, that is orthogonal to the crack front tangent, $\mathbf{t}$, and the normal, $\mathbf{n}$.Abaqus has provision to calculate J-Integral directly in step with applied load for several contours. In this work average J integral is calculated based on J integral for three contours.The FEA results show close match with experimental results which

validate the used FE model and material parameters. Now for each analysis the Weibull stress at the failure point can be computed from the FE simulated results.

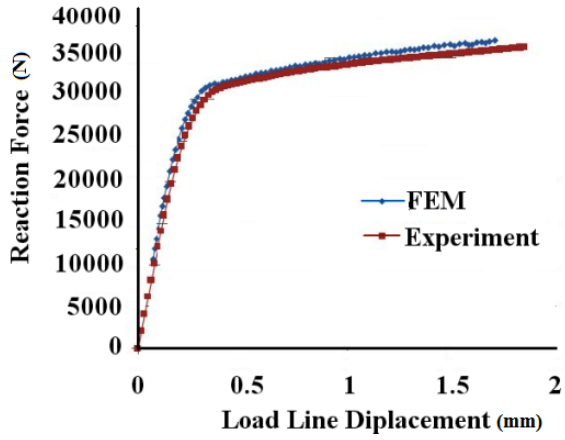

Fig.4.4(a). Comparison of load vs. Load Line Displacement (LLD) -100 °C

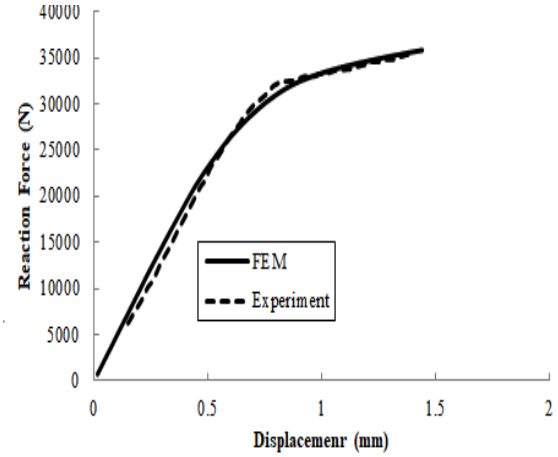

Fig..4.4(b). Comparison of load vs. Load Line Displacement (LLD) -110 °C

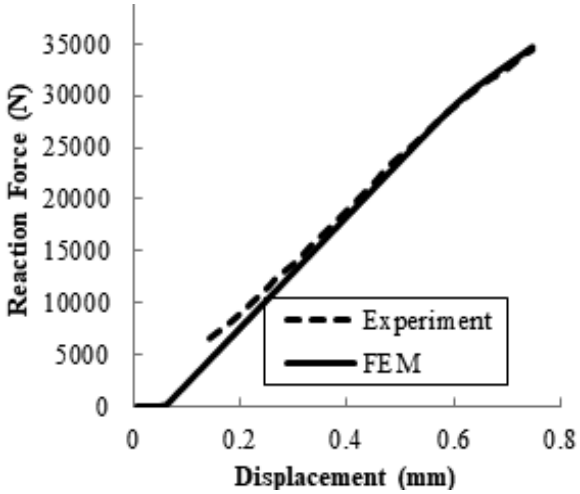

Fig..4.4(c) Comparison of load vs. Load Line Displacement (LLD) -130 °C

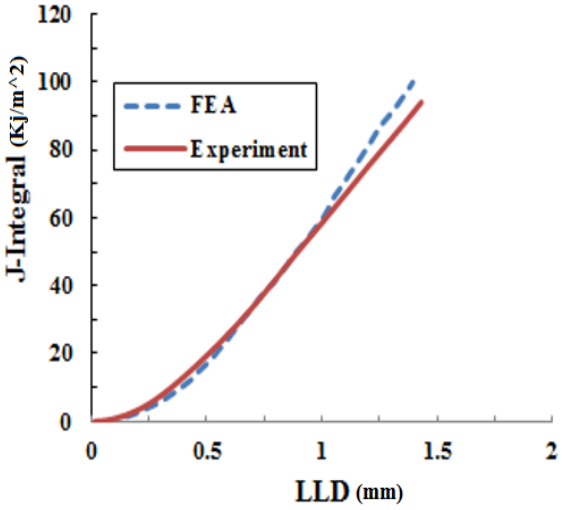

Fig..4.4(d) Comparison of J-Integral vs. Load Line Displacement (LLD) -110

4.8. Computation of Weibull stress at failure point for specimens with different thickness and *a/W* ratio.

Figure 4.2(a) shows the finite element model constructed for analyses of standard quarter (1T) TPB specimen along with the boundary condition used.Fig.4.2 (b) shows the maximum principal stress distribution at the failure displacement of a quarter TPB specimen. From the maximum principal stress distribution the volumes V_j are selected, where the Maximum Principal Stress values has exceeded the Twice the Yield stress values [49,50,75] at the test temperature of (-110 °C) marked the region of the fracture processed zone (FPZ) as shown in Fig. 4.2(b). The Weibull stress is computed most often by integrating the maximum principal stress, σ_1, over the fracture process zone, V_j, at each stage of loading. The hexagonal element size is taken as (0.05X0.05X0.05) mm^3 which will indicate a single volume V_j having 8 nodes. The rationale of choosing this element size is discussed previously. V_j is the volume of the jth element experiencing the maximum principal stress. The length of each side of Reference Volume V_0 is taken as 0.05 mm.[17]

4.9. Determination of Weibull Modulus (*m*) and scaling parameter σ_u

The success of Beremin model for predicting brittle fracture mainly depends on the accuracy of the values of the Beremin material parameters *m* and σ_u. Beremin model describes the failure mechanism as an outcome of distribution of weakest sites in the material which is statistical in nature. Hence any material parameters to represent the failure behaviour should be determined from a large sample containing variation in candidatures as much as possible. With this in mind the values of m and σ_u have been determined from the experimental fracture toughness tests at -110^0 C with specimens of different *a/W* ratio and thickness. All the tests are performed at single temperature to avoid the temperature dependence of *m* and σ_u. The procedural steps are described below.

Step 1. Taking the censored K_{JC} values (38 in number) from experiment for TPB specimens of varied *a/W* ratio and thickness, K_0 is calculated according to the equation 2.4.

Step 2. From the known K_0 value, Probability of failure (P_f) is calculated according to equation 2.1 for each experimental K_{JC}.

Step 3. An initial value of '*m*' is assumed and Weibull stress is calculated for each of the TPB specimens having valid K_{JC} values from equation 4.2.. Probability of failure of the specimen can be calculated from Beremin formula using Weibull stress and m and σ_u.

Step 4. Linear regression method is used as an iterative process to estimate '*m*' [71] Where 'm' is the slope of the linear fit of $\ln[\ln[1/(1-P_f)]]$ vs. $\ln \sigma_w$ and σ_u is obtained from the intercept of the curve.

Step 5. The initial estimates for *m* and σ_u will be updated with the new values. The process is repeated until converged values are obtained to match the slope the process is shown in Fig.4.5 (a) & 4.5.(b). From the above procedure m and σ_u are calibrated as m=21,σ_u=2518 MPa respectively for this material at -110^{0}C. This value matches well with that predicted by Beremin [17] for A508 class 3steel in the transition region and also with the work of Claudio Ruggieri et al. [19] where they suggested that value of m for common structural and pressure vessel steels range from 10 to 50.

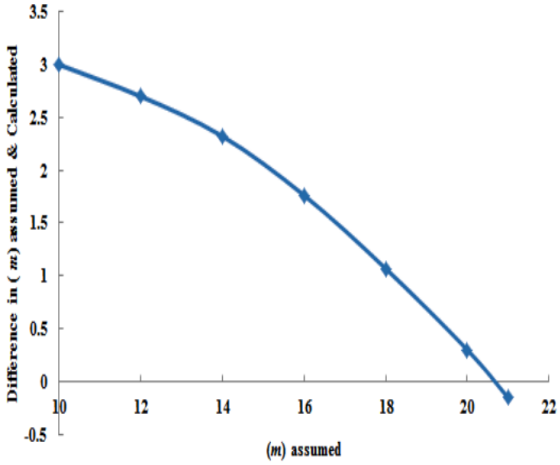

Fig.4.5.(a). Showing convergence in assumed and calculated value of m from linear Regression Analysis.

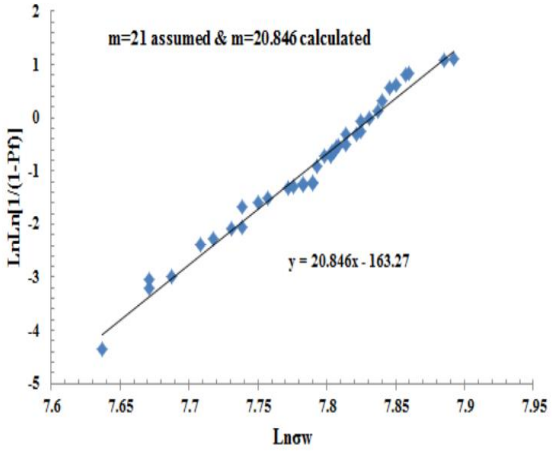

Fig. 4.5.(b). Linear regression analysis of m at T =-110^{0}C.

Linear regression analysis technique gives several correct values of the Beremin model parameters, but from the calculated value of Beremin parameters the K_{JC} and ultimately reference temperature T_0 is predicted which are compared with the experimental results. The values of Beremin parameters which predict ambiguous values of K_{JC} are rejected and the values which predict a matching trend with the experimental results are accepted.

4.10. Estimation of $C_{m,n}$

Beremin model predicts the scatter in the brittle part of the brittle-to-ductile transition curve of ferritic steels but from an engineering point of view, the application of this model has been restricted by the lack of an analytical solution for one of its parameters, $C_{m,n}$ [56] The coefficient Cm,n can be determined by the integration of the following expression[56] provided that m < 2(n+1)/n. Further analytical calculations are not possible because the analytical variations of up and therefore up with θ and n are not known. It is therefore necessary to perform numerical elastoplastic simulations to evaluate Cm;n which is an extremely laborious and time consuming process with respect engineering point of view.

$$\mathbf{C_{m,n} = \left(\frac{1-\nu^2}{\alpha_p I_n}\right)^{\frac{mn}{n+1}} \frac{1}{2-\frac{mn}{n+1}} \int_{-\pi}^{\pi} \sigma_{ij}(\theta) \left[u^{2-\frac{mn}{n+1}} \right]_0^{u_p(\theta)} d\theta}$$

Thus in this work, particular attention is paid to calculate $C_{m,n}$ in a different procedure as described below.

4.10.1 Small-scale yielding (SSY) conditions

The stress-strain field ahead of the crack tip under SSY conditions is simply scaled by the ratio x / (J / σ_{YS}) where x is the distance from the crack front. Under these conditions by the application of the Beremin model, the probability to fracture of a specimen containing a 2D crack expressed in terms of K_{IC} can simply be written as:

$$\ln\left[\frac{1}{1-P_f}\right]=\frac{\sigma_0^{m-4}K_{IC}^4 BC_{m,n}}{V_0\sigma_u^m} \qquad (4.3)$$

Where, $C_{m,n}$ is a numerical factor which depends on the work-hardening exponent n, ($\sigma = K\,\varepsilon^n$) , σ_0 is the yield stress at the test temperature (-110^0C) and V_0 is the reference volume (50x50x50)µm.

Now equation 4.3 can be written in the form

$$Y = AXK_{IC}^4 \qquad (4.4)$$

$$Y=\ln\left(\frac{1}{1-P_f}\right) \qquad (4.5)$$

Where,

$$\text{A=constant=}\frac{\sigma_0^{m-4}C_{m,n}B}{V_0\sigma_u^m} \qquad (4.6)$$

P_f for all valid K_{JC} values are then calculated using rank probability from the following equation

$$P_f=\left((j-0.5)/N\right) \qquad (4.7)$$

Where, j is the rank number and N defines the total number of valid experimental K_{JC} values (N=38 in the present work).

Then the slope of the curve ln (Y) vs. ln (K_{JC}) is measured and is obtained as 4.088 which matches with relation given in equation (10) and then the value of A is estimated from the intercept of this curve, as shown in Fig.4.6. Once the value of A is obtained the value of $C_{m,n}$ is calculated as because the values of σ_0, V_0, σ_u, and B are already known. The value of $C_{m,n}$ thus obtained is as1.64E+09.

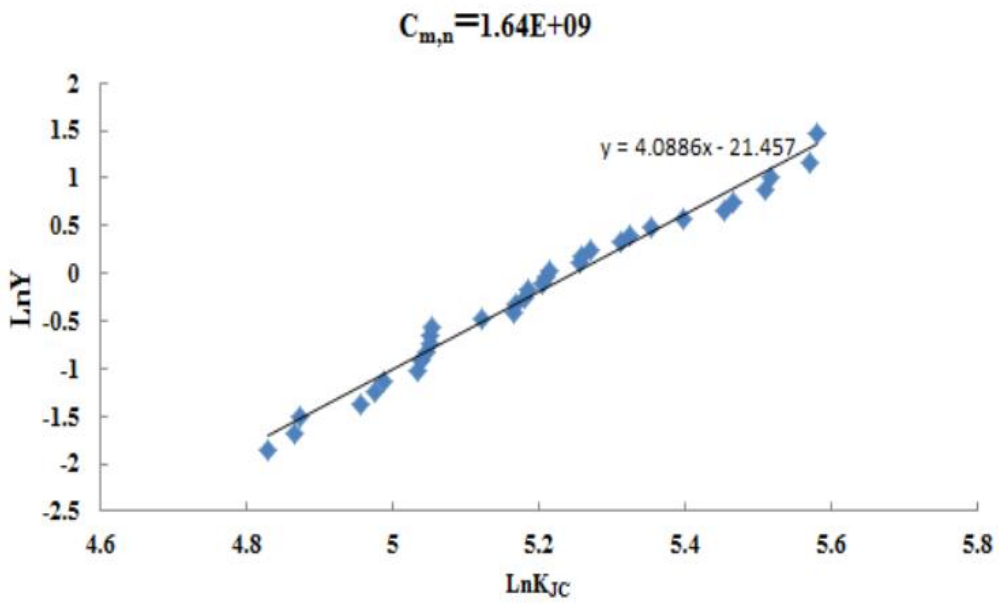

Fig. 4.6.Estimation of $C_{m,n}$ at T = -110^{0}C

4.11. Calculation of Reference Temperature T_0 from Beremin model

Once the value of material parameters $C_{m,n}$, m and σ_u are calibrated from the test data, the prediction of K_{JC} for different thickness and *a/W* ratio considering the effect stress at crack tip based on Beremin model are possible from Eq. (9) if the value of Weibull stress at the failure point is known. From the values of K_{JC} computed from Beremin model for a particular thickness or *a/W* ratio, corresponding T_0 can be computed. The value P_f for the specimen will be computed based on Weibull stress obtained from FE simulation of the specimen which will take care of the particular constraint level.

Table 3.gives a detailed comparison of K_{JC} obtained from experiment and Beremin model for different /W ratio and thickness. The Specimen Identified in the following manner. Name of the Specimen(TPB)_Width of Specimen(W)_Span Length(S)_Thickness(B) _ a/W ratio(a) as shown in Fig.4.7.For Compact tension specimen same specimen identification procedure is followed as shown in Fig.4.7(b).

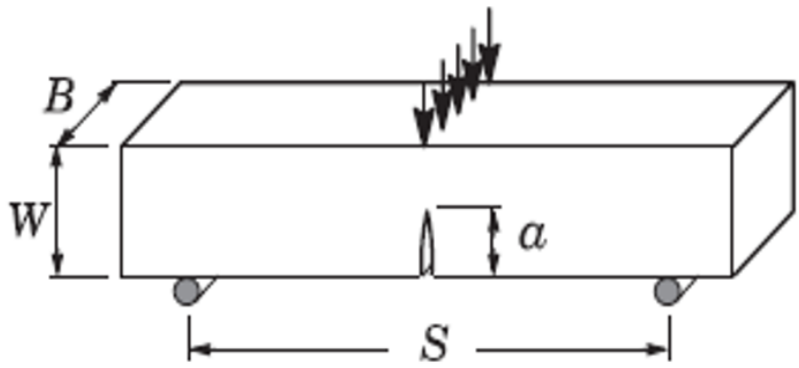

Fig. 4.7(a). Dimensions of TPB specimen.

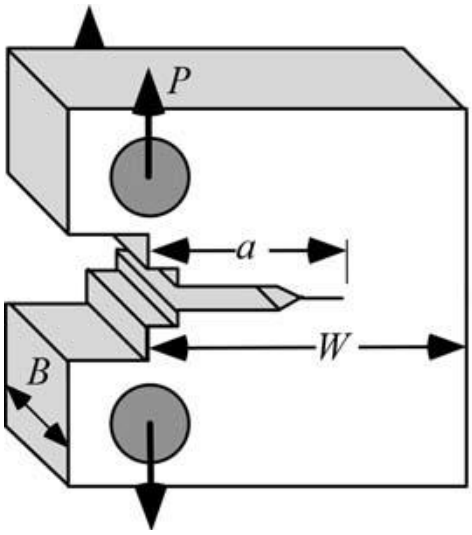

Fig. 4.7(b).Dimensions of CT specimen.

Thus K_{JC} values are predicted from Beremin Model using calibrated values of Weibull Modulus (m), scaling parameter (σ_u) and $C_{m,n}$. Then Reference Temperature T_0 of TPB specimen for different a/W ratio and thickness are evaluated and compared with experimental result. Tables 4.4 and 4.5 show a close matching of predicted Reference Temperature T_0 with experimental values for both a/W ratio and thickness variation of the specimens respectively. From the results it is observed that the maximum error in the estimation of T_0 from Beremin model is less than 6% which is very much hopeful. The limitation of this procedure is due to the requirement of the value of displacement at failure point to be fed in FE simulation to calculate corresponding Weibull stress. But it is

evident from the results that the variation in T_0 due to constraint level if can be captured through the Weibull stress at the failure point the scatter in T_0 is reduced. Besides, it also can be concluded that the calibrated values of Weibull Modulus (m), scaling parameter (σ_u) and $C_{m,n}$ are acceptable considering the correctness in predicted values of T_0 from Beremin model.

$P_{f,}$ the failure probability, obtained from Beremin model is compared with that of obtained from ASTM E1921, Wallin's Master Curve Methodology as per Eq.1 from experimental values and the comparison are shown for a/W ratio 0.45 and 0.6.in fig. 4.9(a) &4.9(b).

Table 4.3. Comparison of Fracture toughness test results for TPB specimens obtained from Experiment and Beremin Model taking m=21,σ_u=2518 MPa and $C_{m,n}$= 1.64E+09

Specimen Id.	Thickness (mm)	a/W Ratio	K_{IC}(MPa.m0) (From Experiment)	Failure Load Line Disp. LLD (mm)	Weibull Stress (σW)	Probability of Failure Pf (Predicted from Beremin Model)	K_{IC}(MPa.$m^{0.5}$) (Predicted From Beremin Model)
TPB_25_100_30_p5	30	0.50	251.8	1.839	2676.98	0.973	281.488
TPB_25_100_30_p55	30	0.55	150.52	0.96	2474.11	0.499	186.113
TPB_25_100_30_p6	30	0.60	139.2	0.926	2437.42	0.396	172.07
TPB_25_100_30_p65	30	0.65	148.23	1.394	2501.7	0.582	197.273
TPB_25_100_30_p7	30	0.7	156.6	1.452	2473.95	0.498	186.049
TPB_25_100_30_p45	30	0.45	246.62	1.67	2657.47	0.955	270.8
TPB_25_100_25_p4	25	0.40	196.43	1.25	2493.93	0.558	214.78
TPB_25_100_25_p45	25	0.45	183.92	1.08	2532.27	0.68	220.06
TPB_25_100_25_p5	25	0.50	155.93	0.95	2415.75	0.34	171.85
TPB_25_100_25_p55	25	0.55	196.20	1.42	2540.49	0.70	223.84
TPB_25_100_25_p6	25	0.60	248.82	2.082	2591.59	0.84	248.514
TPB_25_100_25_p65	25	0.65	175.48	1.29	2461.23	0.462	189.53
TPB_25_100_20_p4	20	0.40	131.26	0.75	2337.78	0.189	152.96
TPB_25_100_20_p45	20	0.45	249	1.93	2567.35	0.78	250.12
TPB_25_100_20_p5	20	0.50	222.17	1.68	2585.3	0.82	259.44
TPB_25_100_20_p55	20	0.55	213.14	1.446	2517.72	0.63	225.75
TPB_25_100_20_p6	20	0.60	193.45	1.547	2502.65	0.585	218.75
TPB_25_100_20_p65	20	0.65	183.79	1.38	2454	0.44	197.3
TPB_25_100_20_p65	20	0.65	163.33	1.187	2416.25	0.343	181.9
TPB_25_100_20_p65	20	0.65	307.25	2.43	2554.72	0.74	243.73
TPB_25_100_15_p4	15	0.40	158.56	0.887	2321.88	0.16	158.578

TPB_25_100_15_p45	15	0.45	200.26	1.167	2398.27	0.302	187.954
TPB_25_100_15_p5	15	0.50	214.83	1.37	2448.43	0.43	209.53
TPB_25_100_15_p6	15	0.60	205.2	1.676	2450.62	0.43	210.514
TPB_25_100_15_p65	15	0.65	174.73	1.64	2423.52	0.36	198.58
TPB_25_100_15_p35	15	0.35	262.74	1.645	2458.40	0.45	262.74
TPB_25_100_12_p4	12	0.40	314.23	2.14	2399.71	0.31	199.36
TPB_25_100_12_p45	12	0.45	183.53	1.027	2294.8	0.13	157.659
TPB_25_100_12_p5	12	0.50	209.6	1.36	2382.06	0.27	191.783
TPB_25_100_12_p6_1	12	0.60	151.97	0.95	2277.16	0.11	151.4
TPB_25_100_12_p6_2	12	0.60	120	0.69	2180.7	0.05	120.63
TPB_25_100_12_p65	12	0.65	142.74	0.92	2248.5	0.09	141.66
TPB_25_100_10_p4_1	10	0.40	252.7	1.55	2294.84	0.13	165.03
TPB_25_100_10_p4_2	10	0.40	129.1	0.69	2146.27	0.03	116.13
TPB_25_100_10_p5	10	0.50	272.1	1.94	2373.45	0.25	196.95
TPB_25_100_10_p45_1	10	0.45	130.46	0.678	2145.47	0.034	115.90
TPB_25_100_10_p45_2	10	0.45	179.35	0.99	2226.27	0.07	140.73
TPB_25_100_10_p55	10	0.55	98.65	0.537	2073.38	0.02	96.87

Table 4.4. Comparison of Reference Temperature (T_0) for TPB specimens obtained from Experiment and predicted from Beremin Model for different a/W ratio.

a/W	Experimental T_0	Average (Mean)	Standard Deviation	T_0 predicted from Beremin Model	Average (Mean)	Standard Deviation
0.4	-149.44	-151.86	4.78	-144	-151.82	5.15
0.45	-145.8			-150.54		
0.5	-156.2			-160.11		
0.55	-153.57			-152.79		
0.6	-147.16			-152.08		
0.65	-159			-151.43		

Table 4.5. Comparison of Reference Temperature (T_0) for TPB specimens obtained from Experiment and predicted from Beremin Model for different thickness.

Thickness (mm)	Experimental T_0	Average (Mean)	Standard Deviation	T_0predicted from Beremin Model	Average (Mean)	Standard Deviation
30	*-153.36*	-150.78	4.93	-160.16	-149.52	10.07
25	-151.49			-156.31		
20	-158			-154.63		
15	-151.92			-151.35		
12	-147.92			-140.54		
10	-142			-134.12		

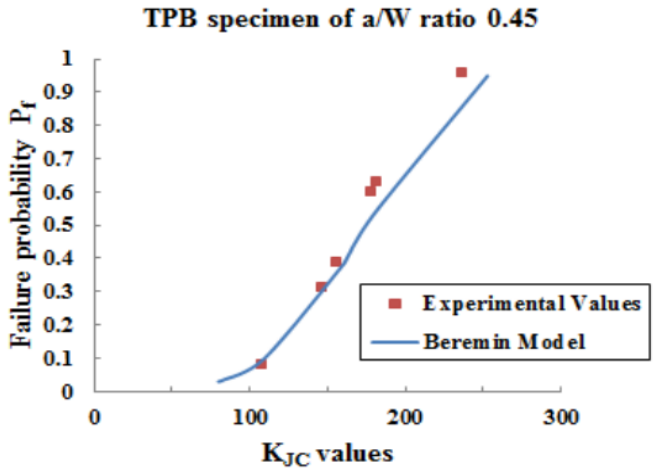

Fig.4.8(a). Failure probability (PR) verses K_{JC}

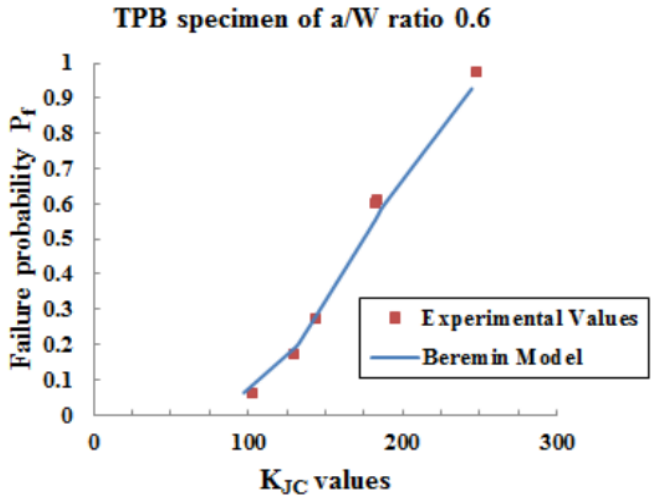

Fig.4.8(b). Failure probability (PR) verses K_{JC}

4.12. Prediction of T_0 of CT specimens using Beremin model and material parameters m and σ_u obtained from TPB specimens at -110^{0}C.

It is observed that Scaling parameter σ_u=2518 MPa, and Weibull Modulus (m) = 21 gives compatible matching with the experimental results for different thickness and a/W ratio of TPB specimen. An attempt is taken to verify acceptability of the values of m and σ_u based on the result with that of CT specimen of the same material and at same temperature.

Finite Element .Analysis are performed on CT specimen taking failure displacements from experimental results [36, 37 & 48]. Again computing the Weibull stress according to equation 4.1 taking m=21 and σ_u=2518 MPa. K_{JC} values are evaluated from equation 4.3. Then Reference Temperature (T_0) is calculated and compared with the experimental results for CT specimen.

Table 4.6 gives a detailed comparison of K_{JC} obtained from two different processes for CT specimen at -110^{0}C .Reference Temperature (T_0) calculated in two ways firstly from experiments using Kim Wallin's Master Curve Metodology (ASTM E1921-02) and Secondly from the K_{JC} values obtained with the help of Beremin model is presented. Table4.7 gives a detailed Comparison of Reference Temperature (T_0), for CT specimens obtained from Experiment and predicted from Beremin Model for different a/W ratio . The maximum error in estimation is observed to be within 3%.

It is observed that calibration of the values of Weibull modulus (m) and Scaling parameter σ_u and $C_{m,n}$ are applicable for both the TPB and CT specimens for the material 20MnMoNi55 steel in the DBT region for a fixed temperature.

Table 4.6. Comparison of Fracture toughness test results for CT specimens obtained from Experiment and Beremin Model taking m=21 σ_u=2518 MPa and $C_{m,n}$= 1.64E+09

Specimen Id.	***a/W* Ratio**	**K_{IC}(MPa.m$^{0.5}$) (From Experiment)**	**Failure Crack Tip Opening Disp. COD (mm)**	**Weibull Stress (σ_W)**	**Probability of Failure P_f (Calculated from Beremin Model)**	**K_{Ic}(MPa.m$^{0.5}$) (Predicted From Beremin Model)**
CT_25_62.5_25_0.45	0.45	183.29	0.845	2395.943	0.296	164.578
CT_25_62.5_25_0.45	0.45	178.75	0.803	2389.799	0.28	162.3749
CT_25_62.5_25_0.45	0.45	166.96	0.747	2378.206	0.26	158.282
CT_25_62.5_25_0.45	0.45	69.75	0.276	2188.108	0.05	102.2075
CT_25_62.5_25_0.45	0.45	62.387	2.44	2153.574	0.037	94.0178
CT_25_62.5_25_0.45	0.45	47.7	0.183	2038.658	0.012	70.498
CT_25_62.5_25_0.5	0.5	62.546	0.267	1969.250	0.005	70.498
CT_25_62.5_25_0.5	0.5	82.807	0.372	2098.529	0.022	82.068
CT_25_62.5_25_0.5	0.5	131.767	0.593	2286.260	0.123	128.685

CT_25_62.5_25_0.5	0.5	172.887	0.714	2350.536	0.21	148.849
CT_25_62.5_25_0.5	0.5	96.3966	0.437	2165.298	0.04	96.73
CT_25_62.5_25_0.5	0.5	134.450	0.769	2373.950	0.25	156.8
CT_25_62.5_25_0.6	0.6	74.5683	0.366	2205.046	0.059	106.430
CT_25_62.5_25_0.6	0.6	157.193	0.925	2340.612	0.193	145.579
CT_25_62.5_25_0.6	0.6	182.846	1.218	2409.143	0.326	169.394
CT_25_62.5_25_0.6	0.6	135.619	0.834	2322.157	0.166	139.653
CT_25_62.5_25_p6	0.6	102.588	0.5709	2192.424	0.053	103.27
CT_25_62.5_25_p6	0.6	171.611	1.0	2354.04	0.215	150.018

Table 4.7. Comparison of Reference Temperature (T_0) for CT specimens obtained from Experiment and predicted from Beremin Model for different a/W ratio.

a/W	Experimental T_0	Average (Mean)	Standard Deviation	T_0 predicted from Beremin Model	Average (Mean)	Standard Deviation
0.45	-133.98	-130.709	5.64	-129.06	-126.99	4.03
0.5	-124.197			-122.35		
0.6	-133.95			-129.56		

4.13. Variation of Weibull Modulus (m) & Weibull Scalar Parameter (σ_u) with temperature, for the Brittle dominated portion of DBT region.

Reference Temperature T_0 predicted from the Beremin model shows a matching trend with that of ASTM E1921 for both TPB and CT specimen at -110°C, which reflects the accuracy in calibrating the Beremin parameters for our material (20MnMoNi55 steel) as discussed in the first half of the chapter .With this understanding we calibrated the parameters for -100°C,-130° to study the effect of temperature on the Beremin Parameters specially in lower self of the DBT region. The process of calibration remains identical as used for -110°C by performing more than 30 number of fracture tests at -100°C, -130°C and then calibrating the values as discussed in index 4.9..Results obtained from, fracture test of 30 1T, TPB specimen for temperature -100°C,-130°C and -110°C for the material (20MnMoNi55 steel) are shown in figure 4.9(a) , 4.10(b) and 4.10(c) respectively. The results are also plotted on Master curve obtained from test temperature of -110°, shown in fig.4.11.The Reference Temperature (T_0) calculated is -151°C.

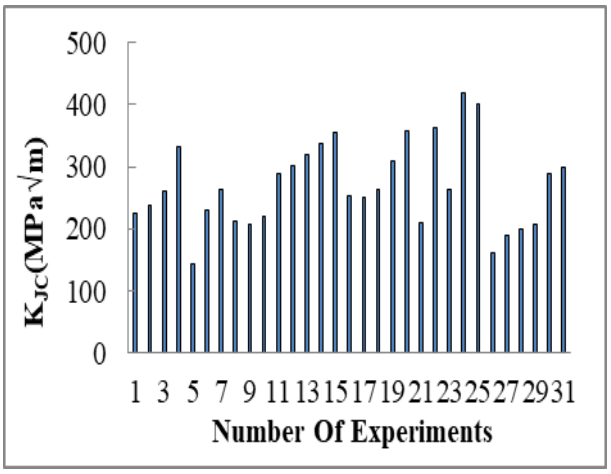

Fig.4.9.(a).K_{JC} calculated from Fracture Toughness Test at -100°C

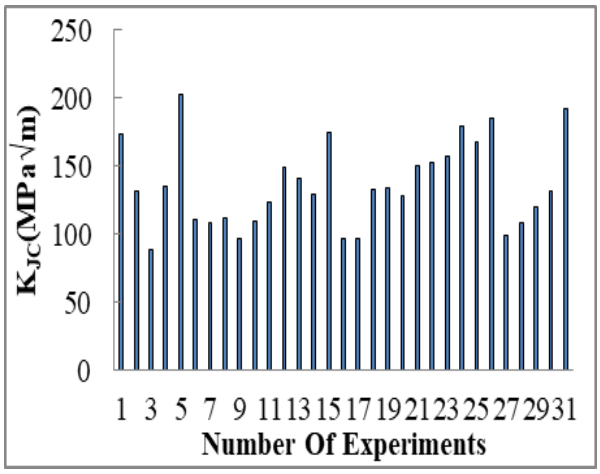

Fig.4.9.(b).K_{JC} calculated from Fracture Toughness Test at -130°C

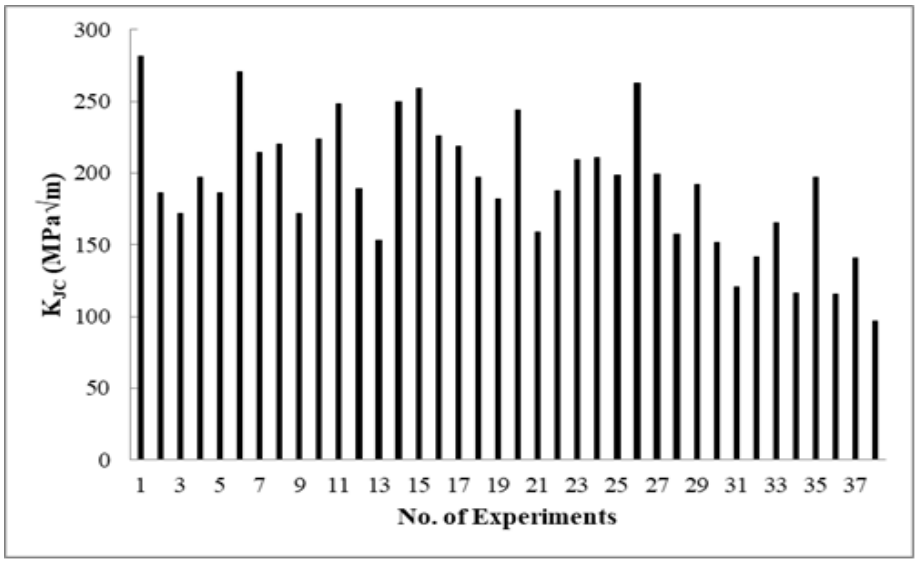

Fig.4.9(c.) K_{JC} calculated from Fracture Toughness Test at -110°C

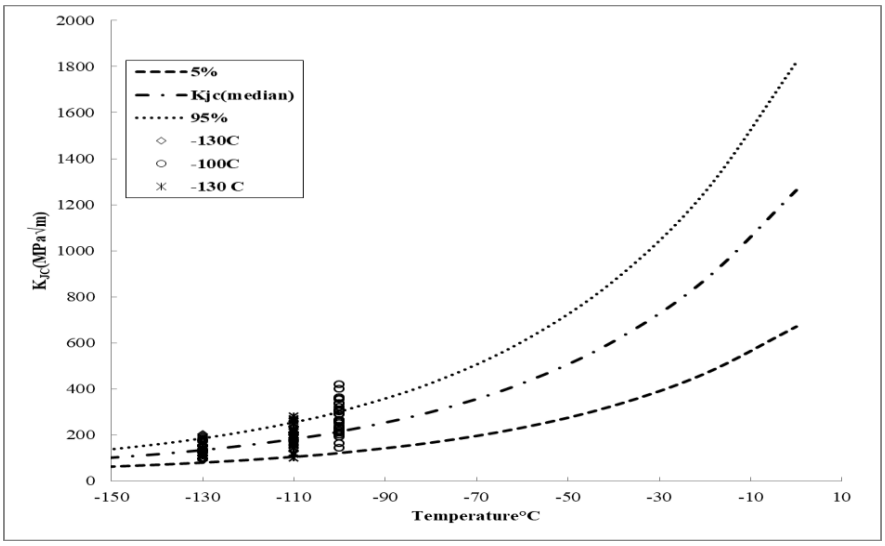

Fig.4.10 Master Curve for 20MnMoNi55 Steel

From the figure 4.10 it could be established that the Master curve along with Reference Temperature (T_0), obtained from Test temperature -110°C satisfactory captures the fracture toughness values obtained at temperature -100°C ,-110°C and -130°C.

With the help of direct calibration strategy and from the results of finite element analysis the values of Weibull Modulus 'm' and scalar parameter 'σ_u' are calibrated for temperatures -100°C ,-110°C and -130°C as shown in fig.4.11(a),4.11(b) and 4.11(c) respectively.

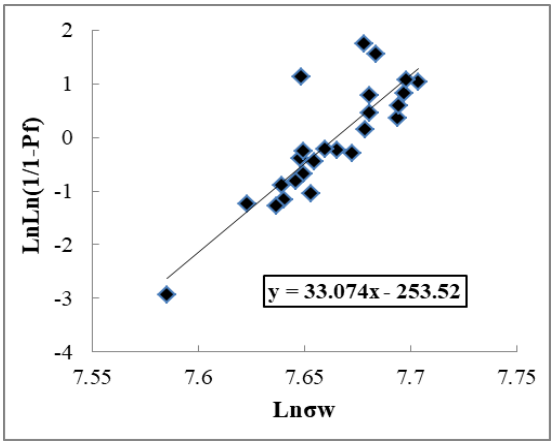

Fig.4.11.(a) Test Temp.-100°C,m predicted 32.5 & m Calculated 33,σ_u=2170 MPa.

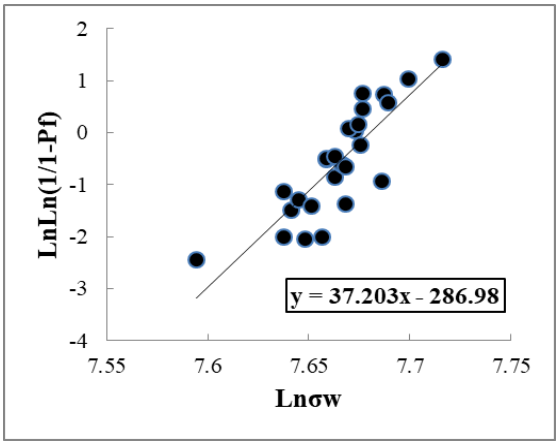

Fig.4.11(b) b.Test Temp.-130°C,m predicted 37 & calculated 37.2, σ_u=2106 MPa

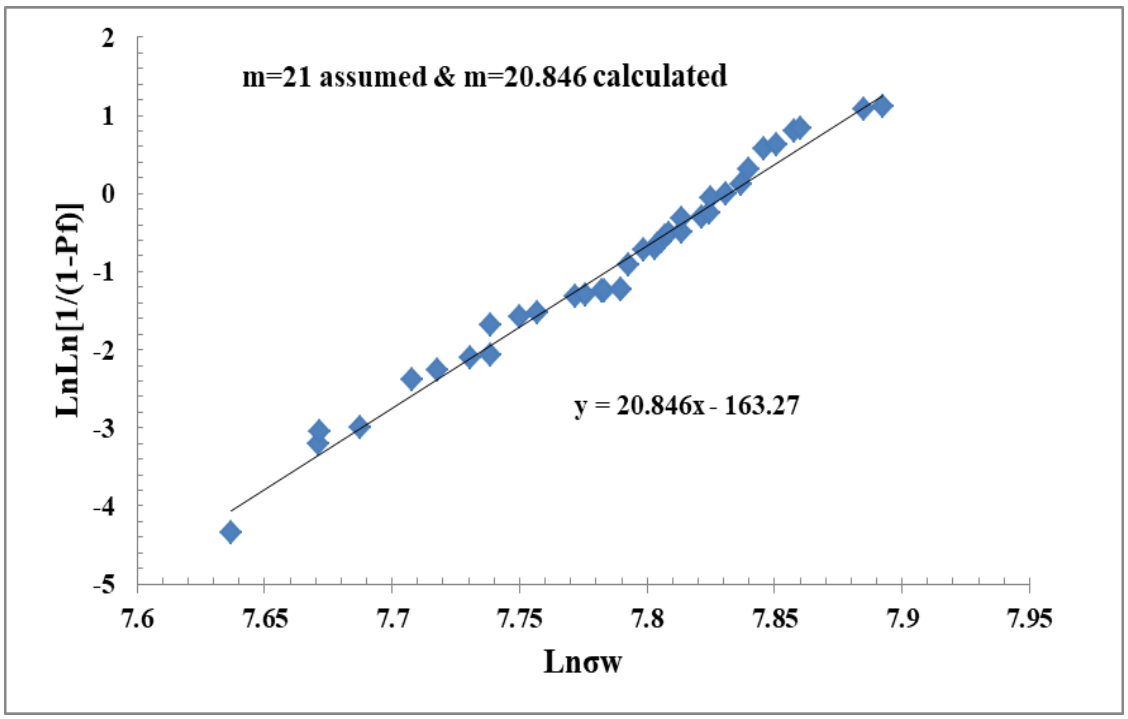

Fig.4.11(c) Test Temp.-110°C, m predicted 21 & m Calculated 20.846,σ_u=2518 MPa

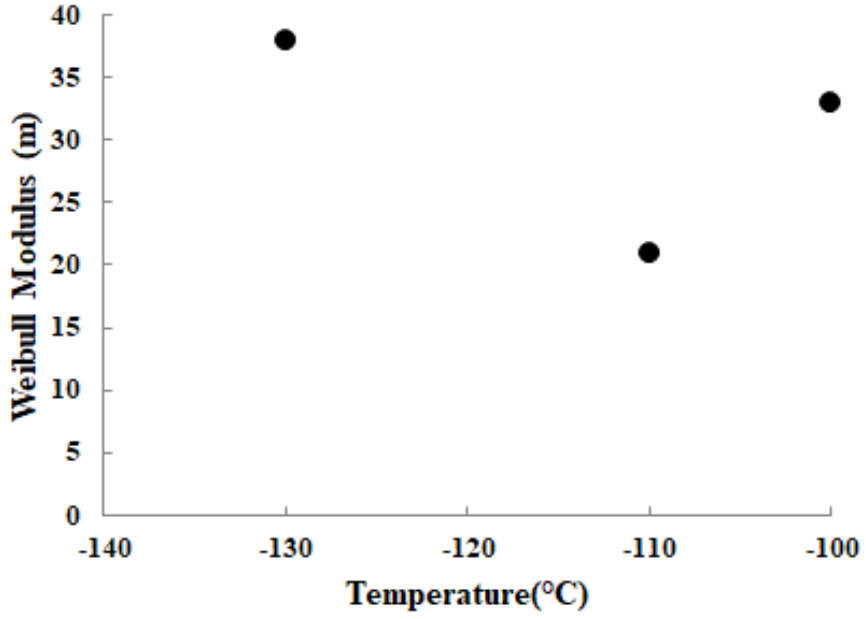

Fig.4.12(a) Variation of Weibull modulus 'm' with temperature

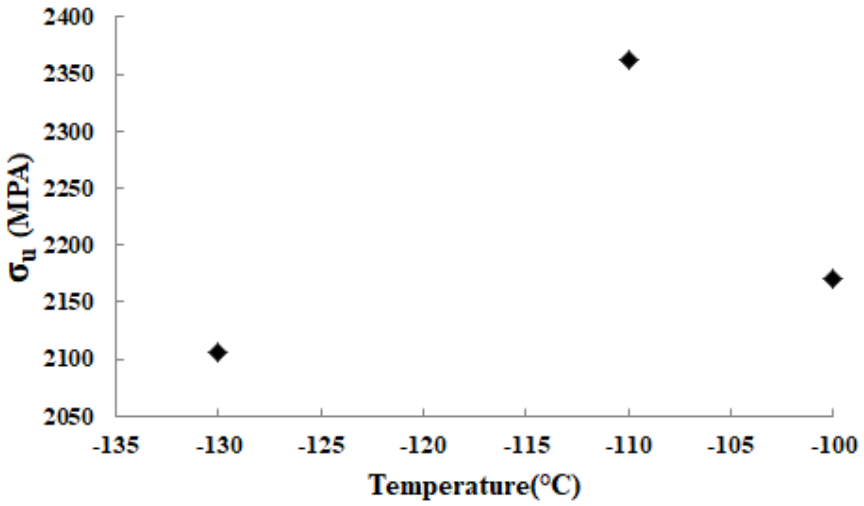

Fig.4.12(b) Variation of Scalar Parameter 'σ_u' with temperature

Fig.4.12(a) & 4.12(b) shows, the variation of Weibull modulus (m) and Weibull Scalar Parameter (σ_u) with temperature in brittle dominated portion of ductile to brittle transition region.

4.14. Observations and Conclusion

1. Large numbers of experiments (38 in number) are performed on TPB specimen of different thickness and a/W ratio in the DBT region at a fixed temperature of -110^0C.
2. Kim Wallin's Master Curve Methodology (ASTM E1921-02) is used to evaluate Master Curve Reference Temperature (T_0) from the valid experimental results for sample of different a/w ratio and thickness.
3. The variation of Reference Temperature (T_0) is observed with thickness and a/W ratio of the specimen is within 10% in both the cases. An attempt is taken to evaluate T_0 for different sample relating stress state at the crack tip using Beremin model.
4. Beremin parameters are calibrated from the experimental results and finite element analysis of TPB specimen, at the above mentioned test temperature.
5. Reference temperature T_0 calculated from Beremin model with the calibrated parameters are compared with Reference temperature T_0 obtained from Kim

Wallin's Master Curve Methodology (ASTM E1921-02) obtained through experiments for different thickness and a/W ratio of TPB specimens. An excellent case specific matching (maximum deviation is within 5%) of Reference temperature T_0 calculated from two different procedures are obtained.

6. As Beremin parameters are material properties an attempt is taken to predict Reference temperature T_0 for CT specimen of the same material and at the same test temperature using the same Weibull Modulus (m), scaling parameter (σ_u) and $C_{m,n}$ as obtained from TPB specimens. Again an excellent matching of Reference temperature T_0 calculated from two different procedures are obtained, which supports the acceptability of calibrated Weibull parameters.

As expected the Beremin parameters which rely on micro level distribution of cracks are not sensitive with geometry and loading conditions but are quiet sensitive with test temperature for a given material. Application of Beremin model and Weibull stress for evaluation of T_0 is observed to capture the effect of stress state at the crack tip also along with the probabilistic nature of failure in Ductile to brittle transition zone of Ferritic steel. This makes possible to use Beremin parameters determined from specimen level for assessment of embrittlement of nuclear components where effect of stress state may be significant.

7. Then we proceed to calibrate the parameters for -100°C and -130°C using the same procedure which is used for calibrating the parameters at -110°C in order to study the variation of Weibull Modulus (m) & Weibull Scalar Parameter (σ_u) with temperature, for the brittle dominated portion of DBT region.

8. The trend of the variation of the parameters were found to in agreement with the available results in literature.

The content of this chapter is published in Journal of Failure Analysis and Prevention. 2018 Dec 1;18(6):1534-47.(Springer)with the title Calibration of Beremin Parameters for 20MnMoNi55 Steel and Prediction of Reference Temperature (T_0) for Different Thicknesses and a/W Ratios

Chapter 5

Determination of Weibull Modulus (m) & Weibull Scale Parameter (σ_u) at different temperatures using Monte Carlo Simulation for 20MnMoNi55 steel.

Outline of the chapter

In this chapter variation of the Beremin parameters with temperature for RPV material 20MnMoNi55 steel is studied. Beremin model is used, including the effect of plastic strain as originally formulated in the Beremin model. A set of six tests are considered at a temperature of -110°C in order to determine Reference Temperature (T_0) and Master Curve for the entire DBT region as per the ASTM Standard E1921. Monte Carlo simulation is employed to produce a large number of 1T TPB (Three Point Bending specimen) fracture toughness data randomly estimated from the scatter band obtained from the Master curve, at different temperatures of interest in the brittle dominated portion of DBT region to determine Beremin model parameters variation with temperatures. The results are then compared with that of experimentally obtained values from the direct calibration strategy as discussed in Chapter4.Utilisation of Monte Carlo simulation transcend the burden of performing a huge number of experiments for proper calibration of Beremin parameters for a fixed temperature. Once the Beremin parameters are calibrated for different temperatures in the brittle portion of DBT region then with the help of $C_{m,n}$,another Beremin model parameter, K_{JC} is predicted for 5%,50%and 95% probability of failure for the corresponding temperatures and compared with the existing Master Curve.

5.1. Introduction

In the previous chapters an idea of successful application of Beremin model is incurred for 20MnMoNi55 steel, after calibrating its parameters from experimental results. Effects of variation in temperatures on these parameters are also discussed. In this chapter an attempt is taken to transcend the burden of performing 30 replica experimental tests for each temperature in the transition region which is quite expensive by the use of Monte Carlo simulation technique with the help of Master Curve methodology. The prediction of the parameters with the utilization of the new technique is marked as "Indirect Calibration" strategy whereas calibration from experimental results is marked as "Direct Calibration" strategy. The predicted values of the Beremin parameters are compared by the two methodologies for 3 temperatures in brittle dominated portion of DBT region.

Proper calibration of Weibull modulus (m) and Weibull scale parameter (σ_u) is a major criterion for the implementation of Beremin model for a given material. Once the parameters are calibrated, the next area of debate put forward by different researchers for the last twenty years is the sensitivity or dependence of the parameters on temperatures. Hojo et al.[73] calibrated distribution of Weibull stress (σ_w) in the brittle fracture region using notched round bar specimens and CT specimen for A533B steel and showed that m and σ_u are insensitive to temperature at least in the lower-self portion of DBT region. Gao et al. [74] also showed in their work that 'm' does not vary with temperature for A508 steel in the transition region. They used a 3-parameter Weibull distribution model where the first parameter 'm' remains constant with temperature while the second parameter σ_u increases with temperature and third parameter the threshold value Weibull stress $\sigma_{w\text{-}min}$ decreases with temperature. Wasiluk et al.[75] studied the variation of Beremin parameters on 22Ni–MoCr37 steel similar to ASTM A508 Cl.3. They also used a 3-parameter Weibull distribution model .They have calibrated the parameters at two extreme temperatures of DBT region that is at -40°C and at -110°C.From the results obtained they have concluded that "m" remains practically insensitive to temperatures, (m=20 at -40°C and m=18 at -110°C) while "σ_u" and $\sigma_{w\text{-}min}$ shows a marked increases with temperature. Petti and Dodds [76] proposed from their study on A533B and A508 steels that, "σ_u", increases with temperature, while they assumed "m" remains invariant

with temperature. But the work done by C.S. Wiesner and M.R. Goldthorpe [77] reveals a different trend. The direct calibration procedure by calculating the Weibull stress for each experimental data from any FEA package and then using Linear regression analysis is the best solution for the calibration scheme. But test with a small number of replica specimens, 10 to 15 creates a lot of uncertainty in the calibrated value of "m" and "σ_u". In the numerical work done by Khalili and Kromp [23],they have shown that test of at least 30 replica specimens are required to provide a reliable result of the parameters, for a single temperatures. But on the other hand, test of such huge number of specimens is notably expensive. To transcend the huge burden of test such a large number of specimens an alternative approach have been put forward in this paper by employing Monte Carlo technique. The aim of this work is to verify the applicability of Monte Carlo simulation to calibrate Beremin Parameters for cleavage fracture in DBT region at different temperatures from six tests at a single temperature to reduce the burden of experiments at different temperatures. Beremin used Weibull stress as local stress Parameter to estimate the failure Probability for a given set of Beremin Parameters m and σ_u. Weibull stress represents the level of driving force whereas σ_u, and m respectively represent the material resistance and scatter in fracture toughness values i.e. the level of likelihood of cleavage fracture. Though cleavage fracture, the value of plastic strains at failure points influences the value of fracture toughness and thus the value of Beremin parameters are likely to be influenced. Because of this observation Beremin modified the expression for calculating Weibull stress including plastic strain with an anticipation that resistance against cleavage fracture will decrease with increase in plastic strain. In our earlier work [48] on the same material enhancement in fracture toughness due to loss of constraint in DBT region and effect on Master Curve was observed. In this work we started with this primacy to consider the effect of plastic strain on Beremin parameters using Beremin's modified Equation and focused on to study the predictability of Monte Carlo simulation. But the findings of Ruggeri and Dodds [58] is that the likelihood of cleavage fracture should increase with increase in plastic strain due to availability of more micro-cracks. As discussed above, the effect of plastic strain on cleavage fracture is explained by the two renowned researchers in two different ways. Beremin considered that the resistance against cleavage fracture will decrease with increase in plastic strain

[17] and Ruggeri considered cleavage fracture should increase with increase in plastic strain due to availability of more micro-cracks. Future study on Experimental results with both the ideas is required verify which theory predicts more accurate fracture toughness data. However, this work is restricted with Beremin's correction and focussed to validate the outcomes from Monte Carlo Simulation.

5.2. Formulation

5.2. 1. Master curve analysis and calculation of Reference Temperature (T_0)

According to Wallin [1,2,3],Brittle fracture probability which is defined as P_f for a specimen having fracture toughness K_{Jc} in the transition region is described by a three parameter Weibull model as shown by

$$P_f = 1 - \exp\left[-\left(\frac{K_{Jc} - K_{\min}}{K_0 - K_{\min}} \right)^4 \right] \tag{5.1}$$

Where,

$$K_{JC} = \sqrt{\frac{J_c E}{(1-\nu^2)}} \tag{5.2}$$

K_0 is a scale parameter dependent on the test temperature and specimen thickness, and K_{min} is the minimum possible fracture toughness which is assumed to be equal to 20 MPa√m. as suggested by Wallin and International Atomic Energy Agency [78]

For single temperature evaluation, the estimation of the scale parameter K_0, is performed according to equation (5.3)[92]

$$K_0 = \left[\sum_{i=1}^{N} \frac{\left(K_{Jc(i)} - K_{\min} \right)^4}{N} \right]^{1/4} + K_{\min} \tag{5.3}$$

Where, K_{JC} (i) is the individual K_{Jc} value and N is the number of K_{Jc} values.

$$K_{JC(median)} = K_{\min} + (K_0 - K_{\min})(\ln 2)^{1/4} \qquad (5.4)$$

Here, T_0 is the temperature at which the value of $K_{Jc\ (median)}$ is 100 MPa$\sqrt{m}$ and known as Reference temperature. T_0 can be calculated from Eq.(4)and Eq.(5)

$$T_0 = T_{test} - \frac{1}{0.019}\ln\left[\frac{K_{JC(median)} - 30}{70}\right] \qquad (5.5)$$

T_{test} is defined as the test temperature where the $K_{Jc\ (median)}$ value is determined from the data set at that temperature.

5. 2.2. Modified Beremin Model

According to Beremin model [17], the probability of failure is given as,

$$p_f = 1 - \exp\left(-\left(\frac{\sigma_w}{\sigma_u}\right)^m\right) \qquad (5.6)$$

$$\sigma_w = \sqrt[m]{\left(\left(\sum_{j=1}^{n}\sigma_1^j\right)^m \frac{V_j}{V_0}\right)} \qquad (5.7)$$

n is the number of volumes V_j, or elements in a FEM calculation and σ_1^j the maximal principle stress of the element j and V_j/V_0 is just a scaling based on the assumption that the probability scales with the volume. V_0 is the reference volume which is normally taken as cubic volume containing about 8 grains i.e., (0.05X0.05X0.05) mm^3. The stressed region of the specimen is divided into n volumes of V_0. Each volume, number i, is subjected to a quasi-homogeneous stress state σ_i, where σ_i is the maximum principal stress. This indicates that the stress variation within V_0 is small, which is possible only when the size of V_0 is small enough in the order to account in the variation of stress with in the volume. But on the contrary V_0 also have to be large enough so that the probability of finding a micro crack of reasonable length will not be vanishingly small. Therefore V_0 can be arbitrarily chosen based on the above two criterions as cubic volume containing

about 8 grains, *i.e.*, (0.05X0.05X0.05) mm^3. These dimensions were also adopted by Beremin and the other co-workers working in this field.

To implement three parameter Weibull distribution σ_w in equation 5.6 should be replaced by (σ_w -$\sigma_{w.min,}$), the value of $\sigma_{w.min}$ is attempted to evaluate from σ_w vs. K_{Jc} results for this material at test temperature but the value appeared negligibly small and hence not included.

Now, this classical model is applicable where plastic strain is negligible or zero that scenario could be present in ceramic or glass materials but this condition cannot be idealised for ferritic steel, especially 20MnMoNi55 steel where an appreciable amount of plastic strain is observed in the crack tip area. To take into account plastic strain a correction formulation has been introduced by Beremin himself in his work [17].

$$\sigma_w = \sqrt[m]{\sum_j \left(\sigma_1^j\right)^m \frac{V_j}{V_0} \exp\left(-\frac{m\varepsilon_1^j}{2}\right)} \qquad (5.8)$$

ε_1^j is the strain in the direction of the maximum principal stress σ_1^J

Throughout the paper the Weibull stress is calculated according to equation 5.8.

Beremin used Weibull stress as local stress Parameter to estimate the failure Probability for a given set of Beremin Parameters m & σ_u. Weibull stress represents the level of driving force whereas $\sigma_{u,}$ and m respectively represent the material resistance and scatter in fracture toughness values i.e. the level of likelihood of cleavage fracture. Though cleavage fracture, the value of plastic strains at failure points influences the value of fracture toughness and thus the value of Beremin parameters are likely to be influenced. Because of this observation Beremin modified the expression for calculating Weibull stress including plastic strain with an anticipation that resistance against cleavage fracture will decrease with increase in plastic strain. In chapter 4 our prime work was to determine the Beremin model parameters from experimental data consisting of 38 TPB specimens without considering the effect of local plastic strain as interpreted in ASTM E1921. But the role of plastic strain on T_0 was indicative in the experimental results. With the later

course of research the effect of plastic strain is observed in the cleavage failure of the specimen. Chapter 5 is started with this primacy to consider the effect of plastic strain on Beremin parameters using Beremin's modified equation and focused on to study the acceptability of Monte Carlo Simulation**.**

5.2.3. A brief discussion on Monte Carlo Simulation

Monte Carlo simulation is name given after the name of the city of Monte Carlo in Monaco. The city is famous for gambling such as roulette, dice, and slot machines. As the simulation process involves generating chance variables and exhibits random behaviours, it is called as Monte Carlo simulation. This simulation is a powerful statistical analysis tool which is widely used in both non-engineering fields and engineering fields. At the beginning it is used to solve neutron diffusion problems in atomic bomb work at Alamos Scientific Laboratory in 1944. Now Monte Carlo simulation has been applied to solve various problems ranging from the simulation of complex physical phenomena such as atom collisions to the simulation of traffic flow and Dow Jones forecasting. It is also suitable for solving complex engineering problems because it can deal with a large number of random variables, various distribution types, and highly nonlinear engineering models.

In comparison from a physical experiment, Monte Carlo simulation performs random sampling and conducts a large number of experiments on computer. Then the statistical characteristics of the experiments (model outputs) are observed, and conclusions on the model outputs are drawn based on the statistical experiments.

In each experiment, the possible values of the input random variables $\mathbf{X} = (X1, X2, , Xn)$ are Generated in accordance to their distributions. Then the values of the output variable Y are calculated through the performance function $Y = g(\mathbf{X})$ at the samples of input random variables. With a number of experiments performed in this manner, a set of samples of output variable Y are available for the statistical analysis, which estimates the characteristics of the output variable Y.

The simulation is normally performed in three steps which are as follows

Step 1 – sampling on random input variables **X**,

Step 2 –evaluating model output Y, and

Step 3 – statistical analysis on model output.

5.3. Methodology For Determination of Weibull modulus (m) & Weibull scale Parameter (σ_u)

1. A set of six fracture tests are performed at temperature of -110°C as per ASTM standard [92] and reference temperature (T_0) is calculated with the help of equation 5.2, 5.3, 5.4 and 5.5.
2. Once reference temperature (T_0) is calculated for the material, Master Curve is drawn for the entire DBT region where the scattered band of fracture toughness with variation in temperature is available.
3. Now with the help of Master curve corresponding to 90 numbers of random input of P_f, random value of 90 numbers of fracture toughness data is generated, for a specific temperature 'T' according to the equation 5.9 and censored according to equation 5.10

$$K_{JC} = 20 + \left[\left\{ \ln\left(\frac{1}{1-P_f} \right) \right\}^{0.25} \left\{ 11 + 77 \exp\left(0.019\left(T - T_0 \right) \right) \right\} \right] \quad (5.9)$$

$$K_{JC(\lim it)} = \sqrt{\left[\frac{E b_0 \sigma_{ys}}{M\left(1-\nu^2\right)} \right]} \quad (5.10)$$

M is the constraint whose value is fixed as 30[92]

4. Now elasto-plastic finite element analysis of 1T TPB specimen is done, using FE software ABAQUS taking the Young's modulus, Poisson's ratio and stress (above yield stress) verses plastic strain for the temperature 'T' as the material parameter.
5. J-Integral and detail of stress near the crack tip at different displacement level are computed from the FE analysis results. This application is ready available in ABAQUS 6.13 which calculates the J-Integral over a predefined number of contours surrounding the crack tip. From the J-Integral K_{Jc} is calculated according to the equation 5.2

6. An initial value of ‘m’ is assumed.
7. ‘σ_W’ is calculated for each displacement level with the assumed value of ‘m’ from the FE simulated results for a specific temperature ‘T’ by a post processing program which reads the Abaqus output files. Then ‘σ_W’ verses K_{Jc} is plotted, where K_{Jc} is obtained from Step-5.
8. Corresponding Weibull stress for each fracture toughness value (generated according to Eq.9) is obtained from ‘σ_W’ verses K_{Jc} plot for the assumed value of ‘m’
9. Now the 90 values of Weibull Stress obtained from Step-8, is arranged in ascending order and Probability Of Failure ‘P_f’ is assigned for each values according to equation 5.11

$$P_f = \left(\left(j - 0.5 \right) / N \right) \tag{5.11}$$

Where j is the rank number and N defines the total number of ‘σ_W’ values.

10. Now ln σ_W is plotted along X-axis and ln[ln[1/(1-P_f)]] is plotted along Y-axis according to equation 5.12.Linear fit is done and the slope of the fit is the calculated Weibull modulus ‘m’ which is assigned a different name ‘m_n’ This procedure is designated as Linear Regression Analysis

$$P_f = 1 - \exp\left(-\left(\frac{\sigma_w}{\sigma_u} \right)^m \right) \tag{5.12}$$

11. If $m=m_n$, then Scalar Modulus ‘σ_u’ is calculated from the intercept of the Straight Line. If, $m \neq m_n$ Then the Step 6 to 10 is repeated with a modified value of m and the process continues till a convergence value is achieved within a tolerance value of 0.1 to 1 units.

12. Then Step 3 To 11 is repeated for 1000 times except Step 4 & 5 which are performed only at the first iteration.

13. The average values of ‘m_n’ and ‘σ_u’ are the calibrated values for the specific Temperature ‘T’.

1 Cryo-chamber 2 Controller 3 Operator panel
4 Support computer 5 Liquid nitrogen cylinder
6 Temperature indicator.

Fig.5.1. Experimental arrangement for low temperature Jc test.

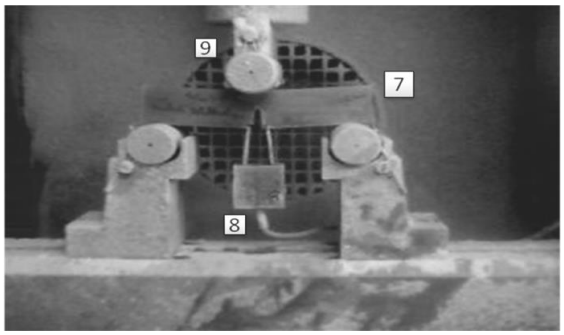

7. TPB Specimen 8.COD Gauge 9.Rigid roller

Fig.5.2 . Experimental set up of TPB specimen for low temperature Jc test

Figure 5.1and 5.2 shows the experimental set up for the determination of reference temperature (T_0) at test temperature of -110°C as described in Step 1 and Figure 4.7(a) reveals the specimen geometry of TPB specimen used in this work.

5.4. Finite Element Analysis for Computing Weibull Stress at Failure Point for TPB Specimen.

The entire Finite Element Analysis for Computing Weibull Stress at Failure Point for TPB Specimen along with validation of the FE model and material properties, also the procedure for Computation of Weibull stress at failure point for specimens are discussed vividly in article 4.6, 4.7 and 4.8 of Chapter 4.

5.5. Results and Discussions

According to Step 1 and Step 2, six numbers of fracture tests are performed at temperature of -110°C as per ASTM standard E1921-02 and Reference Temperature (T_0) is calculated as -151°C.The test data is provided in table 4.2.With the help of (T_0) Master curve is plotted for the entire DBT region shown in Figure 5.3.a. With the help of this Master Curve 90 set of random numbers are generated at respective temperatures shown

in figure 5.3.b .As discussed previously in the consequence steps calibration of Beremin parameters are done with the help of Monte Carlo Simulation employing master curve methodology.

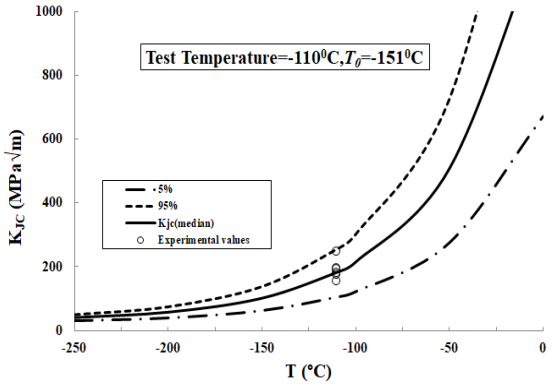

Fig.5.3.a. Master Curve from 6 test data set

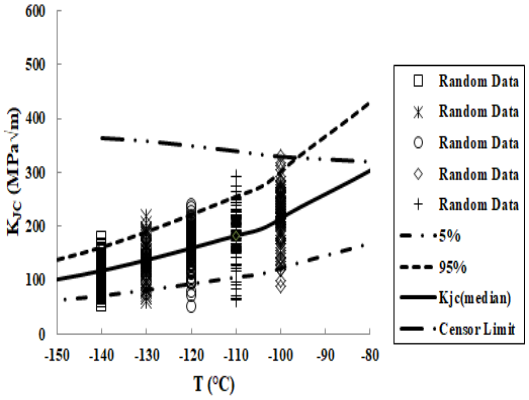

Fig.5.3.b.Randomly generated K_{Jc} by Master Curve and temperature relation

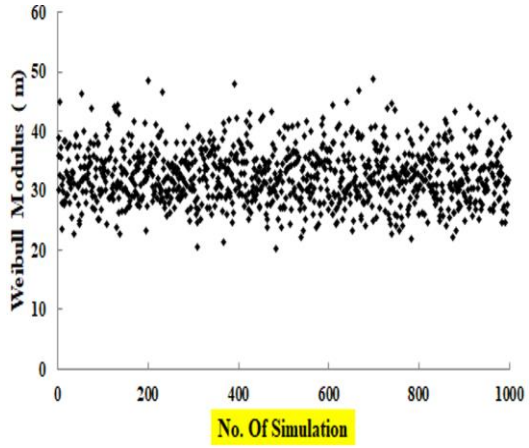

Fig.5.4.a. Relation between Weibull Modulus and the simulation number (test temperature-100°C,average m = 32)

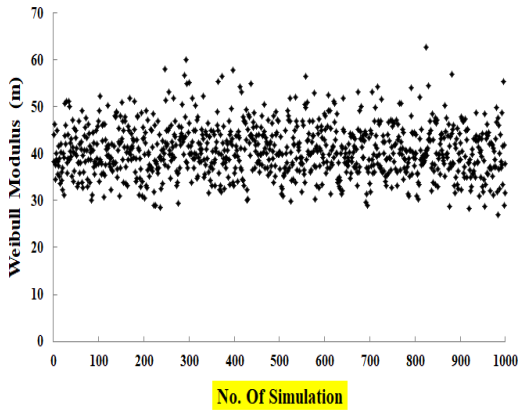

Fig.5.4.b. Relation between Weibull Modulus and the simulation number (test temperature-130°C,average m = 41)

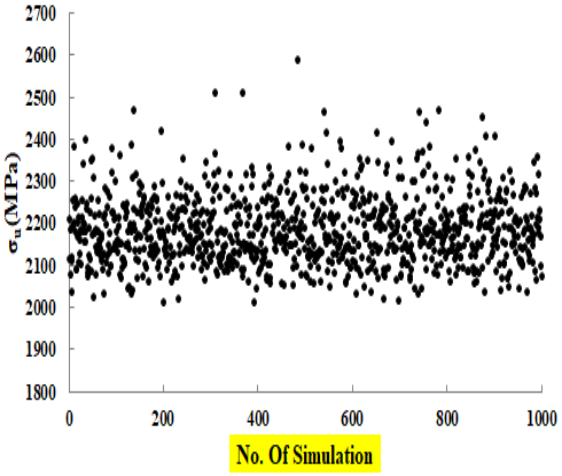

Fig.5.5.a. Relation between Scale Parameter and the simulation number (test temperature-100°C,Average σ_u = 2186 MPa)

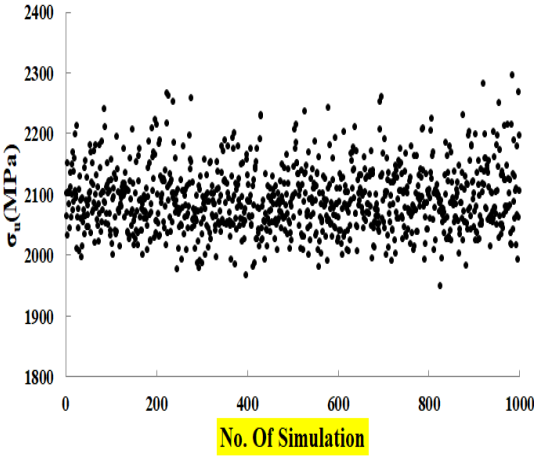

Fig.5.5.b Relation between Scale Parameter and the simulation number (test temperature-130°C,Average σ_u = 2092 MPa)

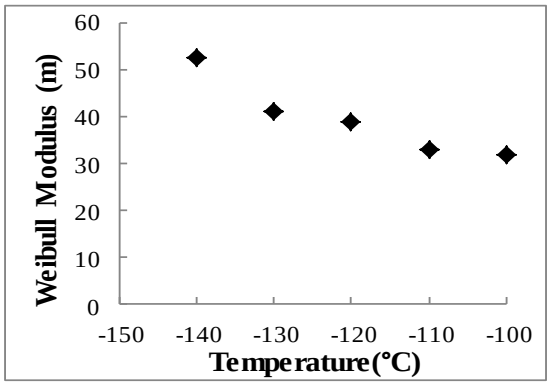

Fig.5.6.a.Variation of 'm' with temperature

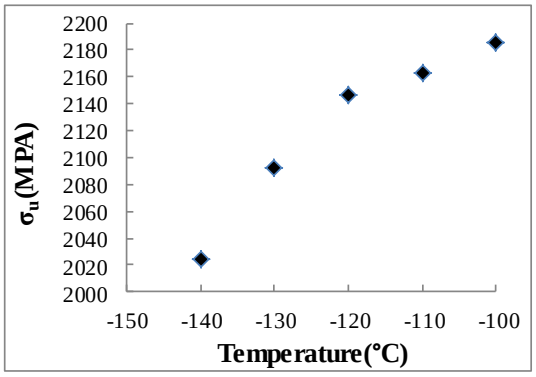

Fig.5.6.b. Variation of 'σ_u' with temperature

Figure 5.4.a and 5.4.b. shows the calibrated values of 'm' for -100°C and-130°C evolved from 1000 Monte Carlo simulation as discussed previously similarly Figure.5.5.a and 5.5.b. shows the calibrated values of 'σ_u' for -100°C and-130°C.

Figure 5.6.a and 5.6..b shows the variation of 'm' and 'σ_u' with temperature for the lower shelf that is in brittle dominated DBT region.

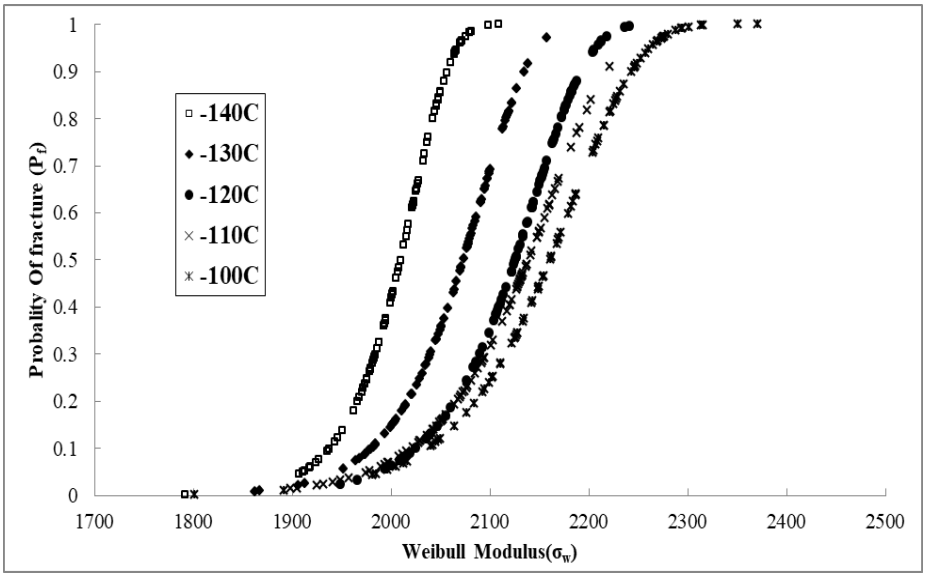

Fig.5.6.c Probability of Failure verses Weibull Stress distribution for -100°C, -110°C, -120°C, -130°C and -140°C.

The Probability of failure verses Weibull Stress (σ_W) calculated from equation 5.7 using calibrated value of Weibull modulus 'm' and 'σ_u' for temperatures -100°C , -110°C , -120°C , -130°C and -140°C are shown in Fig.5.6.c

The variation of Weibull modulus 'm', and 'σ_u' with temperature, calibrated from direct calibration strategy as discussed in chapter 4, for three temperatures data set ,along with indirect calibration by using Monte Carlo simulation for 5 temperature data sets are shown in Fig.5.7 & 5.8. .It is observed that as temperature increases Weibull Modulus 'm' decreases, which is applicable for both way calibration strategy expect experimental value of -110°C. But 'σ_u' increases with temperature showing similar trend for both calibration strategy, except discrepancy shown at temperature -110°C due to variation in thickness and a/W ratio of TPB specimen used for Calibration of the parameters at temperature. Which is axiom that as temperature increases stability of the material increases. This similar trend has been observed by Yupeng Cao et al.[24] for another type of Ferritic Steel material C–Mn steel (the16MnR steel in China).The results shows a clear matching of 'm', and 'σ_u' with temperature for both calibration strategy.

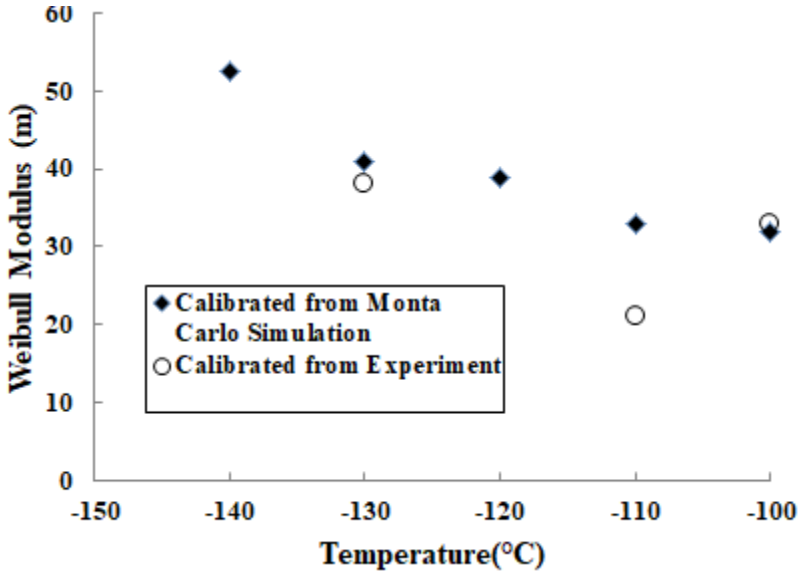

Fig.5.7. Variation of Weibull modulus 'm' with temperature

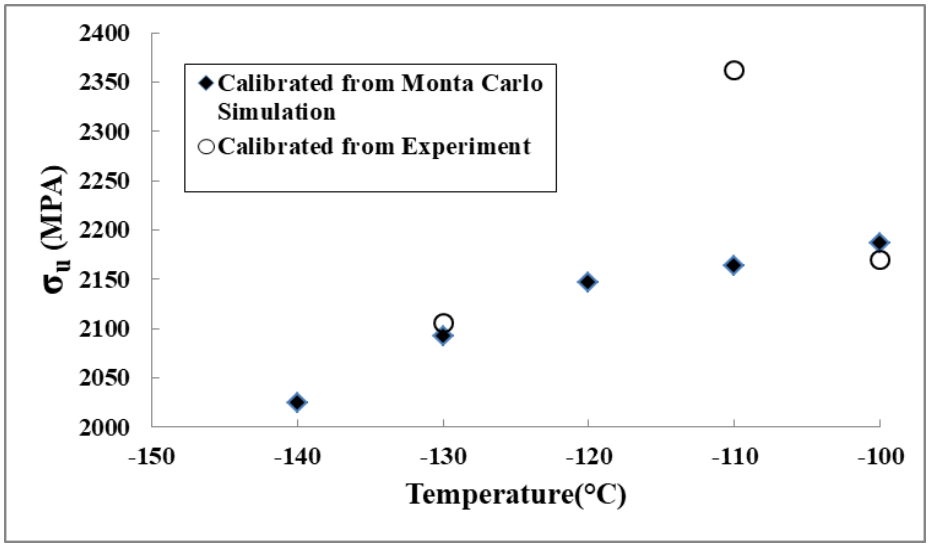

Fig.5.8. Variation of Scalar Parameter 'σ_u' with temperature

Application of Monte Carlo simulation to predict Beremin parameters 'm' and 'σ_w' is useful considering requirement of less number of experiments but validation of the predictability is essential. From the results in Fig 5.7 & 5.8 it is apparent that prediction from Monte Carlo simulation match with the results calibrated from experimental results very well at -130^{0}C and -100^{0}C. The mismatch appeared at -110 ^{0} C may be due to huge variation in thickness and a/W ratio of the test specimens at that temperature. A

comparison of P_f versus σ_w from experiment and FEA for three temperatures -100°C, -110°C -130°C are shown in fig.5.9.a and 5.9.b respectively.

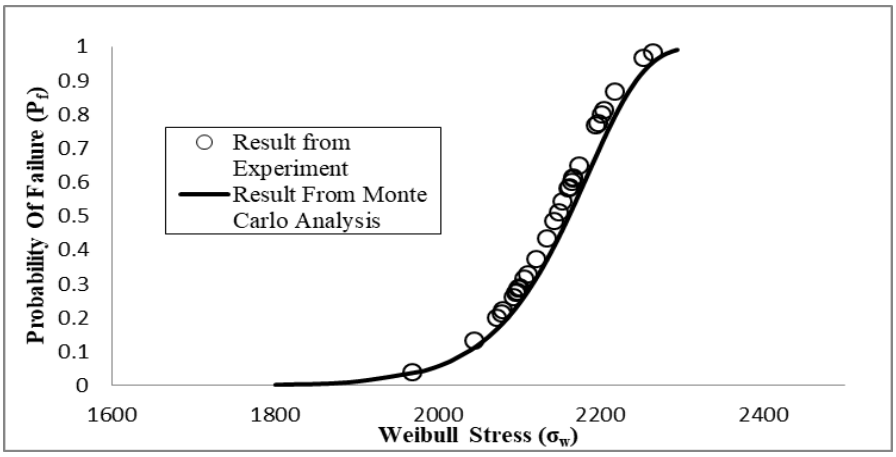

Fig.5.9.a. Probability of Failure verses Weibull Stress distribution for -100°C

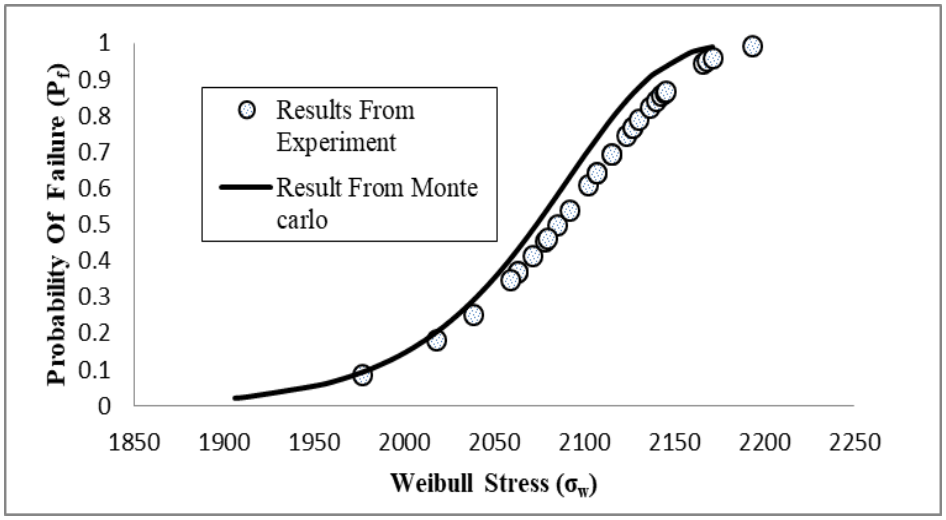

Fig.5.9.b. Probability of Failure verses Weibull Stress distribution for -130°C

5.6. Prediction of Fracture Toughness (K_{JC}) with the help of Modified Beremin Model and from the calibrated value of 'm', and 'σ_u'.

Once the calibrated values of 'm', and 'σ_u' are determined, K_{JC} can be easily predicted with the help of equation 5.13 [17]

$$Ln\left[\frac{1}{1-P_f}\right]=\frac{\sigma_0^{m-4}K_{1C}^4 BC_{m,n}}{V_0\sigma_u^m} \qquad (5.13)$$

Where $C_{m,n}$ is a numerical factor which depends on the work-hardening exponent n, ($\sigma = K' \varepsilon^n$) , σ_0 is the yield stress at the test temperature (-100°C, -110°C, -120°C ,-130°C, -140°C) and V_0 is the reference volume (50 x 50 x 50)μm. The entire process for determination of $C_{m,n}$ is described elaborately in article 4.10 of chapter 4.Now from the equation 5.13 after determination of 'm','σ_u'& $C_{m,n}$ and σ_0(Yield Stress) for a fixed temperature 'T',K_{JC} could be predicted for 5%,50% & 95% probability of failure for that temperature. Similarly for other temperatures in the DBT region K_{JC} could be predicted for 5%,50% & 95% probability of failure and cold be compared with the Master Curve predicted by ASTM E1921.This comparison is shown in Fig.5.10.The K_{JC} predicted for 5%,50% & 95% probability of failure matches well, with the Master Curve predicted determined by performing 6 tests at -110°C.This reflects the successes in calibration of 'm','σ_u' with variation in temperature at least in brittle dominated DBT region.

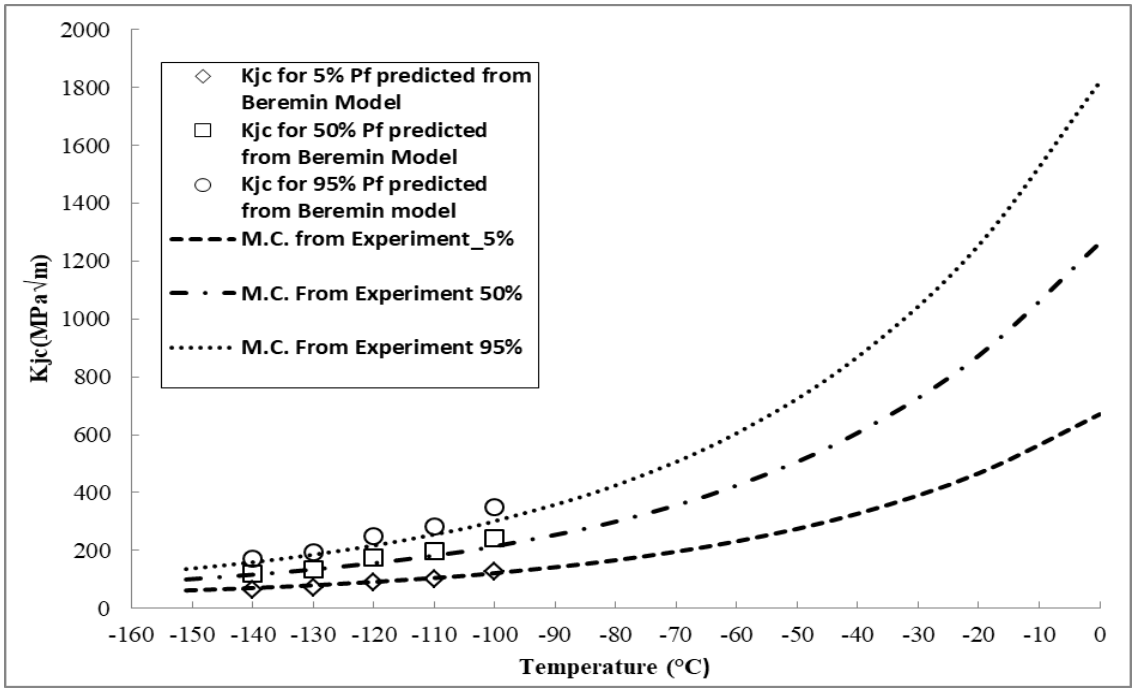

Fig.5.10. K_{JC} predicted from Modified Beremin Model and from Master curve. Its variation with temperature in the Brittle Dominated DBT region

Conclusion

- The application of Master curve along with Reference temperature in estimating the embrittlement of structural steel is widely accepted.

- Beremin model and proposition for brittle fracture in DBT temperature based on Weibull stress considering the constraint level is found to be effective to use this model even at component level.

- The variation of Beremin parameters Weibull modulus 'm' and 'σ_u' with temperature, calibrated by using Monte Carlo simulation for 5 temperature data sets are shown in this work. The values obtained for m and 'σ_u' and their variation with temperature are found to be matching with the values available for the steel of same grade. It is observed that as temperature increases Weibull Modulus 'm' decreases but 'σ_u' increases with temperature which is as expected because as temperature increases stability of the material increases.

- Successful application of Monte Carlo Simulation considerably reduces the burden of performing a huge number of experiments Considering the parameters as material properties they could be used widely in the component level resolving the transferability issue. Only finite element analysis is required at the component level and the probability of failure can be easily predicted, providing the values of the parameters are known for the material at the specific temperature.

- Variation of Beremin parameters with temperature is studied including the effect of plastic strain correction as originally formulated in the Beremin model. Beremin modified the expression for calculating Weibull stress including plastic strain with an anticipation that resistance against cleavage fracture will decrease with increase in plastic strain. But there are findings by other researchers [8] that the likelihood of cleavage fracture should increase with increase in plastic strain due to availability of more micro-cracks. A new strategy to take care of both the effects of plastic strain will be more effective**.**

- The values of Beremin Parameters for temperatures -100°C ,-110°C ,-130°C predicted from Mote Carlo Simulation are validated to that obtained from Experiments. New Calibration procedure of $C_{m,n}$ is also shown in this work for prediction of Fracture Toughness from Beremin Model. With the help of Weibull modulus m, Scale parameter σ_u and $C_{m,n}$ for different temperatures in the DBT region fracture toughness is predicted for 5%, 50%and 95 % probability of fracture. This rresults are then compared with the Master Curve obtained from Experiments as per ASTM E1921

The content of this chapter is published in Journal of Pressure Vessel Technology. 2019 Apr 1; 141(2):021401.(ASME)with the title Variation of Beremin Model Parameters With Temperature by Monte Carlo Simulation

Chapter 6

Observations, Conclusions and Scope of Future Work

6.1Aim Of the Thesis as planned and achieved :

The thesis begins with the objective of determination and to study the effect of constraints on reference temperature T_0 for 20MnMoNi55 steel using Three Point Bending and CT Specimen. The effect of each constraint due to variation in thickness and a/w ratio on reference temperature T_0 is studied vividly in **Chapter 2**.

In **Chapter 3** an attempt is explored to capture the effect of constraints on reference temperature T_0 by comparing different stress based parameters (Q-Stress, T-Stress and Triaxiality ratio) representing constraint level for ductile fracture w.r.t a reference specimen of 25 mm thick and 0.5 a/w ratio.. Prediction yields good results in upper shelf of DBTT but deviate from experimental values in transition and lower shelf of DBTT.

In **Chapter 4** Beremin's brittle fracture model is applied to take care of the constraint effect on reference temperature T_0 specially in the Lower Self of Ductile to Brittle Transition region. A calibration Strategy using linear regression analysis is used in determination of the parameters of the model for the material (20MnMoNi55 steel) used in the work. Then the fracture toughness are predicted by the model, using the calibrated values for the referred material and then compared with those obtained from experiments for TPB specimens. Utilising the calibrated values fracture toughness are predicted for a different Specimen (Compact Tension) of the same material and again compared with the experimental results and good matching is observed.

Later, an attempt is taken to calibrate the parameters of the model for different temperatures in the Brittle Fracture dominated portion of the DBT region.

In **Chapter 5** an attempt is taken to calibrate the parameters used in the Brittle fracture model by the help of Master Curve methodology and a Statistical tool namely Monte Carlo simulation, in order to transcend the burden of performing a huge no of experiment.

The results are then compared with that of experimentally obtained values from the direct calibration strategy as discussed in Chapter 4.

With the knowledge of the values of the calibrated parameters for different temperatures the fracture toughness are predicted for 5%, 50%and 95% probability of failure for the corresponding temperatures and compared with the existing Master Curve.

6.2 Observations & Conclusions

From **Chapter 2** the following conclusions can be drawn.

- ✓ The propositions related to master curve methodology is well applicable for this particular RPV steel to characterize the fracture behavior in DBT region.
- ✓ The reference temperature (T_0) is found to be influenced by geometry and also by the loading condition while comparing the CT results with the TPB results.
- ✓ The value of T_0 obtained by Single Temperature at -110^{0}C matches with the multi temperature value. For the other Temperatures T_0 obtained by Single Temperature at -120^{0}C,-130^{0}C and -140^{0}C lies within a range of ±10^{0}C.
- ✓ According to this study we observe that even after incorporating thickness correction on TPB specimens, T_0 is mildly dependent on the thickness of the specimen.
- ✓ It is observed for the material 20MnMoNi55 that, fracture toughness remains practically constant for a/w above 0.4, which matches with the result of Kim Wallin's observation on quantifying T_{stress} controlled constraint by the master curve transition temperature T_0,[7].

- ✓ While studying on Censor Parameter it is observed that the optimum value of censor parameter (M) could be taken 50 for TPB specimen instead of 30 as is taken for CT specimen., because it is seen that increasing the value of M beyond 50 has insignificant effect on reference temperature (T_0).

From **Chapter 3** the following conclusions can be drawn

- ✓Constraint Effect on Master Curve is pronounced.
- ✓A mathematical model is put forward with the help of Q-Stress, Triaxiality Ratio and T-Stress to co-relate the constraint effect with the Master Curve.
- ✓Reference temperature (T_0) is predicted with the help of the above discussed stress based parameters with respect to a generally accepted a/W ratio 0.5 and thickness of 25 mm for TPB specimen.
- ✓Predicted T_0 provides a qualitative and quantitative matching with the experimental results.
- ✓Q-stress is found to be the best parameter to capture constraint effect on T_0 in the upper shelf of DBT region.

From **Chapter 4** the following conclusions can be drawn

- ✓Satisfactory correlation of the constraint effect in the upper domain or in the ductile failure dominated region of the DBT region is observed. But deviate in brittle failure dominated region or the lower transition region.
- ✓A Brittle failure model is used to capture the constraint effect in a satisfactory way in the lower transition region.
- ✓Beremin Model is employed with the above discussed concept to study the constraint effect on Master Curve and Reference Temperature (T_0).

- ✓Beremin parameters are then calibrated for the referred material from the experimental results and finite element analysis of TPB specimen, at the above mentioned test temperature for the effective utilization of the model.

Then Reference temperature T_0 calculated from Beremin model with the calibrated parameters are compared with Reference temperature T_0 obtained from Kim Wallin's Master Curve Methodology (ASTM E1921-02) obtained through experiments for different thickness and a/W ratio of TPB specimens.

- ✓ An excellent case specific matching (maximum deviation is within 5%) of Reference temperature T_0 calculated from two different procedures are obtained.

- ✓To verify whether Beremin parameters are material properties, an attempt is taken to predict Reference temperature T_0 for CT specimen of the same material and at the same test temperature using the same Weibull Modulus (m), scaling parameter (σu) and $C_{m,n}$ as obtained from TPB specimens.

- ✓ Again an excellent matching of Reference temperature T_0 calculated from two different procedures are obtained, which supports the acceptability of calibrated Weibull parameters.

- ✓As expected the Beremin parameters which rely on micro level distribution of cracks are not sensitive with geometry and loading conditions but are quiet sensitive with Test temperature for a given material.

- ✓Application of Beremin model and Weibull stress for evaluation of T_0 is observed to capture the effect of stress state at the crack tip also along with the probabilistic nature of failure in Ductile to brittle transition zone of Ferritic steel. This makes possible to use Beremin parameters determined from specimen level for assessment of embrittlement of nuclear components where effect of stress state may be significant.

Then it is attempted to calibrate the parameters for -100°C and -130°C utilizing the same procedure which is used for calibrating the parameters at -110°C in order to study the

variation of Weibull Modulus (m) & Weibull Scalar Parameter (σ_u) with temperature, for the Brittle dominated portion of DBT region. The variation of the parameters matches well with the available literature.

From **Chapter 5** the following conclusions can be drawn

- ✓ Calibration of Beremin Parameters are done for temperatures -100°C, -110°C , -120°C ,-130°C and -140°C with the help of Monte Carlo simulation and Master Curve methodology in order to transcend the burden of performing huge number of experiments.

- ✓ Although Beremin model is a brittle fracture model but during experimental determination of fracture toughness in the lower self of DBT region considerable amount of ductile stretch is observed, to incorporate this effect in the said model strain correction is imposed in determination of Weibull stress.

- ✓ The values obtained for m and 'σ_u' and their variation with temperature are found to be matching with the values available for the steel of same grade.

- ✓ It is observed that as temperature increases Weibull Modulus 'm' decreases but 'σ_u' increases with temperature which is as expected because as temperature increases stability of the material increases.

The Beremin parameters Calibrated from Monte Carlo simulation, are validated with the Calibrated values obtained from direct Calibration strategy using experimental results for three temperatures -100°C,-110°C and-130°C .

- ✓The results shows an appreciable matching trend except some amount of variation is observed at -110°C, that could be due to various a/W ratio and thickness of TPB specimen used in calibrating the values from experimental results at that temperature.

- ✓With the knowledge of the values of the calibrated parameters for different temperatures the fracture toughness are predicted for 5%, 50%and 95%

probability of failure for the corresponding temperatures and compared with the existing Master Curve and an acceptable matching is observed.

- ✓Therefore it could be concluded that if the Beremin parameters at different temperatures in the DBT region are known for any material then Reference temperature (T_0) could be predicted in component level for the same material after calculating the Weibull Stress from Finite Element Analysis.

- ✓From all the above observation the final proposition of the work is " *Using only Master Curve (based on six tests in a single temperature) Beremin parameters can be calibrated in various temperature and T_0 at different constraint level can be determined using Beremin Model"*

6.3 Limitations of the study

From the results in Fig 5.7 & 5.8 it is apparent that prediction from Monte Carlo simulation match with the results calibrated from experimental results very well at -130^{0}C and -100^{0}C. The mismatch appeared at -110^{0}C, which may be due to huge variation in thickness and *a/W* ratio of the test specimens at that temperature. So fracture toughness test of more than 30 Specimen of same thickness and *a/W* ratio are required to be performed at -110^{0}C which may give the value of Weibull Modulus (m) and Weibull Scale parameter (σ_u) in agreement with the Monte Carlo Simulation results.

6.4 Scope Of Future Work :

In the present work calibration of Beremin model parameters are performed on the basis of linear regression analysis taking data either from direct experimental fracture toughness values or randomly from scattered distribution presented by Master Curve with the help of Monte Carlo simulation. But some of the existing concepts have not been attempted in this work which are as follows

a) **Toughness scaling model** :But many researchers calibrate the values on the basis of toughness scaling model. They plot Fracture toughness verses Weibull Stress for a shallow crack (*a/W*=0.1) and on the same graph they plot Fracture toughness

verses Weibull Stress for a deep crack (a/W=0.5) for the same type of specimen of the same material. They assume a value of Weibull Modulus (m) for calculating Weibull Stress. For a fixed value of Weibull Stress the fracture toughness are different for different constraint level (different a/W ratio) this is marked as an error function. Then different values of 'm' are selected in iterative process for which the error function is minimized. That value of Weibull modulus (m) is marked as the calibrated value for that material. This method can be applied for determination of Beremin parameters for the material used in this thesis. But in accordance to the protocol of testing of TPB specimen of shallow crack of a/W ratio 0.1 will violate the testing procedure as referred in ASTM E399–90 standard. So in this region specific attention is required in the future.

b) **Comprehensive fracture model in DBTT**: Within the cleavage fracture model (specially in the lower self of DBT region) we assumed that cleavage fracture occurs by unstable micro crack initiated by brittle second phase inclusion. A two-parameter Weibull modulus was used to take into account the statistical nature of cleavage fracture. On the other hand ductile crack tearing (specially in the upper self of DBT region) was described by the mechanism of growth of voids and coalescence of these voids nucleated at second phase inclusion. The Void nucleation, growth and fracture is described by a stress controlled nucleation criterion. For cleavage fracture, after some ductile tearing the nucleation criteria for cleavage and ductile fracture are competitive. Once a void has been nucleated at an inclusion, that inclusion cannot contribute to the mechanism of cleavage fracture. Therefore a model has to be designed which incorporates the combined effect of both, ductile failure model to capture the effect of ductile failure in the Upper Self of DBT region and Brittle failure model to capture the effect of brittle failure in the Lower Self of DBT region. The initial crack growth should be guided by a damage model (like GTN model or Bonora Model).Followed by Brittle failure model like Beremin model. That is Weibull stress should be calculated from FEA which is guided by a damage model like GTN model or Bonora Model instead of Elasto plastic model to take into account the ductile tearing.

Correction for strain :The aim of the last part of the work was to verify the applicability of Monte Carlo simulation to calibrate Beremin Parameters for cleavage fracture in DBT region at different temperatures from six tests at a single temperature to reduce the burden of experiments at different temperatures. Beremin used Weibull stress as local stress Parameter to estimate the failure Probability for a given set of Beremin Parameters m & σ_u. Weibull stress represents the level of driving force whereas $\sigma_{u,}$ and m respectively represent the material resistance and scatter in fracture toughness values i.e. the level of likelihood of cleavage fracture. Though cleavage fracture, the value of plastic strains at failure points influences the value of fracture toughness and thus the value of Beremin parameters are likely to be influenced. Because of this observation Beremin modified the expression for calculating Weibull stress including plastic strain with an anticipation that resistance against cleavage fracture will decrease with increase in plastic strain. In our earlier work [48] on the same material enhancement in fracture toughness due to loss of constraint in DBT region and effect on Master Curve was observed. In this work we started with this primacy to consider the effect of plastic strain on Beremin parameters using Beremin's modified equation and focused on to study the acceptability of Monte Carlo simulation. Later we also appreciated the findings of Ruggeri and Dodds [58] that the likelihood of cleavage fracture should increase with increase in plastic strain due to availability of more micro-cracks. To take care of both the effects of plastic strain one on value of fracture toughness Considered by Beremin) and another on possibility of cleavage fracture (Considered by Ruggeri) a new modification strategy will be studied. In our understanding correction by Beremin to capture the effect of plastic strain on Weibull stress is not reverse to that of By Ruggeri at crack tip influences rather those are complementary. Therefore in this work we decide to be restricted with Beremin's correction and in future course of work a comparative study based on two propositions and also a combined correction model for plastic strain is required to be attempted. Ruggieri and his co-workers basically proposed the three models to take account of the plastic strain. The effect of plastic strain is induced in the formulation of probability of failure and Weibull Stress σ_w , by the introduction of ψ_c. The ψ_c keep on changing for different models which are as follows.

$$P_f\left(\sigma_1,\varepsilon_p\right)=1-\exp\left[-\frac{1}{v_0}\int_{\Omega}\psi_c\left(\varepsilon_p\right).\left(\frac{\sigma_1}{\sigma_u}\right)^m d\Omega\right]$$

$$\sigma_w=\left[\frac{1}{v_0}\int_{\Omega}\psi_c\left(\varepsilon_p\right).\sigma_1^m d\Omega\right]^{1/m}$$

Local criterion using the distribution of particle fracture stress

$$\psi_c=1-\exp\left[-\left(\frac{l}{l_N}\right)^3.\left(\frac{\sigma_{pf}}{\sigma_{prs}}\right)^{\alpha_p}\right]$$

Where,

$\sigma_{pf}=\sqrt{1.3\sigma_1\varepsilon_p E_d}$

l is the particle size, l_N represents a reference particle size,

σ_{prs} is the particle reference fracture stress,

α_p denotes the Weibull modulus

Influence of plastic strain on micro crack density

$\psi_{c(\varepsilon_p)}=\varepsilon_p^{\beta}$

Where ,

ϵ_p=plastic strain

β=material dependent parameter

Exponential dependence of eligible microcracks on plastic strain (ϵ_p)

$\psi_c=1-\exp\left(-\lambda\varepsilon_p\right)$

Where,

λ=material dependent parameter

Modified Beremin model predicts

$$\sigma_w=\sqrt[m]{\sum_j\left(\sigma_1^j\right)^m\frac{V_j}{V_0}\exp\left(-\frac{m\varepsilon_1^j}{2}\right)}$$

ε_1^j is the strain in the direction of the maximum principal stress σ_1^J

In our understanding correction by Beremin to capture the effect of plastic strain on Weibull stress is not reverse to that of By Ruggeri at crack tip influences rather those are complementary

c) **Application of this method in component level:** A comprehensive method to capture the effect of constraint on T_0 at different temperatures is proposed in this thesis work where only Master Curve at any test temperature is sufficient data. But the success of this method to predict degradation of fracture toughness in component level is not explored. This can be the most important future work related to the output of this thesis.

References

1. Wallin, K., The scatter in K_{IC} result. Engineering Fracture Mechanics, Vol. 19, 1984, pp. 1085-1093.

2. Wallin.K, The master curve method: a new concept for brittle fracture. International Journal of Materials and Product Technology 1999.Vol.14 (2–4):342–354.

3. Wallin.K, Master Curve of ductile to brittle transition region fracture toughness round robin data. The "EURO" Fracture toughness curve. VTT Report 1998.

4. Test method for the determination of reference temperature T_0 for ferritic steels in the transition range (ASTM E1921), Philadelphia: American Society for Testing and Materials; 2013.

5. Kim, S.H., Park, Y.W, Lee, J.H., and Kang, S.S.,1999, Estimation of fracture toughness in the transition region using CVN data, 15th International Conference on Structural Mechanics in Reactor Technology (SMiRT 15),Seoul, Korea, August, 15 – 20ASTM E208-06(2012) Standard Test Method for Conducting Drop-Weight Test to Determine Nil-Ductility Transition Temperature of Ferritic Steels.

6. ASTM E208-06(2012) Standard Test Method for Conducting Drop-Weight Test to Determine Nil-Ductility Transition Temperature of Ferritic Steels.

7. Application of Master Curve Method Fracture Toughness Methodology for Ferritic Steel,1998 EPRI Technical Report.

8. 4 R. K. Nanstad ,J. A. Keeney, D. E. McCabe , Prepared for the U.S. Nuclear Regulatory Commission Office of Nuclear Regulatory Research under Interagency Agreement No. 18986-80 1 1-93 .

9. ASTM E1921-02. Standard Test Method for Determination of Reference Temperature, T_0, for Ferritic Steels in the Transition Range http://www.astm.org/DATABASE.CART/HISTORICAL/E1921-02.htm.

10. ASTM E1921-97. Standard Test Method for Determination of Reference Temperature, T0, for Ferritic Steels in the Transition Range. http://www.astm.org/DATABASE.CART/HISTORICAL/E1921-97.htm.

11. International Atomic Energy Agency, 2005, Guidelines for Application of the Master Curve Approach to Reactor Pressure Vessel Integrity in Nuclear Power Plants, Technical Reports Series No. 429, IAEA, Vienna.

12. Wallin, K., 2002, Master curve analysis of the "Euro" fracture toughness dataset, Engineering Fracture Mechanics, 69, 451 – 481.

13. Wallin, K., 2007, Use of the Master Curve methodology for real three dimensional cracks, Nuclear Engineering and Design, 237, 1388 –1394.

14. International Atomic Energy Agency, 2009a, Integrity of reactor pressure vessels in nuclear power plants: Assessment of irradiation embrittlement effects in reactor pressure vessel steels, IAEA Nuclear Energy Series No. NP-T3.11,Vienna.

15. Marcin Graba.,.The influence of material properties and crack length on the *q*-stress value near the crack tip for elastic-plastic materials for centrally cracked plate in tension. Journal of theoretical and applied mechanics.**50**,1, 23-46, Warsaw (2012), 50th anniversary of JTAM.

16. Kim Wallin, Quantifying T-stress controlled constraint by the master curve transition temperature $T_{0.}$ Engineering Fracture Mechanics.68, (2001). 303-328.

17. Beremin FM. A local criterion for cleavage fracture of a nuclear pressure vessel steel. Metallurgical Trans 1983;14A:2277-87.

18. Ruggieri C, Dodds RH. A transferability model for brittle fracture including constraint and ductile tearing effects: a probabilistic approach. International Journal of Fracture 1996;79:309-40.

19. Ruggieri C, Dodds RH, Wallin K. Constraints effects on reference temperature T0 for ferritic steels in the transition region. Engineering Fracture Mechanics 1998;60:19-36.

20. X. GAO., C. Ruggieri, R.H. Dodds Jr.Calibration of Weibull stress parameters using fracture toughness data. International Journal of Fracture 92: 175–200.1998.

21. F. Minami, A. Brückner-Foit, D. Munz, B.Trolldenier. Estimation procedure for the Weibull parameters used in the local approach. International Journal of Fracture 1992;54:197-210.

22. Robert H. Dodds Jr, .C. Fong Shih, Ted L. Anderson. Continuum and micromechanics treatment of constraint in fracture. International Journal of Fracture 64: 101-133, 1993.

23. A. Khalili, K. Kromp. Statistical properties of Weibull estimators. Journal Of Materials Science 26 (1991) 6741-6752.

24. Yupeng Cao, Hu Hu i, Guozhen Wang, Fu-Zhen Xuan. Inferring the temperature dependence of Beremin cleavage model parameters from the Master Curve.Nuclear Engineering and Design 241 (2011) 39–45

25. Guian Qian, V.F. González-Albuixech, Markus Niffenegger.Calibration of Beremin model with the Master Curve.Engineering Fracture Mechanics 136 (2015) 15–25.

26. Burstow, D.W.Beardsmore, I.C.Howard D.P.G.Lidbury . The prediction of constraint-dependent R6 failure assessment lines for a pressure vessel steel via micro-mechanical modelling of fracture. International Journal of Pressure Vessels &Piping 80, 775–785.

27. K. Wallin, A. Laukkanen, P.Nevasmaa and T. Planman, Recent Advances In Master Curve Technology, VTT Industrial Systems, P.O.Box 1704, FIN-02044 VTT, Finland.

28. W. J. McAfee,P. T. Williams, B. R. Bass, D. E. McCabe. An Investigation of Shallow-Flaw Effects on the Master Curve Indexing Parameter (T0) in RPV material. Letter Report. Division of Engineering Technology Office of Nuclear Regulatory Research. S. Nuclear Regulatory Commission. Published April (2000).

29. IradjSattari-Far &Kim Wallin,Application of Master Curve Methodology for Structural Integrity Assessments of Nuclear Components, SKI Report 2005:55.

30. Kim Wallin, Master curve analysis of ductile to brittle transition region fracture toughness round robin data The "EURO" fracture toughness curve. Vtt Publications 367technical Research Centre of Finl. and Espoo 1998.

31. Philip Minnebo, César Chenel Ramos, José Mendes, Luigi Debarberis,Constraint-Based Master Curve Analysisof a Nuclear Reactor Pressure Vessel Steel,results from an experimental programme carried out within the IAEA CRP-8 project.

32. Z.X.Wang,H.M.li,Y.J.Chao,P.S.Lam, Prediction Of Characteristic Length And Fracture Toughness In Ductile-Brittle Transition, Proceedings of PVP20082008 ASME Pressure Vessels and Piping Division Conference July 27-31, 2008, Chicago, Illinois.

33. J.A. Joyce1 and R.L. Tregoning, Quantification of Specimen Geometry Effects on the Master Curve andTo Reference Temperature,Department of Mechanical

Engineering, US Naval Academy, Annapolis, MD USANaval Surface Warfare Center, Carderock, MD USA.

34. H. J. Rathbun, G. R. Odette, T. Yamamoto, M. Y. He, G. E. Lucas, Statistical and Constraint Loss Size Effects on Cleavage Fracture–Implications to Measuring Toughness in the ,Transition, University of California, Santa Barbara, CA 93106-5050.

35. J. Chattopadhyay, B.K. Dutta and K.K.Vaze and S.Acharyya**.**Advanced Research on Master Curve for Safety Assessment of Reactor Pressure Vessel, Barc Newsletter.

36. Bhowmik,S., Chattopadhyay,A., Bose,T., Acharyya,S.K., Sahoo,P., Chattopadhyay, J., Dhar,S., "Estimation of fracture toughness of 20MnMoNi55 steel in the ductile to brittle transition region using master curve method", Nuclear Engg. & Design, Vol.241, 2011, pp 2831-2838.

37. Bhowmik,S., Acharyya, S.K., Chattopadhyay, J., Dhar, S., "Application and comparative study of master curve methodology for fracture toughness characterization of 20MnMoNi55 steel", Materials & Design, Vol.39, 2012, pp 309-317.

38. B. S. Henry And A. R. Luxmoore,The Stress Triaxiality Constraint And The Qvalue As A Ductile Fracture Parameter,*Engineering Fracture Mechanics* Vol. 57, No. 4, pp. 375-390, 1997.

39. G. Mirone, Elastoplastic characterization and damage predictions under evolving local triaxiality: axysimmetric and thick plate specimens,Mechanics of Materials 40 (2008) 685–694.

40. Chen et al, O. Kolednik, J. Heerens, F.D. Fischer, Three-dimensional modelling of ductile crack growth: Cohesive zone parameters and crack tip triaxiality, Engineering Fracture Mechanics 72 (2005) 2072–2094.

41. S. Cravero and C. Ruggieri.A Two-Parameter Framework toDescribe Effects of Constraint Losson Cleavage Fracture andImplications for Failure Assessmentsof Cracked Components. Dept. of Naval Architect. and Ocean EngineeringUniversity of São Paulo – PNV – EPUSP05508-900 São Paulo, SP. Brazil.

42. Markku J.Nevalainen. The effect of specimen and flaw dimensions on fracture toughness. VTT publications 314.ISBN 951-38-5064-1.

43. Philip Minnebo, César Chenel Ramos, José Mendes, Luigi Debarberis. Constraint-Based Master Curve Analysis of a Nuclear Reactor Pressure Vessel Steel. IAEA CRP-8 project.EUR 24092 EN – 2009.

44. M.R. Ayatollahi,M.J. Pavier And D.J. Smith. Determination of T -stress from finite element analysis for mode I and mixed mode I/II loading. International Journal of Fracture 91: 283–298, 1998.

45. Kim Wallin. Quantifying T-stress controlled constraint by the master curvetransition temperature T_0. Engineering Fracture Mechanics 68 (2001) 303-328.

46. N. P. O 'Dowo and C. F. Shih. Family of crack-tip fields characterized by a triaxiality parameter--i. Structure of fields. J. Mech. Phys. Solids Vol. 39, No. 8, pp. 989-1015, 1991.

47. N. P. O 'Dowo and C. F. Shih. Family of crack-tip fields characterized by a triaxiality parameter-ii. Fracture applications. J. Mech. Phys. Solids Vol. 40, No. 5, pp. 939-963, 1992.

48. Sumit Bhowmik.et al. Evaluation and effect of loss of constraint on master curvereference temperature of 20MnMoNi55 steel. Engineering Fracture Mechanics 136 (2015) 142–157.

49. Claudio Ruggieri, XaoshengGao , Robert H. Dodds Jr. Transferability of elastic plastic fracture toughness using the Weibull stress approach: significance of parameter calibration.Engineering Fracture Mechanics 67 (2000) 101-117.

50. Xiaosheng Gao, Robert H. Dodds Jr. An engineering approach to assess constraint effects on cleavage fracture toughness. Engineering Fracture Mechanics 68 (2001) 263-283.

51. Jason P., Robert H. Dodds Jr. Calibration of the Weibull stress scale parameter, σ_u, using the Master Curve. Engineering Fracture Mechanics 72 (2005) 91–120.

52. A H Sherry1, D P G Lidbury, D C Connors and A R Dowling. Modelling of size effects on fracture in the brittle-to-ductile transition regime. Oral/poster reference: ICF100916OR.

53. Claudio Ruggieri. A probabilistic model including constraint and plastic strain effects forfracture toughness predictions in a pressure vessel steel.International Journal of Pressure Vessels and Piping 148 (2016) 9-25.

54. Xiaosheng Gao ,Guihua Zhang, T.S. Srivatsan. A probabilistic model for prediction of cleavage fracture in theductile-to-brittle transition region and the effect oftemperature on model parameters.Materials Science and Engineering A 415 (2006) 264–272.

55. Wei-Sheng Lei. A statistical model of cleavage fracture in structural steelswith power-law distribution of microcrack size.PhilosoPhical Magazine letters, 2016.Vol. 96, no. 3, 101–111.

56. A. Andrieu , A. Pineau, J. Besson, D. Ryckelynck, O. Bouaziz.Beremin model: Methodology and application to the predictionof the Euro toughness data set. Engineering Fracture Mechanics 95 (2012) 102–117.

57. Claudio Ruggieri and Robert H. Dodds, Jr. An engineering methodology for constraint corrections of elastic-plastic fracture toughness - Part I: A review on

probabilistic models and exploration of plastic strain effects. Engineering Fracture Mechanics 134 (2015) 368–390.

58. Claudio Ruggieri, Rafael G. Savioli and Robert H. Dodds, Jr.Comments on W.S. Lei's discussion of ''An engineering methodology for constraint corrections of elastic–plastic fracture toughness – Part II: Effects of specimen geometry and plastic strain on cleavage fracture predictions" by C. Ruggieri, R.G. Savioli and R.H. Dodds. Engineering Fracture Mechanics (2015), doi: http://dx.doi.org/10.1016/j.engfracmech. 2015.06.087.

59. Hessamoddin Moshayedi ,IradjSattari-Far. The dependence of Weibull parameters on preloads and its implication on brittle fracture probability prediction using a local criterion.Theoretical and Applied Fracture Mechanics 87 (2017) 50–60.

60. Abhishek Tiwari, R. N. Sing, Per Ståhle. Assessment of effect of ductile tearing on cleavage failure probability in ductile to brittle transition region. Int J Fract .DOI 10.1007/s10704-017-0238-7.

61. B.Z. Margolin, V.N. Fomenko, A.G. Gulenko, V.I. Kostylev, V.A. Shvetsova. Further improvement of the Prometey model and Unified Curve method part 1. Improvement of the Prometey model.Engineering Fracture Mechanics 182 (2017) 467–486.

62. M.K. Samal , J.K. Chakravartty , M. Seidenfuss , E. Roos. Evaluation of fracture toughness and its scatter in the DBTT regionof different types of pressure vessel steels.Engineering Failure Analysis 18 (2011) 172–185.

63. Kim Wallin. The Elusive Temperature Dependence of the Master Curve. 13th International Conference on Fracture June 16–21, 2013, Beijing, China.

64. Carl von Feilitzen, Iradj Sattari-Far. Implementation of the Master Curve method in ProSACC. 2012:07 ISSN: 2000-0456.

65. Andrey P Jivkov, Peter James. Cleavage modelling with experimental particle size distribution and novel particle failure criterion. 13th International Conference on Fracture June 16–21, 2013, Beijing, China.

66. Y. Lei, N.P. O'dowd, E.P. Busso And G.A. Webster. Weibull stress solutions for 2-D cracks in elastic and elastic-plastic materials. International Journal of Fracture 89: 245–268, 1998.

67. N.P. O 'Dowd , Y. Lei, E.P. Busso. Prediction of cleavage failure probabilities using the Weibull stress. Engineering Fracture Mechanics 67 (2000) 87-100.

68. Avinash Gopalan , M.K. Samal , J.K. Chakravartty. Fracture toughness evaluation of 20MnMoNi55 pressure vessel steel in the ductile to brittle transition regime: Experiment & numerical simulations. Journal of Nuclear Materials 465 (2015) 424-432.

69. Jason P. Petti, Robert H. Dodds Jr. Coupling of the Weibull stress model and macroscale modelsto predict cleavage fracture.Engineering Fracture Mechanics 71 (2004) 2079–2103.

70. X. Gao, R.H. Dodds, Jr,R.LTregoning, J.A.Joyce and R.E.Link. A Weibull stress model to predict cleavage fracture in plates containing surface cracks. Fatigue and Fracture Of Engineering Materials and Structures. Volume 22(1999)481-493.

71. M.C. Burstow. A re-assessment of parameter tuning for the Beremin model using the toughness scaling technique. International Journal of Pressure Vessels and Piping 80 (2003) 797–805.

72. A.H.Sherry, D.P.G.Lidbury, B.R.Bass and P.T.Williams. Developments in Local Approach methodology with application to the analysis/re-analysis of the NESC-1 PTS benchmark experiment. Volume 78, Issues 2–3, February 2001, Pages 237-249.

73. K.Hojo, I.Muroya, A.Brückner-Foit . Fracture toughness transition curve estimation from a notched round bar specimen using the local approach method. Nuclear Engineering and Design. 174(1997) 247–258.

74. Gao, X., Zhang, G., Srivatsan, T.S., 2006. A probabilistic model for prediction of cleavage fracture in the ductile-to-brittle transition region and the effect of temperature on model parameters. Material Science and Engineering. A 415, 264–472.

75. Bogdan Wasiluk, Jason P.Petti, Robert H.Dodds Jr. Temperature dependence of Weibull stress parameters: Studies using the Euro-material. Engineering Fracture Mechanics 73 (2006) 1046–1069.

76. Jason P. Petti , Robert H.Dodds Jr. . Calibration of the Weibull stress scale parameter, σ_u, using the Master Curve. Engineering Fracture Mechanics 72 (2005) 91–120.

77. C.S.Wiesner and M.R. Goldthorpe. The Effect of Temperature and Specimen Geometry on the Parameters of the "Local Approach" to Cleavage Fracture. 1st European Mechanics of Materials Conference on Local Approach to Fracture '86 - 96'. J Phys.IV. France 06 (1996) C6-295-C6-304.

78. INTERNATIONAL ATOMIC ENERGY AGENCY, 2009b, Master Curve Approach to Monitor Fracture toughness of Reactor Pressure Vessels in Nuclear Power Plants, IAEA-TECDOC-1631, Vienna.

79. ASTM E1921-02. Standard Test Method for Determination of Reference Temperature, *T0*, for Ferritic Steels in the Transition Range, http://www.astm.org/DATABASE.CART/HISTORICAL/E1921-02.htm.

80. Viehrig HW, Boehmert J, Dzugan J. Some issues by using the master curve concept. Nuclear Engineering and Design 2002; 212:115–24.

81. Williams, M.L., ‘‘On the Stress Distribution at the Base of a Stationary Crack.’’ Journal of Applied Mechanics, Vol. 24, 1957, pp. 109–114.

82. Mastaneh Moattari and Iradj Sattari-Far. Modification of fracture toughness Master Curve considering the crack tip Q-constraint. Theoretical and Applied Fracture Mechanics. http://dx.doi.org/10.1016/j.tafmec.2017.02.012.

83. Eisele U, Seidenfuss M, Pitard-Bouet JM. Comparison between fracture mechanics and local approach models for the analysis of shallow cracks. J Phys 1996;III(6):75–89.

84. Bao Y, Weirzbicki T. On fracture locus in the equivalent strain and stress triaxiality space. Int J Mech Sci 2004;46:81–98.

85. Gao X, Kim J. Modeling of ductile fracture: significance of void coalescence. Int J Solids Struct 2006; 43:6277–93.

86. Yan C, Mai YW, Wu SX. Finite element analysis and experimental evaluation of ductile-brittle transition in compact tension specimen. Int J Fract1997;87:345–62.

87. Chibber R, Singh H, Arora N, Dutta BK. Micromechanical modelling of reactor pressure vessel steel. Mater Des 2012;36:258–74.

88. Robert H. DoddsJr., Ted L. Anderson, Mark T. Kirk. A framework to assess a/W ratio effects on elastic–plastic fracture toughness (Jc) in SENB specimens. Int J Fract.48, (1991)1–22

89. Claudio Ruggieri. A New Procedure to Calibrate the Weibull Stress Modulus (m). Department of Naval Architecture and Ocean Engineering, University of São Paulo. São Paulo, SP 05508−900, Brazil.

90. Guian Qian ,Wei-Sheng Lei, Markus Niffenegger**.** Calibration of a new local approach to cleavage fracture of ferritic steels. Materials Science & Engineering A 694. **(**2017)10-12.

91. AbhishekTiwari,AvinashG.,SauravSunil,R.N.Singh,PerStåhle,J.Chattopadhyay,J. K.Chakravartty. Determination of reference transition temperature of In-RAFMS in ductile brittle transition regime using numerically corrected Master Curve approach. Engineering Fracture Mechanics 142, (2015)79–92.

92. ASTM E1921-13 (2013). "Standard Test Method for Determination of Reference Temperature, T0, for Ferritic Steels in the Transition Range," ASTM International, American Society for Testing and Materials, West Conshohocken, PA, USA